PARAMETERS INFLUENCING LONG TERM PERFORMANCE AND DURABILITY OF PEM FUEL CELLS

A THESIS SUBMITTED TO
THE GRADUATE SCHOOL OF NATURAL AND APPLIED SCIENCES
OF
MIDDLE EAST TECHNICAL UNIVERSITY

BY

ELİF SEDA ŞAYİN

IN PARTIAL FULFILLMENT OF THE REQUIREMENTS
FOR
THE DEGREE OF MASTER OF SCIENCE
IN
CHEMICAL ENGINEERING

FEBRUARY 2011

Approval of the thesis

PARAMETERS INFLUENCING LONG TERM PERFORMANCE AND DURABILITY OF PEM FUEL CELLS

submitted by **ELİF SEDA ŞAYİN** in partial fulfillment of the requirements for the degree of **Master of Science in Chemical Engineering Department, Middle East Technical University** by,

Prof. Dr. Canan Özgen _____
Dean, Graduate School of **Natural and Applied Sciences**

Prof. Dr. Deniz Üner _____
Head of Department, **Chemical Engineering**

Prof. Dr. İnci Eroğlu _____
Supervisor, **Chemical Engineering Dept., METU**

Dr. Ayşe Bayrakçeken _____
Co-Supervisor, **Chemical Engineering Dept., Atatürk University**

Examining Committee Members:

Prof. Dr. Işık Önal _____
Chemical Engineering Dept., METU

Prof. Dr. İnci Eroğlu _____
Chemical Engineering Dept., METU

Dr. Ayşe Bayrakçeken _____
Chemical Engineering Dept., Atatürk University

Doç. Dr. Alper Tapan _____
Chemical Engineering Dept., Gazi University

Prof. Dr. Gürkan Karakaş _____
Chemical Engineering Dept., METU

Date: 09/02/2011

I hereby declare that all information in this document has been obtained and presented in accordance with academic rules and ethical conduct. I also declare that, as required by these rules and conduct, I have fully cited and referenced all material and results that are not original to this work.

Name, Last name: Elif Seda ŞAYİN

Signature :

ABSTRACT

PARAMETERS INFLUENCING LONG TERM PERFORMANCE AND DURABILITY OF PEM FUEL CELLS

Şayin, Elif Seda

M.Sc., Department of Chemical Engineering

Supervisor: Prof. Dr. İnci Eroğlu

Co-supervisor: Dr. Ayşe Bayrakçeken

February 2011, 111 pages

Fuel cells are the tools which convert chemical energy into electricity directly by the effective utilization of hydrogen and oxygen (or air). One of the most important barriers for the fuel cell commercialization is the durability of the fuel cell components in the long term operations. In this study, the durability of the PEM fuel cell electrocatalysts were investigated via cyclic voltammetry (CV) and rotating disk electrode (RDE) experiments in order to determine the hydrogen oxidation reaction (HOR) and oxygen reduction reaction (ORR) which corresponds to the half cell reactions in the fuel cell. PEM fuel cell electrodes mainly composed of carbon supported Pt catalysts. In long term operations due to Pt dissolution and carbon corrosion some properties of the electrocatalysts can be changed. Performance losses in catalysts mainly depend on; i) decrease in the total metal surface area (SA) and the electrochemically active surface area (ESA) due to the increase in the particle size ii) decrease in the tafel slope potential in ORR and iii) increase in carbon corrosion. In this study, these properties were examined via accelerated degradation tests performed in CV and RDE. The catalysts having different Pt loadings, synthesized with different ink compositions, pH values and microwave durations were

investigated. The commercial catalysts having Pt loadings of 20, 50 and 70 (wt %) were tried and best results were obtained for Pt/V (50 wt %) catalyst. Different carbon to Nafion® ratios of 4, 8, 12 in the ink composition were tried. C/N ratio of 8 gave the best result in Pt dissolution and carbon corrosion degradation tests. The catalysts prepared at different pH values of 1.4, 6.25 and 10 were tried and the catalyst prepared at pH of 10 was less degraded in Pt dissolution test and the catalyst prepared at pH of 6.25 showed better resistance to carbon corrosion. Catalysts prepared under different microwave durations of 50, 60 and 120 s were tried and the catalyst prepared at 60 s gave the best performances.

Keywords: PEM fuel cell electrocatalyst, durability, accelerated degradation test, cyclic voltammetry

ÖZ

PEM YAKIT PILLERİNİN UZUN DÖNEM PERFORMANS VE DAYANIMINI ETKİLEYEN PARAMETRELER

Şayin, Elif Seda
Yüksek Lisans, Kimya Mühendisliği Bölümü
Tez Yöneticisi: Prof. Dr. İnci Eroğlu
Ortak Tez Yöneticisi: Dr. Ayşe Bayrakçeken

Şubat 2011,111 Sayfa

PEM yakıt pilleri, hidrojen ve oksijen gazlarının etkin bir şekilde biraraya gelmesi ile kimyasal enerjiden doğrudan elektrik enerji üreten araçlardır. PEM yakıt pillerinin ticarileşmesi önündeki en önemli engel, yakıt pili bileşenlerinin uzun dönem kullanımlardaki dayanımlarıdır. Bu çalışmada, PEM yakıt pili elektrokatalizörlerinin dayanımı yakıt pilinde yarı hücre reaksiyonları olarak bilinen hidrojen oksidasyon ve oksijen redüksiyon reaksiyonları açısından döngülü voltametri (CV) ve döner disk electrot (RDE) yöntemleriyle araştırılmıştır. PEM yakıt pili elektrokatalizörleri, genel olarak, platin metalinin karbon ile desteklenmesi sonucu oluşur. Pilin uzun dönem çalışması sonucunda, platin çözünmesi ve karbon korozyonuna bağlı, katalizörün önemli özelliklerinde kayıplar gözlenmektedir. Performans kayıpları, genel olarak, i) parçacık boyutu büyümesine bağlı katalizörlerin toplam metal alanında, elektrokimyasal aktif alnında, ii) oksijen redüksiyon potansiyeline bağlı tafel eğimi potansiyelinde düşüşler ve iii) karbon korozyonundaki artışlara bağlıdır. Bu çalışmada, CV ve RDE yöntemleri ile katalizölere hızlandırılmış bozunma testleri

uygulanarak bu özellikler araştırılmıştır. %20,% 50 ve 70 % Pt yüküne sahip ticari katalizörler denenmiş ve en iyi sonuç Pt/V %50 katalizöründen alınmıştır. Katalizör çözeltisi içinde carbonun Nafion çözeltisine oranı 4, 8, 12 olarak denenmiş ve en iyi sonuç hem Pt çözünmesi hem karbon korozyonu açısından C/N oranı 8 olan katalizör tabakasından alınmıştır. Bunların yanında, 1.4, 6.25 ve 10 pH değerlerinde sentezlenmiş katalizörler denenmiş ve pH 10, platin degredasyonu açısından, pH 6.25 ise karbon korozyonu açısından en iyi dayanımı göstermiştir. 50 s, 60 s, 120 s mikrodalga sürelerinde sentezlenene katalizörlerin denenmesi sonucunda da en iyi sonuç 60 s süresinde sentezlenen katalizörden alınmıştır.

Keywords: PEM yakıt pili elektrokatalizörü, dayanıklılık, hızlandırılmış bozulma testi, çevrimsel voltametri

To my family

and

Alp

ACKNOWLEDGEMENTS

First and the most, I would like to express my deepest gratitude to my supervisor Prof. Dr. İnci Eroğlu for her valuable thoughts, suggestions and comments till the completion of the study. Besides her scientific and academic guidance, her energy, understanding and kind attitude always motivated me. I admire her for both her academic carrier and her personality.

I also wish to express my grateful thanks to my co-supervisor, Dr. Ayşe Bayrakçeken for transferring her knowledge about cyclic voltammetry and electrochemistry of catalysts. Even she works in Atatürk University; she always guided me and supported my study. She was the person who tried hard as much as I tried to carry this study to completion.

I am thankful to my dear friends Pelin Yetişemiyen and Nur Kandilli for their support and friendship from the first time I met them in METU.

I want to thank all the members of FCRC laboratory especially Serdar Erkan. I could able to solve many troubles with the help of him. I also want to thank Berker Fıcıcılar. I have learned so much from him. He was the person who encouraged me both entering METU and be a research assistant in the department.

I want to say my best to my boyfriend, Alp Lafcı for being always near me and encouraged me both in my good and hard times. Even we fell apart for now, during this time, he always showed his support and patience. I owe him so much.

Last and specially, I would like to express my deepest appreciations to my family, my father Ahmet Şayin, my mother Güzide Şayin and my sister Burcu Şayin for their help and support they always showed to me during my whole life.

TABLE OF CONTENTS

LIST OF TABLES

TABLES

LIST OF FIGURES

FIGURES

LIST OF SYMBOLS

A Area under curve for hydrogen reduction region excluding double layer capacitance

B Levich constant

CE Counter Electrode

CV Cyclic Voltammetry

E Voltage

ESA Electrochemical Surface Area (m^2/gr Pt)

F Faraday constant

GC Glassy Carbon

GDL Gas Diffusion Layer

HOR Hydrogen Oxidation Reaction

L Platinum loading on glassy carbon electrode ($\mu g/cm^2$),

MEA Membrane Electrode Assembly

N Avogadro number

NHE Normal Hydrogen Electrode

ORR Oxygen Reduction Reaction

PEMFC Proton Exchange Membrane Fuel Cell

Pt Platinum

Q Charge (coulomb)

RDE Rotating Disc Electrode

RE Reference Electrode

S Scan rate (mV/s)

SA Surface Area (m^2/gr)

VX Vulcan XC72

VXR Vulcan XC72R

WE Working Electrode

CHAPTER 1

INTRODUCTION

Energy is a very important issue for humanity. Increase in World' population due to technological growth causes more energy consumption. Fossil fuel based energy sources are the most common energy sources but besides, they are one of the most serious threats for the sake of human beings. First of all, they are limited and will be depleted some day; second of all, they cause serious environmental hazards leading to climate change, air pollution, ozone depletion, etc. Environmental and health effects of fossil fuels lead researchers to find and develop new energy sources which are clean, renewable and sustainable.

From this point of view, hydrogen is thougt to be a good alternative which is a secondary energy source. It can be produced from renewable primary energy sources like wind, solar, geothermal etc. It is light, clean and an efficient fuel that can be converted directly to electricity by fuel cells.

Fuel cells are electrochemical energy converters which converts chemical energy into electrical energy directly. Since its invention, fuel cells are developed for commercialization. Barriers against their commercialization can be summarized by the factors which are high cost of the components, performance losses, gas poisoning and degradation of chemical based components (membrane, catalyst) with time (Zhang et al., 2009). If these factors can be minimized, usage of fuel cells in our daily lives would be increased.

Fuel cells are mostly classified by the electrolyte they have employed. Direct methanol fuel cells (DMFCs) are an exception because in DMFCs, methanol is electrochemically oxidized in the fuel cell. Other types are, proton exchange membrane fuel cells (PEMFCs), phosphoric acid fuel cells (PAFCs), alkaline fuel cells (AFCs), molten carbonate fuel cells (MCFCs) and solid oxide fuel cells (SOFCs). Among these types, proton exchange membrane fuel cell is the most common one. PEMFCs are advantageous because they can be easily handled and assembled. Solid electrolyte is used in PEMFCs and also they work pollution free, easily start-up and shut-down and its operations undergo at lower temperatures relative to other fuel cell types which brings lower thermal losses (Bernay et al., 2002).

The most crucial part of the PEM fuel cells is Membrane Electrode Assembly (MEA). It basically consists of diffusion media, catalyst layer and solid polymer electrolyte. It is accepted as the heart of a PEM fuel cell because main reactions of interest and proton conduction occur in this part. Basically, hydrogen gas is fed to the anode side as the fuel and breaks into proton and electron by the help of the catalyst layer. Proton conductive membrane only transfers protons thus electrons are transferred to cathode through an external circuit. Oxygen gas is fed to the cathode side. Protons, electrons and oxygen are reacted at the cathode side and water is formed (Bayrakçeken, 2008).

PEM fuel cells are tried to become commercial products but there are some barriers that prevents them to be used for stationary and mobile applications. From this point of view, there arises the importance of durable and stable operations and barriers that limit PEM fuel cells to operate for long times without having performance losses. Durability is an important factor which can be stated as the ability of a PEM fuel cell to show resistance against permanent change in performance over time. Decrease in durability does not mean to a catastrophic failure but it causes performance losses that is not recoverable or reversible (Wu et al, 2008). Longer lives for PEM fuel cells

are tried to be achieved in order to make them commercial, handy and alternative energy systems. Factors that affect the durability of PEM fuel cells are mainly; poor water management, fuel and oxidant starvation, corrosion and chemical reactions of cell components. Durability tests are performed to the PEM fuel cells both in-situ and ex-situ. In-situ tests are applied directly to the cell itself and ex-situ tests are applied to the components of the cell, separately.

In-situ durability tests can be performed but takes too much time. For example, 4.5 years of testing is needed in order to accomplish 40000 hour of fuel cell operating time target for stationary applications. This method is time consuming and fuel expense reaches nearly 2 million dollars (Wu et al, 2008). Considering these factors, researchers have tried to develop some tests called accelerated stress tests (ASTs) or in other words accelerated degradation tests (ADTs), which can be performed in shorter times and would also give considerable information about fuel cell performances.

Accelerated stress tests (as ex-situ tests) are mainly performed to the components of the MEA, which are membrane, catalyst layer and gas diffusion layer. Tests that are applied to the membrane are; holding at open circuit voltage (OCV), load cycling and most common one is the Fenton test. Catalysts used in PEMFCs are mainly composed of platinum supported on carbon so tests applied to the catalyst mostly depend on searching the degradation mechanisms of platinum dissolution and carbon corrosion. These degradation mechanisms can be investigated via the tests performed by cyclic voltammetry (CV) technique. For the gas diffusion layer (GDL), tests are carried out by applying in-situ and ex-situ stressors to the GDL. For example, testing PEMFC at higher temperatures or submerging GDL to hydrogen peroxide solution to simulate PEMFC conditions by which weight losses can be observed (Zhang et al., 2009).

Catalyst layer is one of the most important parts of the fuel cell. Its durability would affect the long term performance of the fuel cell without any doubt. Due to dissolution, migration or agglomeration of platinum metal particles and corrosion of carbon support; catalyst loses its properties in the fuel cell environment (Schmittenger et al., 2008). In order to investigate the effect of each component on the durability and find solutions to performance loss problems, components should be tested separately. From this aspect, catalyst layer was decided for testing its durability, separately.

The objective of this thesis is to determine the long term stabilities of the commercially available and already synthesized catalysts in METU Chemical Engineering Department Fuel Cell Research Laboratory with ex-situ testing. Already synthesized catalysts were prepared by microwave irradiation technique having 20 wt % Pt supported on Vulcan XC72 carbon support. They were prepared at different preparation conditions including different pH values and different microwave durations (Bayrakçeken, 2008). Commercial ETEK Pt/V (20 wt %) and Pt/V (50 wt %) and Pt/V (70 wt %) catalysts were used. The comparison of the home made catalysts with the commercial ones is very important in order to determine the electrocatalytic activity of the catalysts prepared in our laboratory. Cyclic Voltammetry and Rotating Disc Voltammetry techniques are well-known techniques used for the characterization of the catalysts in a fast manner. Ex- situ testing protocols were based on searching the effects of platinum dissolution and carbon corrosion by exposing the catalysts to potential cyclic and potential holding operations. The data obtained from the physicochemical and electrochemical characterization techniques were used to calculate the total metal surface area, electrochemical surface area losses, losses due to carbon corrosion, platinum utilization and potential losses of the catalysts. These results were then compared to the results of the commercial catalysts.

CHAPTER 2

LITERATURE SURVEY

2.1 Proton Exchange Membrane Fuel Cells

Proton exchange membrane fuel cells are thought to be one of the most promising energy conversion system alternatives of the present century. Fuel cells draw attention by most of the vehicle companies and researchers because they are simple, viable, can quickly start-up and shut-down. Also, they can be demonstrated in so many conceivable applications from powering a cell phone to a locomotive (Barbir, 2006). Also, they are compact, have light-weight and high power density. Besides, they do not need higher temperatures to operate. Considering all these good features, in recent years, concentration has been given to PEM fuel cells for making them commercial products (Wind et al, 2002).

2.2 Working principle and components

A PEM fuel cell basically made up of two electrodes acting as anode and cathode with a solid polymer electrolyte sandwiched between them. Hydrogen gas is fed to the anode side in which oxidation reaction occurs. Hydrogen splits into proton and electron. The proton conducting membrane transfers only the positively charged ions (protons) to the anode side of the cell. Negatively charged ions (electrons) transfer to the cathode side with an external circuit by which electricity is produced. At the cathode side, oxygen gas is fed and meets with electrons and protons thus water is produced. In Figure 2.1, operating principle of PEM fuel cell is given

(www.biocharfarming.files.wordpress.com/2008/10/fuel_cell_diagram_scientificcomputing.jpg, last accessed at 25.12.2010).

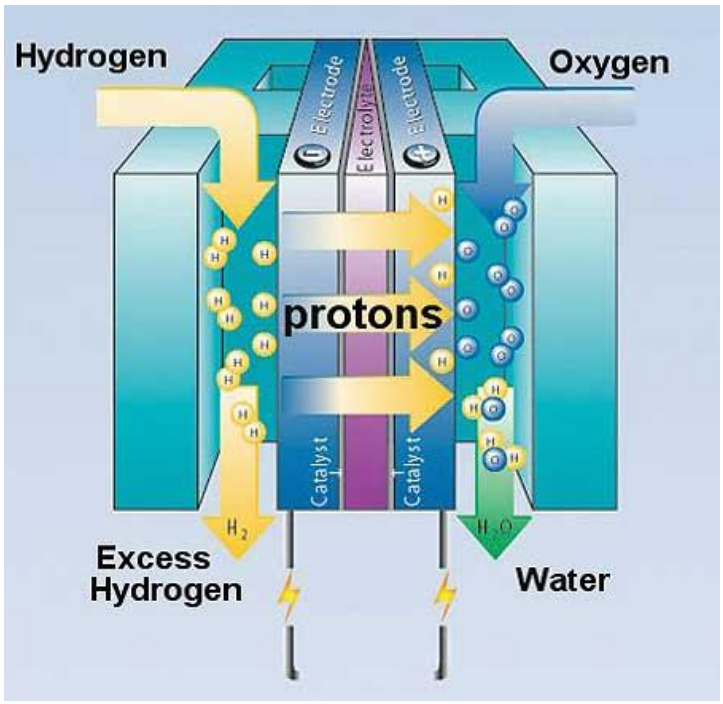

Figure 2.1 How a PEM fuel cell works?

In PEM fuel cells, reactions are mentioned as half reactions because separate reactions occur in anode and cathode sides and their overall gives the production mechanism of water.

Anode half cell reaction: $2H_2 \longrightarrow 4H^+ + 4e^-$ E= 0.00V (2.1)

Cathode half cell reaction: $O_2 + 4H^+ + 4e^- \longrightarrow 2H_2O$ E= 1.23V (2.2)

Overall reaction: $2H_2 + O_2 \longrightarrow 2H_2O$ E= 1.23V (2.3)

Anode half cell reaction (hydrogen oxidation reaction, HOR), establishes the standard potential of 0.0 V and the cathode half cell reaction (oxygen reduction reaction, ORR) states the standard potential of 1.23 V. Total potential of 1.23 V gives the resultant reversible potential of the cell.

PEM fuel cells generally operate between 70-90°C. To limit its working temperature, some water content should be present within the cell, which is provided by humidifying the reactant gases before they are fed to the reactor. This is also a must for the efficient work of the electrolyte because proton conducting membranes should be stated well-humidified in order to conduct the protons and operate for longer times, efficiently (Barbir, 2006).

Components of a PEM fuel cell can be mentioned as, proton conducting electrolyte (membrane), catalyst layer, gas diffusion layer and bipolar plates.

Membranes of PEM fuel cells are typically made up of perfluoro-sulfonic acid ionomer (PSA). The best PEM fuel cell membrane is known as Nafion® produced by Du-Pont which uses perfluoro sulfonylfluoride ethyl-propyl-vinyl ether (PSEPVE) (Barbir, 2006). Membranes should have high proton conductivity and they should supply a strong barrier to the mixing of fuel and reactant gases. They should also stay stable for long times under fuel cell operating conditions.

Catalyst layer is another important component of a PEM fuel cell. It is directly contacted with the membrane and the gas diffusion layer. The other referring for the catalyst layer is active layer. For anode and cathode sides, catalyst layer is the place where the half cell reactions occur. Catalyst layer can be deposited either on the membrane or the gas diffusion layer. The real aim for both of the techniques is to make an effective connection of the catalyst layer components (platinum, platinum or other alloy, supporting material) to the membrane (Litzster et al, 2004). Platinum is the most common material for PEM fuel cell catalysts for providing excellent long term performances to the PEM fuel cell. In spite of this property of platinum it has high cost so researchers have tried to substitute the platinum with other proper

materials (O'Hayre et al, 2002). Besides the Pt loading, there are some other factors that should be optimized to obtain higher performances. Reactant diffusivity, ionic, electrical conductivity and hydrophobicity level of the catalysts are the most important properties that should be taken into consideration. In figure 2.2 the transfer mechanism through the catalyst layer can be easily seen (Litzster et al, 2004).

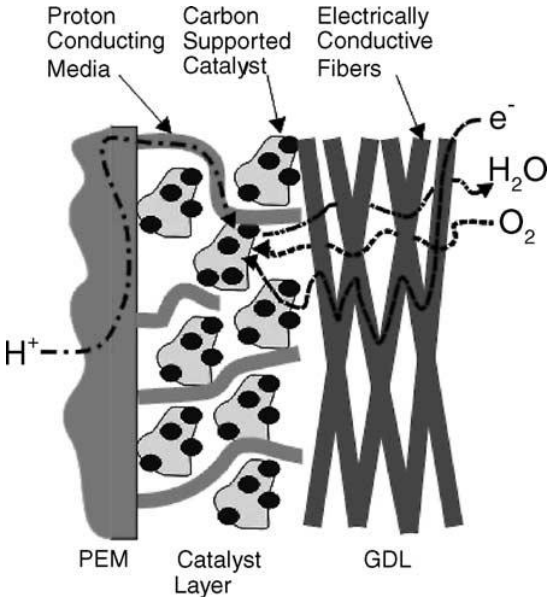

Figure 2.2 Transfer in PEM fuel cell catalyst layer

Gas diffusion layer (GDL) is the other crucial part of a PEM fuel cell. They are carbon based, porous materials mostly called as carbon paper or carbon cloth. Catalyst used in PEM fuel cells are applied to the GDL in an ink form which is comprised of water, isopropanol, Nafion® solution and catalyst itself. This solution is sprayed on two same shaped gas diffusion layers and then they are hot pressed to the both sides of a proton conducting membrane. They are the outer part of the MEA. They provide a connection between electrodes and bipolar plates by supporting membrane mechanically. Their function is to distribute the reactants to the catalyst

layer and they also allow the resultant product water to leave the electrode surface (Willlams et al., 2004).

Final crucial components are the bipolar plates. They have considerable functions in the operating of PEM fuel cells. They supply a good distribution area for distributing the fuel gases and air over the active areas. Also, heat release due to reactions is removed by bipolar plates from active areas. In addition to these, they have conducted current from cell to cell in fuel cell stacks and they are good barriers for prevention of gas leakages. Due to good distribution of fuel gases, channel dimensions have to be met exactly, small deviations may lead to reduced efficiencies and reduced output thus poor gas utilization. On the other hand, to minimize the ohmic losses, the materials used to manufacture the bipolar plates should have lower bulk and contact resistances. Also, they should not contain any ingredients that can poison other components of the fuel cell. Today several types of materials are being used in bipolar plates. Main materials of interest are, electro-graphite, carbon-carbon composites, sheet material, flexible graphite foil and graphite polymer composites (Middelman et al, 2003).

2.3 Electrochemistry of PEM fuel cells

Electrochemistry of PEM fuel cells is based on the reactions occuring both on the anode and the cathode sides. At the anode side basically, hydrogen is fed and seperates into its protons and electrons.

$$H_2 \longrightarrow 2\,H^+ + 2\,e^- \qquad E = 0.00\ V \qquad (2.4)$$

At the cathode side, oxygen gas is fed and meets there with the protons coming from proton conducting membrane and electrons coming from an external circuit by which electricity is produced. Reaction of oxygen, protons and electrons gives water.

$$\tfrac{1}{2}\,O_2 + 2H^+ + 2\,e^- \longrightarrow H_2O \qquad E = 1.23\ V \qquad (2.5)$$

These reactions are called hydrogen oxidation reaction (HOR) for anode side where hydrogen gives electron and oxidizes and oxygen reduction reaction (ORR) for cathode side where oxygen takes electron and reduces.

As an overall, formation of water is occuring by the combination of H_2 and O_2 gases with electricity output.

$$H_2 + ½\ O_2 \longrightarrow H_2O \qquad E= 1.23\ V \qquad (2.6)$$

Cathode side ORR reaction determines the performance of the PEM fuel cell due to having slower kinetics.

2.3.1 Hydrogen oxidation reaction

As mentioned before, hydrogen oxidation reaction takes place at the anode side of the PEM fuel cell and the mechanism would follow via two mechanism as written below (Larminie and Dicks, 2003).

Tafel-Volmer mechanism

$$H_2 \longrightarrow 2\ H_{ads} \qquad (2.7)$$

$$H_{ads} + H_2O \longrightarrow H_3O^+ + e^- \qquad (2.8)$$

Heyrovsky-Volmer mechanism

$$H_2 + H_2O \longrightarrow H_{ads} + H_3O^+ + e^- \qquad (2.9)$$

$$H_{ads} + H2O \longrightarrow H_3O^+ + e^- \qquad (2.10)$$

2.3.2 Oxygen reduction reaction

Oxygen reduction reaction takes place at the cathode side of the PEM fuel cell. The mechanism would follow either complete or incomplete reduction of O_2 (Hamann et al., 1998).

Complete reduction

$$O_2 + 4H^+ + 4e^- \longrightarrow 2H_2O \qquad E = 1.23\ V \qquad (2.11)$$

which is the desired PEM fuel cell overall reaction leading to H_2O formation.

Incomplete reduction

$$O_2 + 2H^+ + 2e^- \longrightarrow H_2O_2 \qquad E = 0.682\ V \qquad (2.12)$$

This reaction may be followed via the following reactions leading to complete the reduction. On the other hand, H_2O_2 may split into OH^- and OOH^- radicals which is a bad case for the durability of the membrane because these radicals will attack the polymer end groups of the membrane and in time membrane gets thinner and loses its proton conductive property (Bayrakçeken, 2008).

1. **Further reduction**

$$H_2O_2 + 2H^+ + 2e^- \longrightarrow 2H_2O \qquad E = 1.77\ V \qquad (2.13)$$

2. **Chemical deposition**

$$2H_2O_2 \longrightarrow 2H_2O + O_2 \qquad (2.14)$$

2.3.3 Polarization curve and voltage losses

PEM fuel cells are used for producing electricity so the energy released is the most crucial factor for a PEM fuel cell. In this point 'Gibbs free energy' is taken into consideration where $\sum G_f$ is the Gibbs free energy of formation, which gives us the energy gained.

$$\sum G_f = \sum G_f \text{ (products)} - \sum G_f \text{ (reactants)} \quad (2.15)$$

Electrical energy is gained from the charge that flows through the external circuit. It can be said due the reactions 2.1 and 2.2 that, for every mole of H_2O produced, two electrons are passed through the external circuit. If –e is the charge of one electron then the charge flows through can be determined as;

$$-2Ne = -2F \quad (2.16)$$

where the F (coulomb/mole) stands for Faraday constant (96485 C/electron-mole) which represents the the magnitude of electrical charge for one mole of electron. The basic relation is;

$$F = eN \quad (2.17)$$

where N is the Avogadro number (6.022×10^{23} mol^{-1}). If the potential needed to be supplied for moving the charge of 1 mole electron is E (volt), then the electrical work gained will be found from equation 2.18, below.

$$\text{Electrical work} = 2F \times E \text{ in (Joules/mole)} \quad (2.18)$$

Assuming no losses in the system, this electrical work stands for Gibbs free energy of formation. Then potential (E) can be written in the form of equation 2.19, which the voltage is called 'Open Circuit Voltage'(OCV) for the fuel cell.

$$E = \frac{-\Delta Gf}{2F} \tag{2.19}$$

Since ΔG and F are already known, the theoretical hydrogen/oxygen fuel cell potential can also be calculated from equation 2.20, below (Barbir, 2006).

$$E = \frac{-\Delta Gf}{2F} = \frac{237340\ \text{J/mole}}{2\times 96485\ \text{A.s/mole}} = 1.23\ \text{V} \tag{2.20}$$

The characteristic performance result of a PEM fuel cell is represented as the polarization curve. It depends on so many factors basing on technical, working and manufacturing properties of the PEM fuel cell. Thickness of the polymer electrolyte membrane, catalyst loading, degree of humidity, design of bipolar plates, flow channels and operating conditions like temperature, pressure and properties of reactant gases are the important parameters which affect the performance of a PEM fuel cell thus the polarization curve.

In PEM fuel cells, potential losses depend on activation polarization losses, ohmic losses and concentration polarization losses which can be seen in Figure 2.3 (Barbir, 2005).

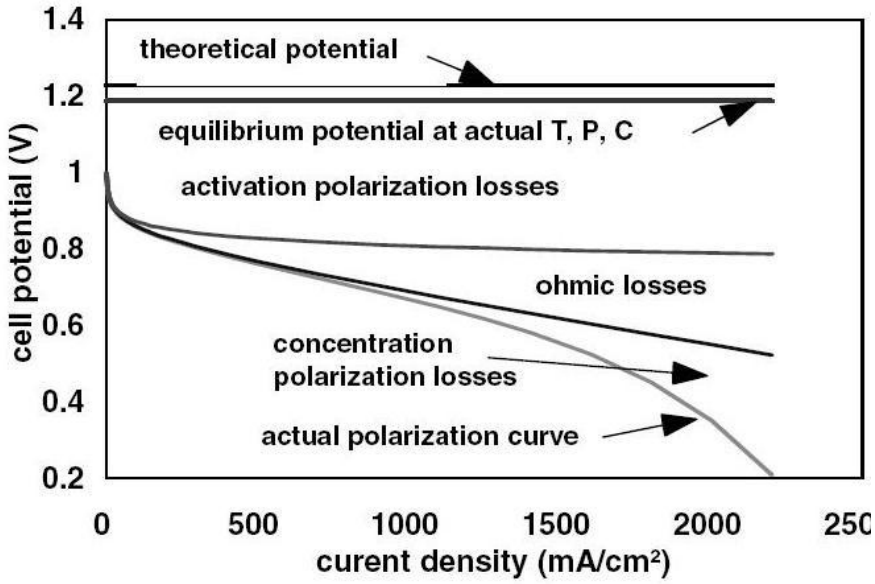

Figure 2.3 Typical polarization curve of a PEM fuel cell

Activation losses occur due to slower reactions taking place on the surface of the electrodes. This results in the loss of some voltage which carries the chemical reactions that transfer the electrons. Ohmic losses are the results of all the resistances within the fuel cell like connecting materials. This results in limiting the transfer of ions through the membrane and catalyst layers. Concentration polarization losses are due to decrease of the reactant concentration on the electrode surfaces.

2.4. Durability of a PEM fuel cell

Durability or endurance of PEM fuel cells has attracted many researchers in recent years. Great deal of research has been dedicated for meeting the Department of Energy (DOE) targets for PEM fuel cells. The life-time of PEM fuel cells is targeted as 5000 h for mobile and 40000 h for stationary applications (Schmittenger and Vahidi, 2008). At this point, there arises the importance of durability of PEM fuel cells which can be stated as the ability of a PEM fuel cell to show resistance against

permanent change in performance over time. This is the most important barrier for a PEM fuel cell to become a commercial product. To make PEM fuel cells commercially viable products, first of all, durability issue should be solved which is based on understanding the degradation reasons and mechanisms followed by recognizing the effects of them to the PEM fuel cell performance.

Durability is a difficult concept to quantify and develop because of the duration of testing times. Required tests should be performed for thousands of hours. This procedure is difficult to perform. Instead of this, to improve the PEM fuel cell durability, components should be tested via simulated fuel cell conditions in shorter times and degradation mechanisms should be well investigated (Borup et al., 2006).

2.4.1 Durability of proton exchange membranes

The durability of membrane is one of the most crucial factors for fuel cells to become commercial products. For PEM fuel cells, widely used polymer is the perfluorosulfonic acid (PFSA) due to its high chemical stability under fuel cell operating conditions (Büchi et al., 2009)

Membranes are used for transferring of protons from anode side to cathode side also prevents the mixing of hydrogen and oxygen. The widespread used proton exchange membrane is Nafion® (perfluorosulfonic acid (PFSA) membrane). It's structure was shown in Figure 2.4.

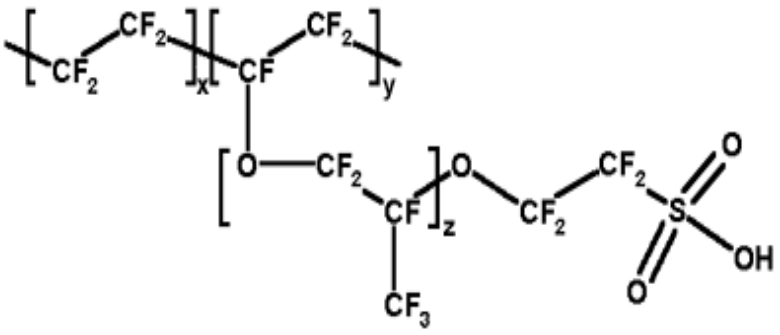

Figure 2.4 Structure of Nafion® membrane

Membrane degradation usually is the results of mechanical, thermal and chemical unstabilities under harsh conditions of the fuel cell (Zhang et al, 2009). Within these mechanisms, chemical degradation is the dominant one. It occurs in two steps. Firstly, due to oxygen reduction reactions, H_2O_2 would be formed. Then, OH^- and OOH^- radicals may be formed from H_2O_2. These radicals will attack the polymer end groups of the membrane. The radical chemical attack is agreed to be an initiator for the membrane degradation. Due to these attacks, in time, membrane gets more and more degredad, then loses its gas permeability function so gas crossover occurs.
Due to mixing of hydrogen and oxygen, more H_2O_2 will be formed within the cell. Membrane degradation due to these radical attacks also is the reason for detecting fluoride (F^-) ion in some amount, in the effluent water. Also, due to unwanted reactions of hydrogen and oxygen not only with each other but also with other reactants will prevent other reactions that should be occuring. With these highly exothermic reactions, released heat will cause hot-spots on the membrane which will then lead to formation of pinholes and after a certain time membrane would lose all its property and fail (Schmittenger and Vahidi, 2008).

Another important reason for the membrane degradation is the membrane dehydration. Membranes should be well-humidified in order not to lose its proton conductive property. Due to decrease in the water content within the cell, proton

conductivity decreases, thus concentration resistances increase leading to voltage and power loss. However, a temporary potential loss in the cell would be accomplished by humidification but for long time operations, dry conditions would cause catastrophic damages in the membrane (Le Canut J. et al, 2009).

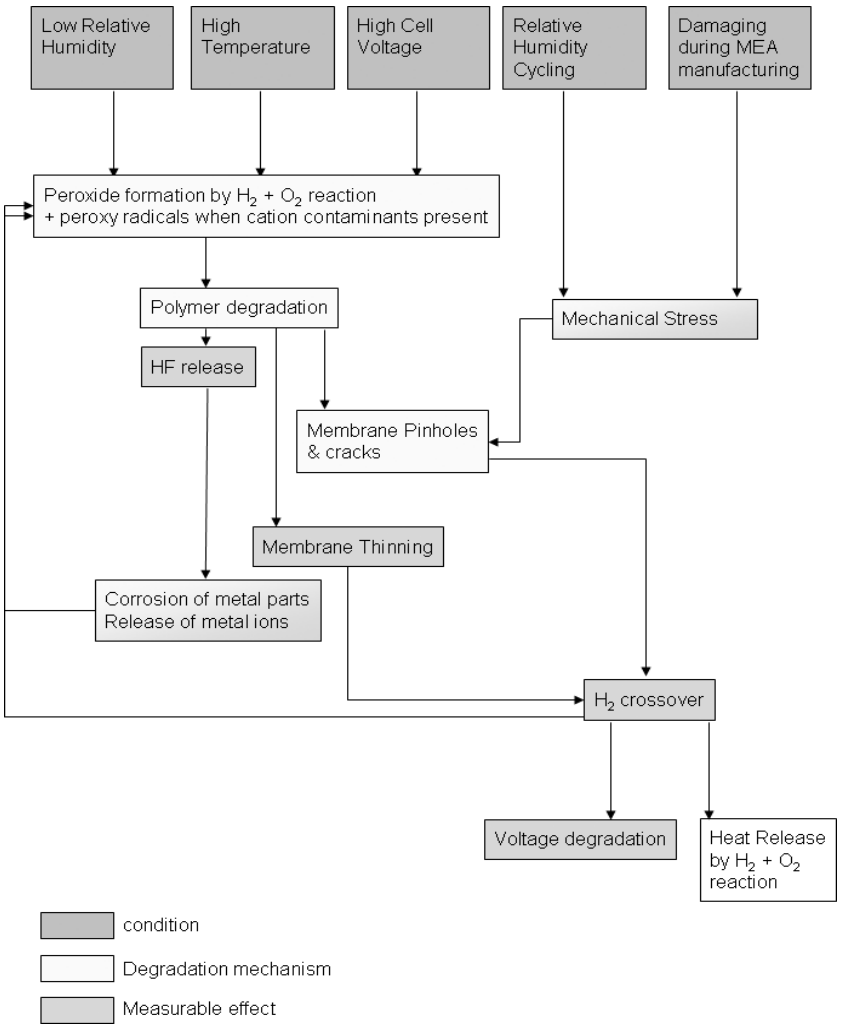

Figure 2.5 Membrane degradation mechanisms, conditions and their results (Bruijn et al., 2007)

2.4.2 Durability of electrocatalyst and catalyst layer

Electrocatalyst and catalyst layer durabilities are another important issues for PEM fuel cells. The most critical property of the catalyst layer is to have an efficient active area because all of the reactions take place on the electrochemical active surface area of the catalyst layer.

PEM fuel cells operate under harsh environments. Anode side catalyst layer undergoes the effects of reducing H_2 atmosphere and on the other hand cathode side is exposed to high oxidized situations under high potentials (Shao et al, 2007). Catalyst failure mostly depends on dissolving of platinum and corrosion of carbon support from the catalyst layer in long periods of operations. Platinum dissolution leads to change in the morphology of the catalyst which causes decrease in the electrochemical surface area of the electrode and corrosion of carbon support occur due to dissolution or loss of carbon particles with platinum particles attached to its surface (Schmittinger and Vahidi, 2008).

Platinum dissolution:

$Pt \longrightarrow Pt^{+2} + 2e^-$ (electrochemical degradation) (2.21)

$PtO + 2H^+ \longrightarrow Pt^{+2} + H_2O$ (degradation by formation of PtO film) (2.22)

Carbon corrosion occurs in three steps:

$C \longrightarrow C^+ + e^-$ (oxidation of carbon) (2.23)

$C + ½\ H_2O \longrightarrow CO + H^+$ (hydrolysis) (2.24)

$2CO + H_2O \longrightarrow CO + CO_2 + 2H^+ + 2e^-$ (gasification to CO_2) (2.25)

The overall reaction is;

$C + H_2O \longrightarrow CO_2 + 4H^+ + 4e^-$ which has potential of 1.2 V. (2.26)

That is the reason of carrying out the carbon corrosion investigation studies at 1.2 V (Ball et al., 2007).

Catalyst layer degradation can be classified into two main parts which are anode corrosion and cathode corrosion. The anode side catalyst does not really play a role in catalyst durability. For the anode side, platinum particle size growth leading to decrease in ESA can be observed only in extended fuel cell operations (Borup et al.,2006).

For the cathode side, it was stated in many studies that, electrochemical surface area (ESA) of the catalyst decreases even for short time operations (Schmittinger and Vahidi, 2008). The decrease in the ESA of the catalyst can be explained by agglomeration, migration and sintering of reoriented or dissolved small platinum particles (Borup et al., 2006).

Potential cycling is one of the main reason of platinum agglomeration resulted with ESA loss. Many studies showed that, as the number of potential cycles increases, the life time and the potential of the cell clearly decrease (Schmittinger and Vahidi, 2008). Secondly, temperature differences during fuel cell operations is another important reason for the catalyst failure. Due to high temperatures, kinetic rates of the reactions increase which results faster growth of platinum particles causes decrease in ESA (Borup et al., 2006). In addition to those, humidification level is another important parameter for the durability of the catalyst. It has a reverse effect on the catalyst rather than the membrane. As the relative humidity of the gases gets lower, particle size growth of the platinum particles decreases so lower humidity values enhances the life time of the catalysts (Schmittinger and Vahidi, 2008).

Bayrakçeken et al (2010) applied the potential cycling test for detecting the morphology change of the PtPd/BP2000 catalysts. Figure 2.6 shows the TEM images for PtPd/BP2000 (2:1) catalyst (a)-(b) before and (c)-(d) after potential cycling test.

The morphology change can be easily detected and as can be seen from the figure that some of the Pd particles left from the surface of the carbon support and also it will surely continue to change under the exposure of longer potential cycles. Since the small particles are not stable, similar results can be obtained for the catalysts having only Pt over the carbon supports.

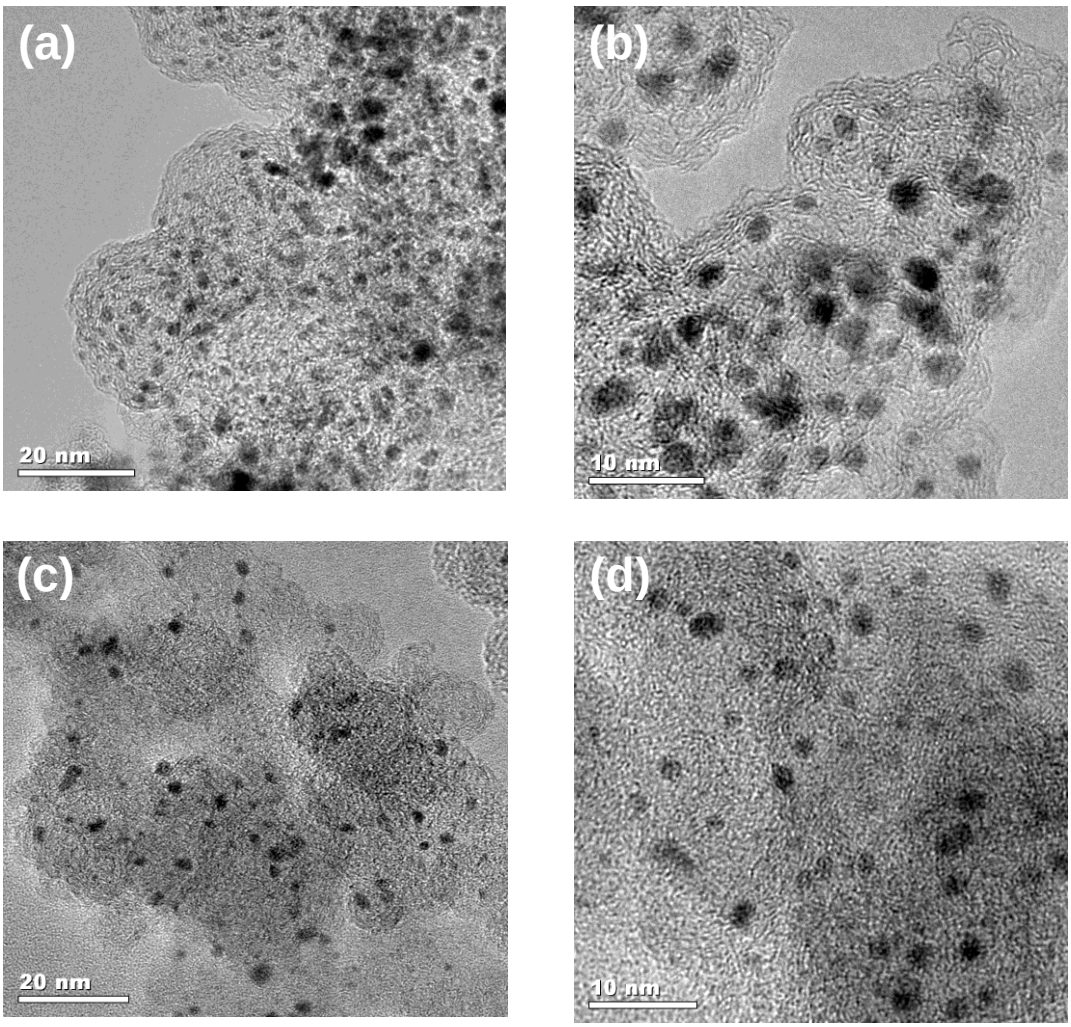

Figure 2.6 TEM images of PtPd/BP2000 (Pt: Pd 2:1), (a)-(b) before potential cycling, (c)-(d) after potential cycling (Bayrakçeken et al., 2010)

2.4.3 Durability of gas diffusion layer (GDL)

A GDL is generally the combination of a thin layer of carbon mixed with PTFE coated on the sheet of macroporous carbon paper. As mentioned before, it is used for permitting the fuel gases to transfer through the catalyst layer. In additon to this, it provides a path for the electrons to be transfered between catalyst layer and bipolar plates. Also it has a crucial role for the management of water. In spite of the fact that, GDL seems to be a minor part of the cell, many researches showed that enhancing its properties would lead to serious improvements in fuel cell operations (Middelman et al., 2003)

Macroporosity of GDL comes from its hydrophobic pores which permits the transportation of gases and hydrophilic pores which permits the transfer of water. The amount of these pores should be balanced in a stable ratio in order to have an efficient mass transfer. Inefficiency of hydrophilic pores will lead to water blockages within the cell which is also called flooding. Due to flooding, water can not be transferred to the membrane, which is very crucial for the membrane in order to provide efficient proton transfer. With lack of proton transfer, surely the performance of the cell will decrease. On the other hand, flooding will cause reactant gas starvation, too. Due to clogging of the pores with excess water, fuel gases can not transfer so critical reactions would not be occur which again leads to performance losses (Zhang et al., 2009).

Besides these failure mechanisms, GDL is mainly composed of carbon and it is a very well known fact that carbon undergoes oxidation within the harsh environment of the PEM fuel cell (Chen et al., 2009).

$$C + 2H_2O \longrightarrow CO_2 + 4H^+ + 4e^- \qquad E= 0.207\ V \qquad (2.27)$$

$$C + H_2O \longrightarrow CO + 2H^+ + 2e^- \qquad E= 0.518\ V \qquad (2.28)$$

2.4.4 Durability of bipolar plates

The function of bipolar plates is to seperate the cells. Also, they provide electronic current between the cell and seperates the fuel gases. They include flow patterns for the reactants and coolants. For bipolar plates, from electric conductivity point of view and for long term operations, the contact resistance is more critical than the bulk resistance (Bruijn et al., 2007). Graphite is the most widely used material for the construction of bipolar plates due to its good corrosion resistance (Hung et. al., 2006).

Metal bipolar plates are mostly covered with some coating materials due to lowering corrosion. In time, deteriorations would occur which indicates the direct contact of the bipolar plate material to the harsh environment of the fuel cell. With lack of corrosion resistance, dissolved metal ions will diffuse to the membrane and kept in the active sites which results a considerable performance loss in the fuel cell. From this aspect, bipolar plates should be coated with different ingredients which have more bonding strength with the substrate material. The other important problem for the durability of the bipolar plates is deformations caused from the compression forces. These forces should be applied in order to have an efficient electric conduction and prevent leakages of the reactant gases. Besides, the operational constraints like thermal cycling, the uniformity of the current or other nonhomogenities related with other components can affect the mechanical properties of the bipolar plates (Wu et al., 2008).

2.5 In-situ durability testing methods on PEM fuel cells

For understanding the durability of PEM fuel cells and the barriers against them, first of all failure mechanisms and their causes should be fully understood. Then tests should be applied to both the fuel cell itself and the components seperately (Zhang et al., 2009).

In situ tests are carried within the environment of PEM fuel cell operating conditions. Performance degradation of PEM fuel cell is observed under long term operations while the fuel cell operation takes place. As mentioned before, long time testings were not preferred by many researchers due to long durations of the tests and higher costs.

Yu et al. (2005) performed a life time test of 2700 h with a commercial Nafion® membrane under a constant current of 300 mA/cm^2. They have searched the parameters which are hydrogen crossover rate and change in electrochemical surface area (ESA). They have found that the H_2 crossover rate increased sharply after 2088 h. They observed an interesting result that, after 300 h testing, the performance of the fuel cell improved. The have stated the main idea behind this result was the increase of the active sites between Nafion and the Pt catalyst because Nafion swells when it first meets with water so its interaction with Pt particles increases. This also can be explained by the increase in the performance at the beginning of the test. In addition to these, they have found that after 1900 h, due to membrane degradation and electrochemical active surface area loss, performance degradation of the cell was clearly observed. Hence, from performance degradation point of view the dominant reason was reported as the hydrogen crossover rather than ESA loss of the catalyst layer.

Cleghorn et al.(2006) performed a single cell PEM fuel cell test which the testing was carried on during 3 years (more than 26000 h). The test was carried on under a constant current of 800 mA/cm^2 . It was interrupted for every 500 h to determine the electrochemical diagnostics which were taken when the open circuit voltage was obtained less than 100 mV. Also, cyclic voltammetry and electrochemical H_2 cross-over measurements were applied to the PEM fuel cell. After the completion of the diagnostic tests, fuel cell was turned into its previous operating conditions and the test was restarted with the same conditions applied before. They have resulted that as the test carried on, the potential of the PEM fuel cell decreased from 0.65 to 0.54

V which was gained from typical polarization curve. Also, they have resulted that the life of the cell was limited due to hydrogen crossover through the membrane. From in-situ cyclic voltammetry tests, they have reached that 66 % of the ESA was lost from the cathode side active catalyst layer.

2.6 Ex-situ durability testing methods on PEM fuel cells

For reducing the testing time and gaining rapid results, researchers and companies such as Ballard Power Systems, Du Pont, General Motors perform different accelerated experiments to the fuel cell components in order to understand the durability of PEM fuel cell components (Wu et al., 2008).

2.6.1 Polymer electrolyte membrane accelerated degradation tests

Basing on several experimental studies, membrane degradation would be mainly based on some parameters like, temperature, humidification level and sudden start-up and shut-down operations. These will be the stressors that are applied during accelerated durability tests of the membrane (Zhang et al., 2009).

Fenton test is the most widely used test for searching the membrane durability. It mainly detects the chemical stability of the membrane by keeping it under Fenton's reagent which is comprised of H_2O_2 solution with some ppm level of Fe^{+2}. Membrane is kept in this solution at 90°C for detecting the F^- ion release amount. With this technique, OH^- and OOH^- radicals are formed within the solution like in PEM fuel cell operations and the amount of degradation of membrane can be observed. As mentioned before, these radicals will attack the polymer end groups of the membrane and in time membrane loses its properties (Chen et al., 2007).

Tang et al. (2007) studied on Nafion membrane by keeping it in 30 % wt. H_2O_2 solution with 12.3 ppm Fe^{+2}, 6.1 ppm Cr and 5.4 ppm Ni. They have analyzed the

solution every 30 min and replaced it by fresh solution. Solutions were analyzed in atomic absorption spectroscopy and they have found 3.6 % weight loss in the membrane due to F^- ion release. The other test performed by the same group were relative humidity (RH) cycling. They tried to understand the effect of relative humidity of the fuel gases from membrane durability point of view. From this aspect, they have put the samples of commercial Nafion membrane into the bottles which have 0.1 M of H_2SO_4 solution and kept them for 1000h. Dry, the humidity level of air and saturated humidity conditions were applied to the bottles, respectively. The bottles were fed with same amount of H_2 and O_2. After testing, the samples were analyzed with FTIR. From FTIR analysis, Nafion shows the main peaks of interest after different times of exposing the Nafion with O_2 and H_2 under the mentioned humidity conditions. This established the stable chemical structure of Nafion under long time exposure of fuel gases. To sum up, they have resulted that the membrane degradation mainly depends on decomposing of the polymer end chains under the environment of radicals rather than exposing the membrane to weak relative humidity conditions.

2.6.2 Platinum catalyst accelerated degradation tests

For Pt catalyst, the accelerated degradation tests mostly include, thermal degradation tests, aging in aqueous media, OCV (open circuit voltage) operations and electrochemical degradation under simulated PEM fuel cell environment (Shao et al., 2007).

Dam and Bruijn (2007) performed an experiment for identifying the effect of temperature and potentials on platinum dissolution by exposing the platinum film into 1 M $HCIO_4$ solution. They have concluded that the platinum dissolution rate was not considerable below 40°C. As the temperature increases from 60°C to 80°C, they have detected that the dissolved platinum amount increased from 0.87 ng/h.cm^2 to 1.58 μg/h.cm^2 under the potential of 1.15 V.

Electrochemical aging under simulated fuel cell environment is the most widely used test. An aqueous acid solution is used instead of Nafion which acts as the proton conductor media. Generally, constant potential is applied in the potential range of cathode which is similar to PEM fuel cell operations. Also, cycling is carried out within a potential region of oxidation and reduction reactions of PEM fuel cell. This experiment is carried by three-cell electrode system and the method is called cyclic voltammetry (Shao et al., 2007).

Cyclic voltammetry tests basing on potential cycling and support durability at 1.2 V were reported as the most efficient and trustworthy experiments for understanding the degradation mechanisms of both the platinum catalyst and the support (Gasteiger et al., 2006).

Wang et al. (2007) studied platinum degradation tests on two catalysts having different supports of Vulcan XC-72 and BP-2000. They have taken an initial cyclic voltammogram and final cyclic voltammogram after 1200 cycles at 50 mV/s scan rate in 0.5 M $HClO_4$ solution, between 0.6 V and 1.2 V potential range, at room temperature. This test was carried out to investigate the change in the electrochemical surface areas of the catalysts before and after the degradation tests. After these tests, for both catalysts, the ESA losses were detected. For further accelerated degradation, both catalysts were also tested under same conditions but for 10000 cycles. Initial and after 10000 cycles, voltammograms were taken for both catalysts and 20.6 % ESA loss was found for Pt/Vulcan XC-72 and 40.9 % for Pt/BP-2000. The highest ESA loss for Pt/BP-2000 was depending on lower corrosion resistance of this catalyst.

2.6.3 Carbon support accelerated degradation tests

Carbon is the most videly used material as the support of platinum catalyst. A support material should have high surface area and catalytic activity. Carbon undergoes oxidation at the potentials which the oxidation-reduction reactions of the cathode side are occurring (Wang et al, 2007).

Carbon oxidation proceeds into two mechanisms which are formation of surface groups as a result of incomplete oxidation and formation of CO_2 with complete oxidation. Direct carbon oxidation happens above 1V so in cycling experiments at potentials below 1 V, the main influence of the carbon corosion is platinum. Below 1V, platinum is reacted with water and formed Pt-OH adsorbed intermediate species. These intermediate species will cause carbon corrosion shown in the mechanism given in 2.29, below (Merzougui and Swathirajan, 2006).

$$Pt\text{----------}OH + C \longrightarrow C(OH) + Pt \qquad \text{(between 0.6-1 V)} \qquad (2.29)$$

Wang et al. (2007) stated that the corrosion of Vulcan XC72 can be observed by keeping the catalyst under constant potential of 1.2 V. They have resulted that carbon corrosion occurs due to surface oxide formations caused by quinone- hydroquinone redox couples formed on the surface of the carbon support. The mechanism was shown in 2.30, below.

$$C = O + e^- + H^+ \longleftrightarrow C - OH \qquad (2.30)$$

Ball et al. (2007) performed a potentiostatic corrosion experiment on commercial carbon supports. Experiments were carried out within a temperature range of 20°C to 80°C. Samples were kept at 1.2 V for 24 h. Cyclic voltammograms were analyzed before and after aging tests for detecting the double-layer capacitance and carbon

corrosion due to quinone-hydroquinone couples which were active at around 0.6V. They have resulted that carbon corrosion increases with increase in the temperature.

Wang et al. (2007) studied the corrosion of carbon support on Vulcan XC-72 and BP-2000 supports by applying them a fixed potential of 1.2V at room temperature. They have kept both of the supports for 0, 24 and 120h in 0.5 M H_2SO_4 solution at 10 mV/s scan rate. They have observed the carbon corrosion peaks at around 0.6 V due to surface formations of hydroquinone and quinone redox species. For both supports carbon oxidation peaks gets wider as the experiment duration increased.

Kangesniemi et al. (2004) performed another experiment basing on extending the potentiostatic hold of widely used commercial carbon support Vulcan XC72. Experiments were carried out in 1 M H_2SO_4 solution and the samples were kept under 1.2 V potentiostatic hold for 0, 16, 60 and 120 h. The characteristic anodic peak resulted from carbon corrosion around 0.6V got more pronounced with increasing potentiostatic hold durations. Same group also performed a similar experiment at 65°C to have more realistic PEM fuel cell conditions. This time samples were kept for 16 h at 0.8, 1, 1.2 V potentials. They have found that as the potential increased from 0.8 to 1.2 V, the anodic peak resulted from carbon corrosion appears more vividly. Also, they have observed that temperature enhanced carbon corrosion because the peak gained after 16 h hold at 1V at 65°C is nearly twice the peak gained with the same conditions but at room temperature.

2.6.4 Gas diffusion layer accelerated degradation tests

As mentioned before GDL is the component between the flow field and the catalyst layer which has crucial functions. It allows the fuel gases transfer through the catalyst layer. Also, it builds an electron pathway between catalyst layer and bipolar plates. GDL is a very important component for balancing the water management within the cell.

Researchers mainly performed ex-situ tests rather than in-situ tests for gas diffusion layers to eliminate the adjoining effects caused by other components of the fuel cell (Zhang et al., 2009).

Frisk et al. (2004) performed an experiment by submerging the gas diffusion layer into H_2O_2 solution for simulating the environment of PEM fuel cell and detected the weight loss.

2.7 Cyclic Voltammetry

Cyclic voltammetry is an electrochemical potential controlled technique which the potential sweep is applied on a working electrode and current is observed. Observing the current response is a good way to understand the thermodynamics and mechanisms of chemical reactions occurring between the electrode surface and the proton supply solution (usually an acidic solution). For cyclic voltammetry experiments, a potentiostat system is used by which the control parameters are set which are scan rate, total sweeps and potential range. The function of the potentiostat is to apply a potential within a selected potential range and to show the taken current in a current vs. potential curve (David and Gosser, 1993).

Current is generated on the surface of the working electrode by the transfer of electrons to the redox species. All these mechanisms occur by transporting of ions

within an acidic solution. The electrode solution interphase is the main part of interest where the oxidation and reduction reactions occur so the behavior of the electrode surface should be examined in detail. When a potential is exposed to the electrode surface, first of all, electrode develops a charge on its surface. Then, excess of ions localize near to the surface of the electrode to neutralize it. The mentioned mechanism was represented in Figure 2.7, below.

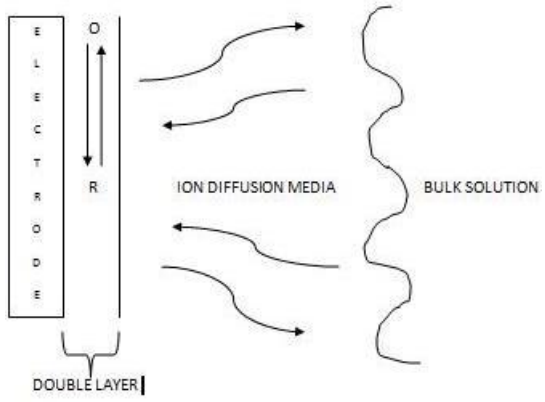

Figure 2.7 Electron transfer between the electrode surface and the bulk solution

Current on the surface of the electrode is generated by the electron transfer carried by redox species. All the species is in a solution so current is generated by the transfer of these ions to or from the surface of the electrode. There are two different currents generated on the surface of the electrode in cyclic voltammetric experiments. These are capacitive and faradaic currents. Faradaic current is the dominant one because capacitive current is occurring when there is no redox species in the solution. That's just generated as the solution electrode interphase acts as a capacitor.

Capacitors are the parallel plate electric conductors separated by an insulator and capacitance is the ability of the conductors to store energy. When a potential

difference is applied between the conductors, a static electric field is developed between the conductors which stores energy. In cyclic voltammetry, it can be thougt that the electrode surface and the solution surface are two conductors. When a potential difference is applied, ions transfer to the electrode surface and accumulate there. This ion accumulated layer is termed to be an insulator like in capacitors and called double layer in cyclic voltammetry point of view. As the potential of the electrode is varied, ions begin to transfer to the surface of the electrode. Due to this movement a theoretical layer is formed just on the surface of the electrode which is called double layer. This capacitor model is used for describing the electrochemical systems. The charge on the capacitor can be described basing on the potential loss across the capacitor.

$$Q = C.\ E \tag{2.31}$$

Taking the derivative of the equation gives equation 2.32 shown, below.

$$\frac{dQ}{dt} = C\,\frac{dE}{dt} \tag{2.32}$$

$\frac{dQ}{dt}$ is the definition of current (i) so capacitive current can be written as in equation 2.33, below.

$$i = C.v \tag{2.33}$$

Faradaic current occurs when there are active redox species in the solution. It depends on both the kinetics of the electron transfer and and the diffusion rate of the redox species to the electrode surface. The concentration of the redox species on the electrode surface can be described by Nernst equation, shown in 2.34, below. Basing on the fact that, the reaction occuring on the surface of the electrode is reversible, it can be written as below.

$$Ox + e^- \rightleftharpoons Red$$

$$E = E^0 - 0.0592 \log\left(\frac{B}{A}\right) \quad (2.34)$$

where A and B represents the concentrations of oxidized and reduced redox species, respectively. E is the applied potential at that time and E^0 is the standard electrode potential.

Due to Nernstian behaviour of the electrode surface, as the applied potential decreases, the concentration of A (oxidized species) should decrease leading to reduction. If the potential increases, the concentration of B (reduced species) should decrease.

Before a potential is applied to the system, there is no concentration change on the surface of the electrode because as mentioned before redox species accumulate on the surface of the electrode when the voltage is applied. As the potential gets negative, concentration of the oxidized species begin to decrease on the surface of the electrode according to Nernstian behaviour. Due to Fick's Law of diffusion, as the concentration of the oxidized species decreases on the surface, the concentration gradient between the surface and bulk solution increases so the flux of the oxidized species from bulk solution to the surface of the electrode will increase. This brings a higher cathodic current (shown as i_{pc} on Figure 2.8).

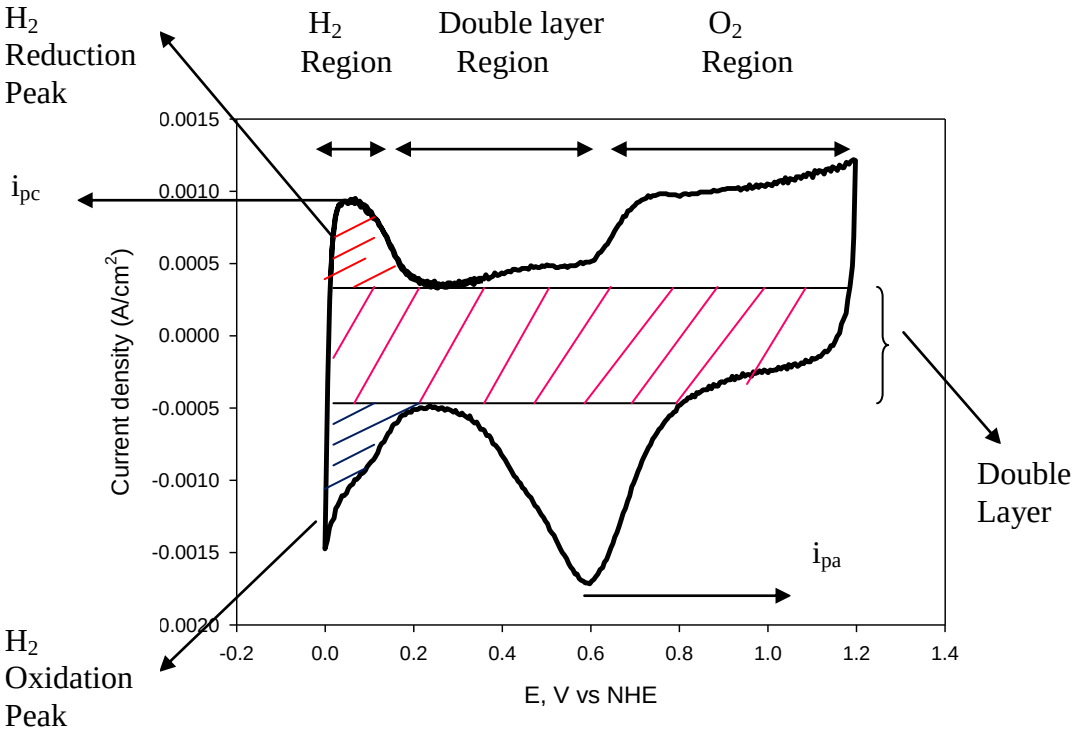

Figure 2.8 Typical shape of a cyclic voltammogram adapted to Nernstian behaviour

As the potential gets more negative, the oxidized concentration on the electrode surface will finally become zero. This is the maximum point of the i_{pc} curve. As the oxidized concentration on the electrode going to zero the concentration in the bulk solution decreases, too, leading the concentration gradient to decrease. As the concentration gradient decreases, the current begins to decrease till the turning point. After the reverse scan begins, the potential begins to increase leading to increase in the concentration of oxidized species on the electrode surface but still the concentration gradient decreases so the current continues to decrease till the point E_0. At this point due to Nernst equation, concentration of oxidized and reduced species on the electrode surface become the same. As the potential increases, the concentration of the oxidized species increases both on the surface of the electrode

and the solution so the concentration gradient begins to increase leading the current to increase. The maximum current in the reverse cycle is called the anodic current showed as i_{pa} in Figure 2.8. Again like in cathodic region, the concentration of oxidized species finally becomes zero thus the concentration in the solution, too. Due to decrease in the concentration gardient, current begins to decrease and the cycle is completed.

2.8 Rotating Disc Voltammetry

Rotating disc voltammetry is another type of analysis which can be gained besides cyclic voltammetry in potentiostat. The working electrode used in cyclic voltammetry experiments is attached to a motor. While the cyclic voltammetry proceeds the motor does not work but for rotating disc voltammetry experiments working electrode rotates at different angular velocities. The most important advantage of the rotating disc voltammetry is that the rotation makes the solution to move in a steady flow which the solution firstly pulled upward and then thrown downward with the movement of the rotator.

The main important barrier against efficient contact of ions with the working electrode surface is the stagnant film. It occurs when the electrode contacts with the solution at the first time. With rotating disc voltammetry, the thickness of the stagnant layer gets thinner as the speed of the rotator increases, allowing the ions transfer to the electrode surface more easily. That's why for rotating disc voltammetry experiments, the current increases as the velocity of the rotator increases.

The other advantage of the RDE testing technique is that the steady state conditions are drawn quicker which depends on faster mass transfer to the electrode surface by diffusion than stationary electrode. It can be said that the RDE system is a convective system which the hydrodynamic and convective-diffusion equations are solved together.

The current density gained on the surface of the electrode basing on the thickness of the stagnant layer can be found as shown below. Also, the current density felt on the surface of the electrode directly depends on the diffusion of the reactants so the relation can be also based on Fick's Law of diffusion.

$$i_d = n.F.\frac{D}{\delta RDE} . c_0 \quad (2.35)$$

Where i_d represents current density, n is the number of electrons on the surface of the electrode, F is the Faraday constant, D is the diffusivity constant of the reactant in the present electrolyte and c_0 is the bulk concentration of the reactant.

The thickness of the stagnant layer where the diffusion takes place can be found via Navier Stokes equation. The thickness of the stagnant layer between the surface of the electrode and the bulk solution can be calculated by using the equation 2.36 below.

$$\delta_{RDE} = 1.61. v^{1/6}. D^{1/3}. \omega^{-1/2} \quad (2.36)$$

Where v is the kinematic viscosity of the electrolyte solution and ω is the rotation speed of the electrode in the unit of (rad/s). Substituting equation 2.36 into 2.35 gives the relation called *Levich equation*.

$$i_{d,RDE} = 0.620. n. F. D^{2/3}. v^{-1/6}. c_0. \omega^{1/2} \quad (2.37)$$

In equation 2.37, all the parameters except rotation speed are substituted by the Levich constant B so it can be rewritten as in equation 2.38, below.

$$i_{d,RDE} = B. \omega^{1/2} \quad (2.38)$$

This equation leads to find the current density related with diffusion. There is also another current which is formed kinetically on the surface of the electrode. From this aspect, current density can be written as in equation 2.39, below.

$$\frac{1}{\mathrm{i}} = \frac{1}{\mathrm{ik}} + \frac{1}{\mathrm{B}.\omega^{1/2}} \qquad (2.39)$$

From RDE(rotating disc electrode) experiments, Koutecky-Levich plot is obtained by drawing the plots of $\frac{1}{i}$ versus $\frac{1}{\omega^{1/2}}$. The relation should be linear and the slope gives the Levich constant. From this, n, the number of electrons transferred per unit mole of oxygen can be found.

Merzougui and Swathirajan (2006) performed cyclic voltammetry and rotating disc voltammerty tests on both supported platinum and nonsupported platinum catalysts. First, they have tried 500 cycles on different platinum loaded catalysts which had 46.5 %, 47.7 % and 30 % platinum. They have found that the ESA decreased for all of them but the highest ESA was gained from 30 % Pt catalysts. On the other hand, the degradation parameter is nearly 25 % higher for 30 %Pt loaded catalyst than the others. The initial higher ESA at lower platinum loaded catalysts may be due to good dispersions of smaller platinum particles but the highest degradation rate of the lowest platinum loaded catalyst may depend on platinum sintering and agglomeration due to carbon corrosion.

CHAPTER 3

EXPERIMENTAL

3.1 Materials

For catalyst ink preparation, catalysts (Tables 3.1, 3.2 and 3.3) or Vulcan XC72 (Cabot) were used for testing. Deionized water and 1,2 propandiol (Sigma-Aldrich %99.5) were used as solvents. Nafion solution (%15, Ion Power Inc.) was used for building a network within the catalyst layer for transferring of protons.

For cyclic voltammetry and rotating disc voltamettry tests, KCI (Sigma) and $HCIO_4$ (%70, Sigma) were used for making 0.1 M KCI solution for reference electrode and 1 M $HCIO_4$ solution to act as proton conducting media.

3.2 Catalyst ink preparation

In the experiments, all catalyst inks were prepared by 1 ml of 1, 2 propandiol, 1 ml of deionized water, Nafion solution (%15) and required amounts of Pt/C catalysts depending on its Pt loading on carbon support. Components should be added in the order of catalyst, water, 1, 2 propandiol and finally Nafion solution. After that, catalyst ink was kept in ultrasonic bath (Bandelin Sonorex) for 1 hour and in addition to this for better mixing and homogeneity, catalyst ink was continued to be mixed in homogenizer (Ultra-Turrax IKA T25 Digital) for 5 min. after ultrasonication.

3.3 Loading of the catalyst ink on the electrode surface

Catalysts are applied as an ink form in PEM fuel cell operations as well as cyclic voltammetry (CV) tests. In PEM fuel cells, catalyst ink is sprayed on the gas diffusion layers which are generally a carbon paper or a cloth. In cyclic voltammetry tests, the prepared ink is deposited on the glassy carbon part of the working electrode (Figure 3.1) which has a surface area of 0.1963 cm^2. The Pt loading on the GC electrode was set to 28 $\mu g/cm^2$ for all inks.

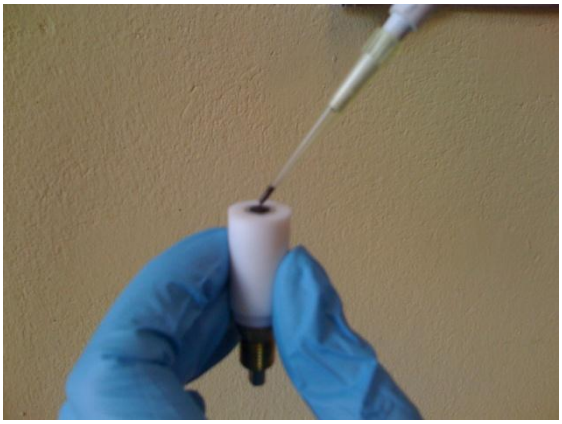

Figure 3.1 Loading on the GC (glassy carbon) electrode

The 2 µL of the ink is taken by micropipette and loaded on the GC (glassy carbon) electrode. Glassy carbon electrode should not contain any scrathes. If there is a scratch then it has to be removed by using 0.5 micron alumina. Afterwards, the deposition of the catalyst ink should be done. The homogeneity and well distribution of the catalyst ink on the electrode surface is very crucial for reproducible results.

After deposition of the ink, electrode was left in room temperature overnight for drying.

3.4 Cyclic Voltammetry (CV)

CV is a very useful technique in order to determine the real electrochemical surface area of the catalysts. The CV set up is given in Figure 3.1 and Figure 3.2 (Pine Instrument Company, Grove Cty, Pennsylvania 16127, Bipotentiostat Model AFCBP1). CV analyses were carried in a three electrode electrochemical cell system, which is composed of working, reference and counter electrodes.
Working electrode (WE) is the electrode where the reactions of interest are taking place. It is mainly made up of glassy carbon surrounded by Teflon. The catalyst ink is deposited on GC electrode.

Reference electrode (RE) is usually made up of Ag/AgCI electrode filled with KCI solution. Its main function is to detect if the applied potential at the electrode surface is gained. Ag/AgCI electrode contains the Ag metal wire and its AgCI salt.

Counter electrode (CE) is made up of platinum wire and its function is to control if the potential difference between the reference electrode and the working electrode is the potential that is applied. Reference and counter electrodes were shown in Figure 3.2, below.

Figure 3.2 Reference electrode (RE) (left) and counter electrode (CE) (right)

The importance of these electrodes is to keep the electrode neutralized. If the measured potential at the working electrode is not the potential that is applied then the potential is adjusted by increasing or decreasing it. The reaction occurring at the working electrode should be the same as in counter electrode but to the opposite direction. This means if reduction takes place on the surface of WE then oxidation should take place in CE.

RE acts as a reference to the potential applied to the WE. The applied potential should be enough to oxidize or reduce the species of interest (Pt, carbon) on the surface of the WE. The required potential is determined by removing or adding an electron to or from the species on the GC electrode. The adjustment of the potential is due to this electron transfer within the solution because the potential is applied by an external source (potentiostat).

RE allows a redox reaction that will accept or release of the electrons to the electrolyte. The reaction is shown below.

$$Ag \rightleftharpoons Ag^{+} + e^{-} \qquad (3.1)$$

At this point, KCI solution is used by the electrode. It has K^{+} and CI^{-} ions. If the reaction goes to the right side K^{+} ion is released to the electrolyte and if it goes to the left side CI^{-} ion is released to preserve the neutrality of the electrolyte.

These three electrodes are placed in a glass reactor having a proton rich solution (1 M $HCIO_4$ solution). Also, the glass reactor allows the entrance of nitrogen and oxygen gases while the experiment is taking place.
Before starting the tests, the glass electrochemical cell was filled with 0.1 M $HCIO_4$ solution, a double junction reference electrode compartment was filled with 0.1 M KCI solution. All three electrodes were placed in the electrochemical cell.

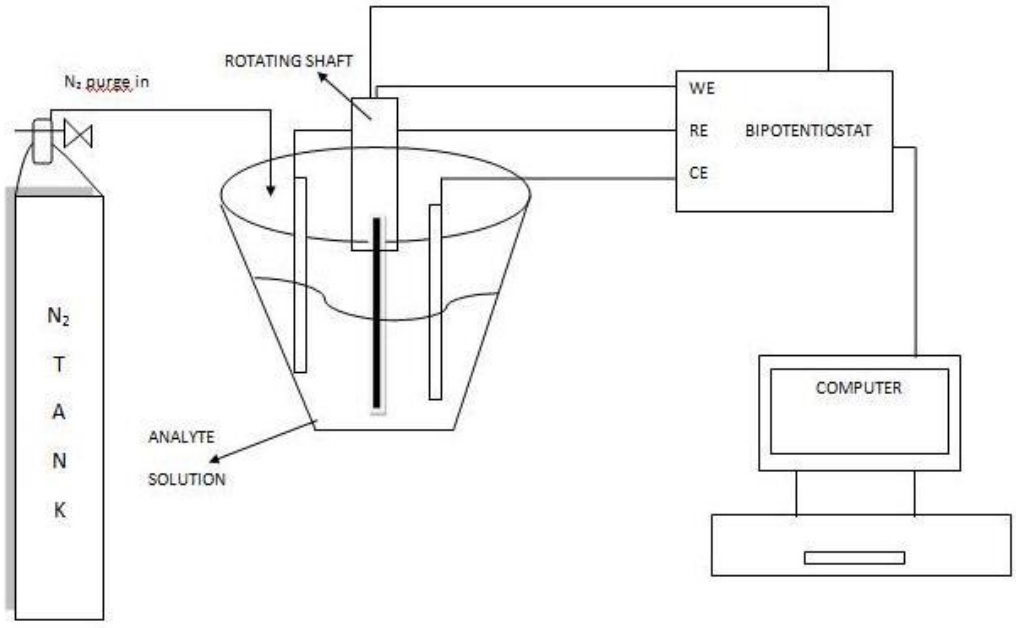

Figure 3.3 Schematic representation of three electrode cell configuration connected to bipotentiostat

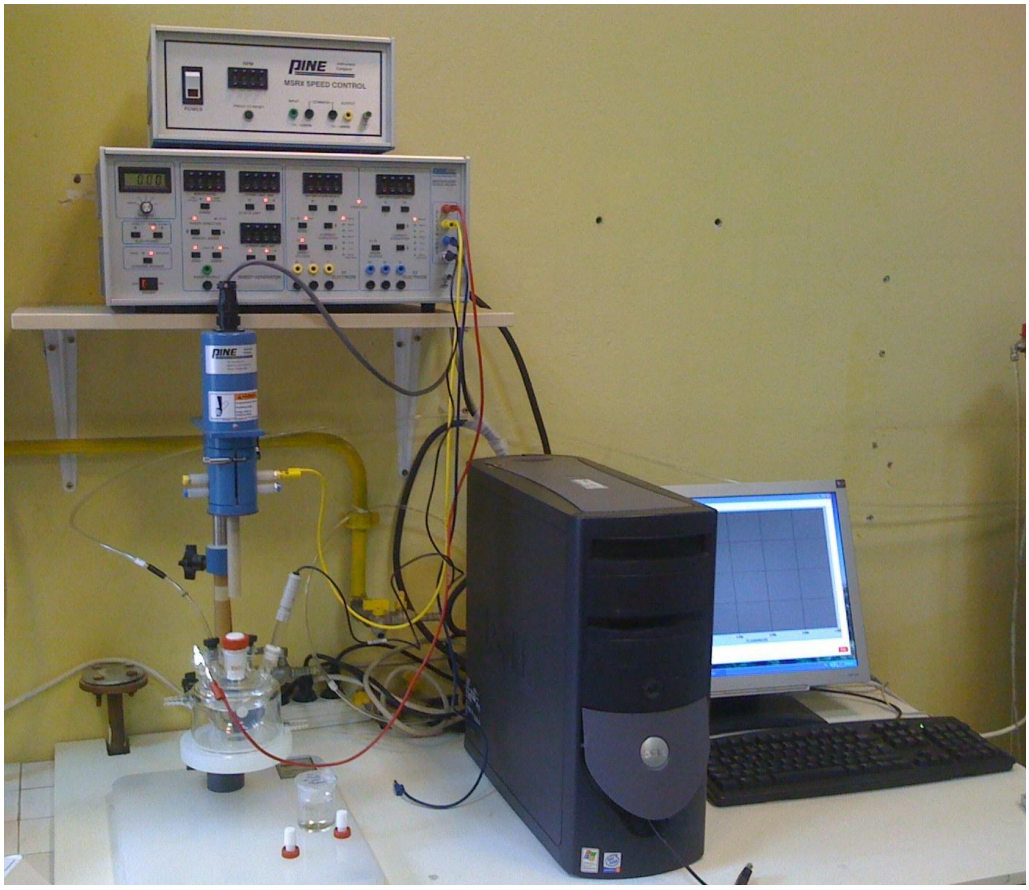

Figure 3.4 Experimental set-up for cyclic voltammetry

3.5 Procedure to get a cyclic voltammogram

1. The potentiostat is opened.
2. The software that is used is opened on the computer.
3. Parameters set are: scan rate, total sweep, potential range
    - Scan rate: The electrode potential ramps linearly versus time which is known as the experiment's scan rate (V/s).
    - Total sweep: Number of the linear sweeps.
    - Potential range: The range between the initial and final potentials that the linear sweeps start and end.

4. After setting the parameters, the potential was cycled.
5. The data taken after the cyclic experiment a voltage-current relation is taken which means the response current taken due to applied potential range (Chapter 2, Figure 2.8).
6. The scan is made within a given potential range forwards and backwards. For example 1 cycle (2 sweeps) for the potential range of 0-1.2V is set. For the forward scan, the CV is taken from 0 to 1.2 V. After turning point, the cycle reverses and the CV continued to be taken from 1.2 to 0 V and the cycle is then completed. For repeated cycles, for example for 100 cycles (200 sweeps), the scan is taken for 100 times within given potential range.

3.6 Accelerated Aging Test Procedures

3.6.1 Platinum dissolution test

Most of the PEM fuel cell catalysts are made up of platinum supported on carbon. Platinum is the crucial part of the catalyst on which the reactions of interest are taking place. Commercial and already prepared catalysts were tested by cyclic voltammetry and rotating disc electrode techniques.

In the procedure, HOR and ORR were investigated via cyclic voltammetry and rotating disc voltammetry experiments. The main idea on observing both the Pt dissolution and carbon corrosion is based on observing the situations of the catalysts before and after aging periods. That’s why the procedure is splitted into two parts which are before platinum dissolution and after platinum dissolution.

3.6.2 Carbon corrosion test

Most of the PEM fuel cell catalysts are made up of platinum supported with carbon. Besides platinum dissolution, carbon corrosion is another crucial factor for limiting the durability of the catalyst layer. Tested commercial and already prepared catalysts were all made up of platinum supported with commercial carbon, Vulcan XC-72. For all the catalysts after platinum dissolution tests, new electrodes with the same ink compositions were prepared and the carbon corrosion tests were applied.

In testing procedure, like in platinum dissolution experiments, cyclic voltammetry and rotating disc voltammetry experiments were performed together. As like in platinum dissolution tests, carbon corrosion tests were splitted into two parts which were based on searching before and after situation of the catalysts from carbon corrosion point of view.

3.7 Rotating Disc Voltammetry Tests

As mentioned before experiments were performed in both cyclic voltammetry and rotating disc voltammetry. The schematic representation of rotating disc voltammetry can be seen in Figure 3.2. For this purpose, GC electrode was embedded into a rotating shaft and connected to a speed control device. All rotating disc voltammetry tests were carried out in O_2 environment.

The results taken from RDE experiments would give us the potential losses of the catalysts after degradation tests (from Tafel plots). Also, the number of electrons transferred per mole of O_2 (from Koutecky-Levich plots) can be found. This is another important parameter which shows if the reduction of O_2 leads to H_2O_2 formation or H_2O formation.

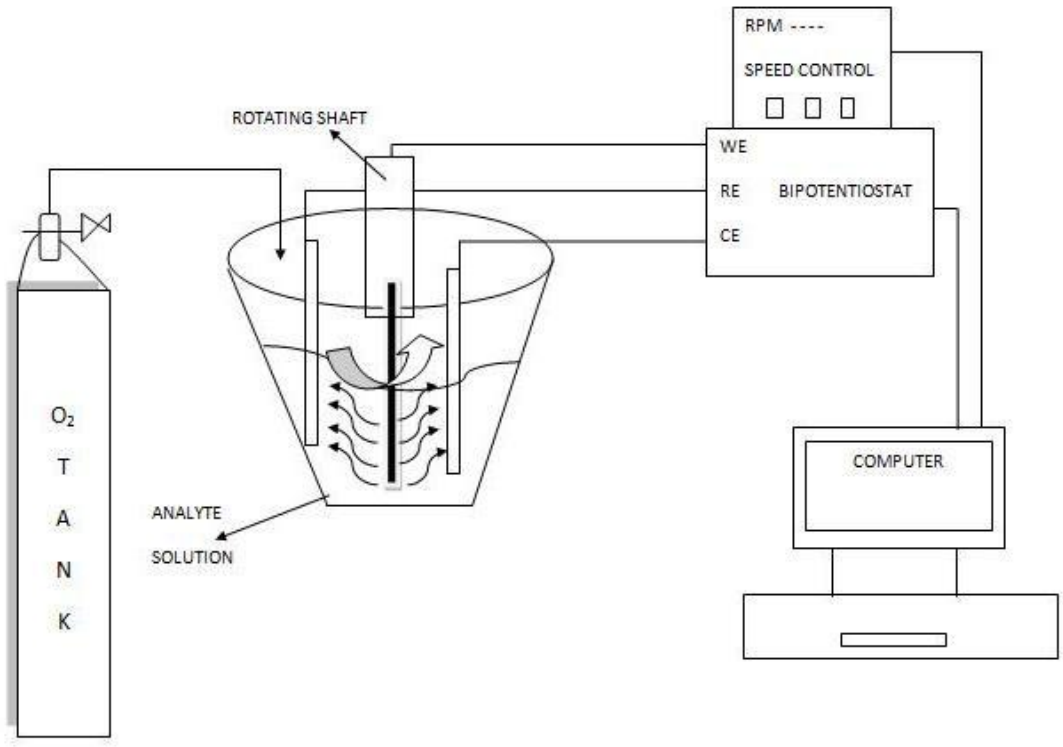

Figure 3.5 Schematic representation of rotating disc voltammetry experimental set-up

For both carbon corrosion and platinum dissolution testing procedures, ORR was investigated via RDE (rotating disc electrode). For each procedure, ORR was investigated for 100, 400, 900, 1600 and 2500 rpm angular velocity values at a scan rate of 5 mV/s between 0-1.2 V potential range and taken for 1 cycle before and after the degradation tests. The voltammograms were used to obtain the electrochemical surface area, tafel slopes, number of electrons transferred per oxygen molecule of the related catalyst for before and after aging tests.

3.8 Scope of the experiments

Electrochemical characterization methods including cyclic voltammetry and rotating disk voltammetry techniques were used in order to determine the long term stability of the commercial catalysts (having different Pt loadings) and the catalysts synthesized by microwave irradiation technique. These catalysts were prepared by using polyol process in which the reduction was achieved by microwave irradiation. The details were given, elsewhere (Bayrakçeken, 2008, Güvenatam, 2010). Briefly, a domestic microwave oven was used during the experiments. The polyol environment was provided by ethylene glycol. Hexachloroplatinic acid, Vulcan XC72 put into ethylene glycol and the pH is adjusted with the addition of KOH (1.4, 6.25 and 10). The microwave duration was also changed between 50s-120s.

Average particle sizes for platinum were calculated from Scherrer equation shown below.

$$t = \frac{K\,\lambda}{B\cos\theta} \tag{3.2}$$

Hydrogen oxidation and oxygen reduction reaction activities of the catalysts were investigated before and after the aging tests. Pt dissolution and carbon corrosion of the catalysts were investigated. During Pt dissolution tests potential was cycled in between 0-1.2 V and 0.6-1.2 V for several cycle numbers. Carbon corrosion of the catalysts was investigated by holding the potential at fixed potential of 1.2 V. Hydrogen oxidation and oxygen reduction reaction activities before and after these Pt dissolution and carbon corrosion aging tests were evaluated to determine the stability of the catalysts. The tested catalysts were shown in Tables 3.1, 3.2, below.

Table 3.1 Tested commercial catalysts (Platinum on Vulcan XC72)

Catalysts	Nominal Pt (%)	Average Particle size (nm)
ETEK Pt/V	20	2.6
X Pt/V	50	2.4
Y Pt/V	70	3.2

Table 3.2 Catalysts synthesized by microwave irradiation technique (Platinum on Vulcan XC72)

Catalysts number	Nominal loading (wt %)	Catalysts synthesis pH	Microwave duration (s)	Average Particle size (nm)
1	20	1.4	50	4
2	20	6.25	50	3.9
3	20	10	50	3.3
4	20	1.4	60	4.6
5	20	1.4	120	5.7
6	32	1.4	120	3.4
7	44	1.4	120	4.2

The testing procedures were given in Figure 3.7. The preparation of the catalyst ink, it's loading and drying steps were mentioned. After the catalyst ink was dried on the surface of the GC electrode, one of the aging tests (Pt dissolution or carbon corrosion) begins. For understanding the situation of the catalyst before aging, first of all HOR test procedure was applied and the CV of the catalyst was taken under given conditions. After that, ORR test procedure was applied and the ORR activity of the catalyst was analyzed before aging tests.After these observations, one of the aging tests (Pt dissolution or carbon corrosion) was performed on the catalyst under given conditions. The situations of the catalysts after aging tests were determined by applying firstly HOR then ORR test procedures.

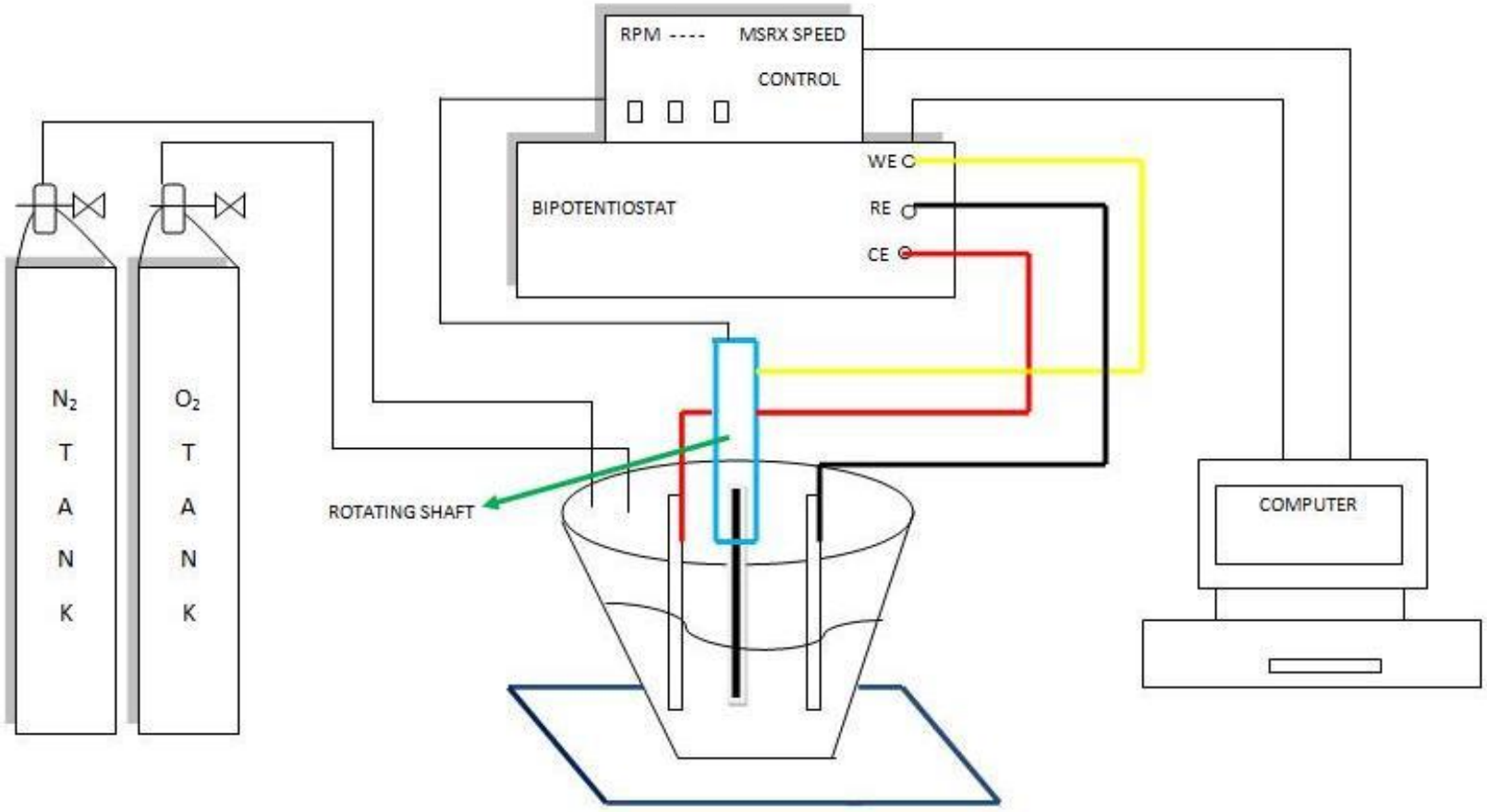

Figure 3.3 Experimental set up (both cyclic voltammetry and rotating disc voltammetry)

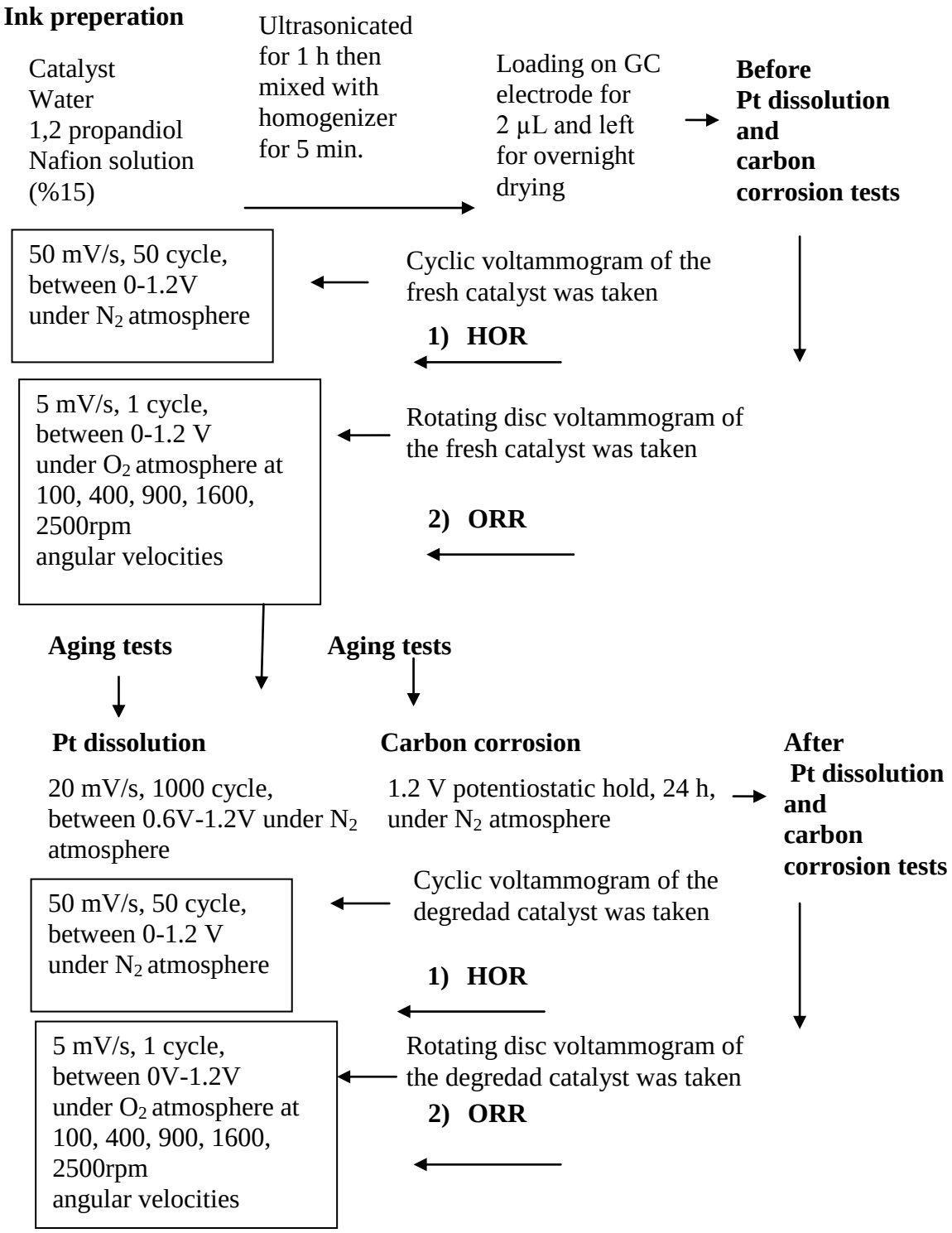

Figure 3.7 Experimental procedures for cyclic voltammetry and rotating disc voltammetry

CHAPTER 4

RESULTS AND DISCUSSION

4.1 Data Analysis for the Results of Cyclic Voltammetry and Rotating Disk Voltammetry Techniques

The data obtained from the CV and RDE tests were used to determine the properties of the catalysts before and after aging tests. These properties that are investigated are listed below.

- The real electrochemical surface areas (ESAs)
- Pt utilization
- Carbon corrosion
- Potential losses due to Tafel plots

All these properties were observed before aging tests and after aging tests. The aim is to determine how these parameters are changed for the catalysts after degradation tests. These results will give an opinion about the catalysts how they would behave for long term operations when they are used in PEM fuel cell applications.

Electrochemical surface areas (ESAs) of the catalysts were found from the average areas of hydrogen reduction (A_r) and hydrogen oxidation (A_o) peaks by using the equation below.

$$\mathrm{ESA} = \frac{(\mathrm{Ar}+\mathrm{Ao})/2}{\mathrm{K.L.S}} \qquad (4.1)$$

where A is in A.V/cm^2, K corresponds to the charge when the Pt surface is covered with monolayer of hydrogen 0.21 mC/cm^2, S is the scan rate in mV/s and L is the platinum loading on the electrode which is 28 μg Pt/cm^2 (Bayrakçeken, 2008). Sample calculation for ESA is given in Appendix A.1.1.

The particle sizes of the catalysts determined by XRD were used to calculate the metal total surface area (SA) of the catalysts. The platinum metal particles were assumed to be spherical and SA of the catalysts can be calculated by using equation 4.2 as shown below.

$$SA = \frac{4\pi r^2}{\rho \frac{4}{3} \pi r^3} \tag{4.2}$$

where ρ is the density of platinum metal which is 21.4 g/cm^3, d is the particle size of platinum taken from XRD measurements in nm (Bayrakçeken, 2008). Sample calculation for SA is given in Appendix A.1.2.

Platinum utilization is based on the interaction of the platinum particles with the electrolyte. It can be found by using equation 4.3 below (Bayrakçeken, 2008). Sample calculation for Pt utilization is given in Appendix A.1.3.

$$Pt_{ut}\ (\%) = \frac{ESA}{SA}\ 100 \tag{4.3}$$

4.1.1 Effect of potential cycling on commercial and synthesized catalysts having different Pt percentages (HOR activity)

Cyclic voltammetry tests were performed on synthesized and commercial catalysts. Catalysts were synthesized by microwave irradiatioın technique (Bayrakçeken, 2008). Catalysts have 32 and 44 % platinum percentages according to TGA results.

XRD results showed that they have average particle sizes of 3.4 and 4.2 nm, respectively (Güvenatam, 2010). All the tests were performed at a scan rate of 50 mV/s. Commercial ETEK and Pt/V (32 %) catalysts were tried up to 1000 cycles and Pt/V (44 %) catalyst was tried up to 7000 cycles.

Electrochemical surface areas of the catalysts were calculated for all the catalysts after exposing to 50 cycles to see the ESA of them before aging. ESAs were continued to be calculated as the number of cycles increased in order to determine the decrease in ESA.

Figures 4.1, 4.2 and 4.3 showed the current density versus voltage relationships of the catalysts Pt/V %20 ETEK, Pt/V %32 and Pt/V %44, respectively. It can be easily seen from the figures that different Pt loadings and different carbon amounts of the catalysts affect the double layer capacitance. As the Pt loading increases while the amount of carbon decreases, double layer capacitance decreases.

The total metal surface areas (SA) of the catalysts and the platinum utilizations were calculated by using the CV data and tabulated in Table 4.1. Due to having the smallest particle diameter and lowest Pt loading the SA of Pt/V %20 was the highest but due to its lowest ESA values, its %Pt utilization value was the lowest among other catalysts.

In Table 4.1 the total metal surface areas (SA) and %Pt utilizations of the catalysts were shown. The highest %Pt utilization belongs to the catalyst Pt/V %32.
In Table 4.2, the ESA values can be seen, which the Pt/V (32 %) catalyst showed the highest ESA. The irregular ESA change with Pt loading (Pt/V (32 %) has the highest ESA) can be explained by so many factors. Xing et al. (2004) studied carbon nanotubes having 10, 20 and 30 % Pt and the CV results showed that as the Pt percentage of the catalyst decreased, ESA of the catalysts increased due to decrease in particle size. Another study, Cho et al. (2007) studied on the catalysts having Pt

percentages of 20, 40 and 60 %. They have found that as the %Pt increased the ESA values decreased.

In the present case, an increase in the ESA value as the %Pt increased up to 32 % may be attributed to better utilization of the available Pt active sites than other catalysts. But further increase in the Pt loading resulted in an increase in the particle size which causes a decrease in ESA.

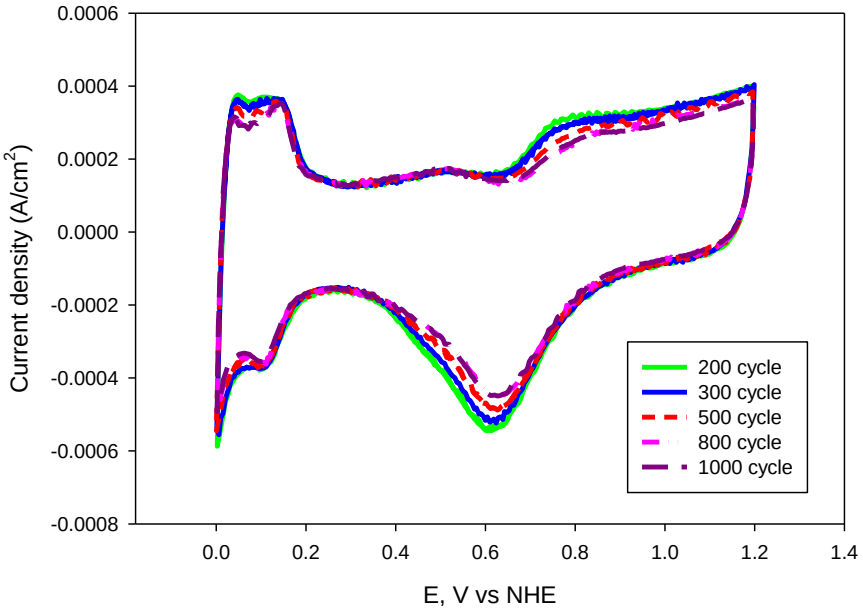

Figure 4.1 Cyclic voltammograms of commercial Pt/V (20%) catalyst taken at a scan rate of 50mV/s in 0.1 M $HClO_4$ solution after potential cycling up to 1000 cycles

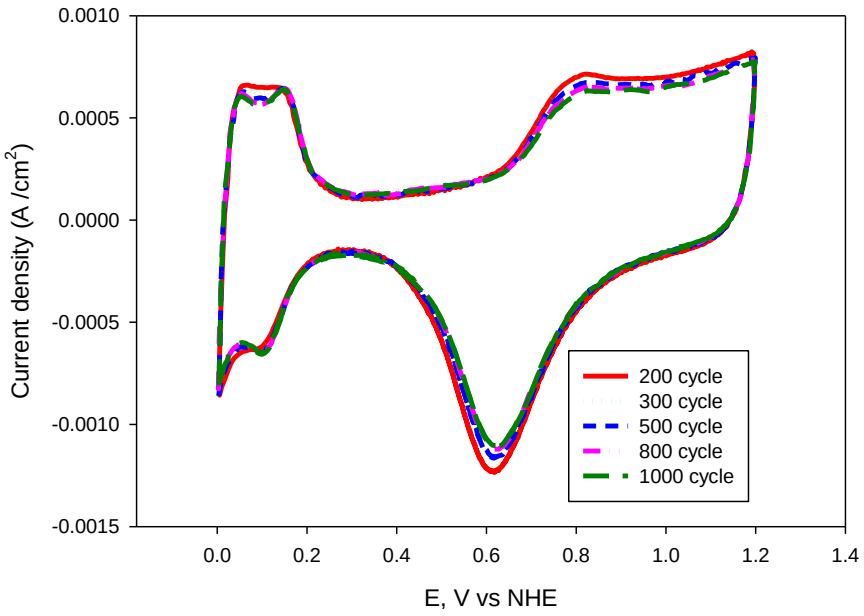

Figure 4.2 Cyclic voltammogram of Pt/V (32 %) catalyst taken at a scan rate of 50mV/s in 0.1 M $HClO_4$ solution after potential cycling up to 1000 cycles

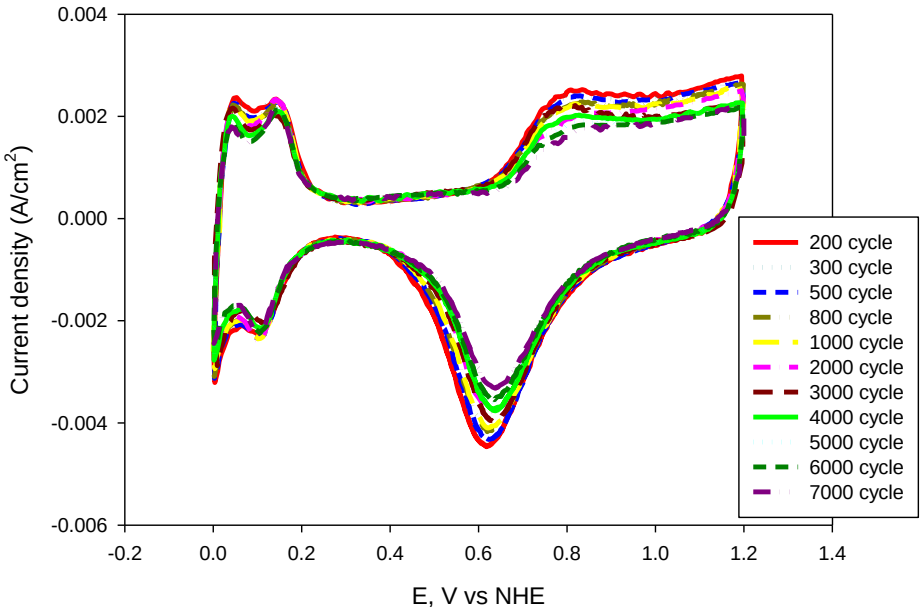

Figure 4.3 Cyclic voltammogram of Pt/V (44 %) catalyst taken at a scan rate of 50mV/s in 0.1 M $HClO_4$ solution after potential cycling up to 7000 cycles

Table 4.1 Total metal surface areas (SA) and Pt utilizations of catalysts having different %Pt

Catalysts	SA (m^2/g)	Pt utilization (%)
Pt/V (20 %) ETEK	108	21
Pt/V (32 %)	67	71
Pt/V (44 %)	83	44

In Figure 4.4, the ESA changes of the catalysts were shown. For all the catalysts, the decrease in the ESA can be seen. The highest ESAs were gained from the catalyst Pt/V %32.

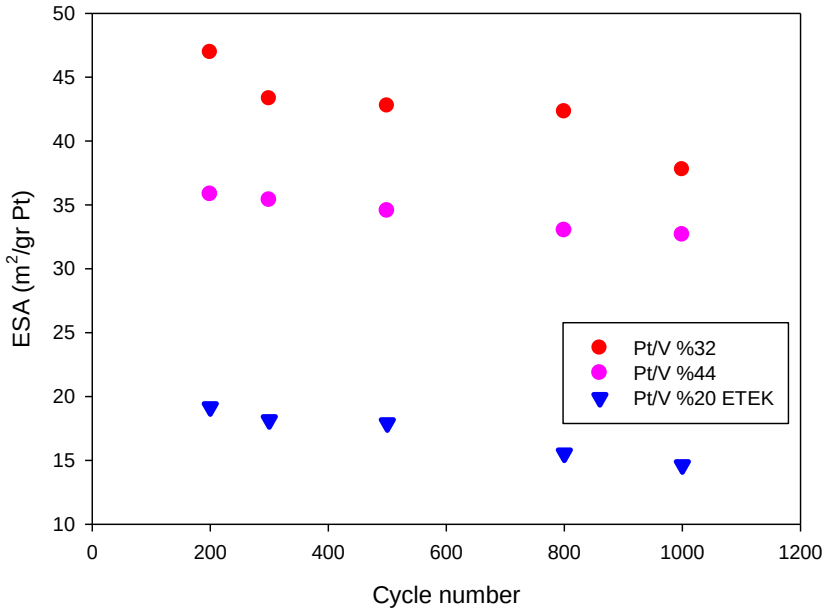

Figure 4.4 ESA changes of the catalysts after cycled up to1000 at a scan rate of 50 mV/s in 0.1 M $HClO_4$ solution

Table 4.2 ESA values for the catalysts having different platinum percentages after potential cycling experiments

CYCLE NUMBER	**ESA (m^2/g Pt) Pt/V (20 %) (ETEK)**	**ESA (m^2/g Pt) Pt/V (32 %)**	**ESA (m^2/g Pt) Pt/V (44 %)**
50	23	48	36
200	19	47	36
300	18	43	35
500	17	43	35
800	15	42	33
1000	14	37	32
2000			31
3000			30
4000			30
5000			28
6000			27
7000			26

4.1.2 Effect of carbon to Nafion (C/N) ratio on catalyst activity

In PEM fuel cell applications, as mentioned before, an ink is prepared made up of catalyst itself, Nafion solution, water and 1, 2 propandiol. This ink is then sprayed on two same shaped gas diffusion layers which then become the anode and the cathode parts of the fuel cell. There are so many catalyst related reasons that affect the durability of the PEM fuel cells but catalyst is not the only part of the catalyst layer. Nafion is another important parameter and its role as a proton pathway is so critical. In this part of the study, the effect of the catalyst ink composition including carbon to Nafion (C/N) ratio was investigated with commercial Pt/V %20 ETEK catalyst.

Catalyst inks were prepared with different C/N ratios (4, 8, and 12) and the ink which has no Nafion solution.

Figure 4.5 showed the cyclic voltammograms of Pt/V (20 %) (ETEK) catalyst having different C/N ratios in the catalyst ink taken at a scan rate of 50 mV/s for 50 cycles between 0 V-1.2 V potential ranges to see the changes in ESAs of the catalysts. By using the CV data, the total metal surface areas (SA), ESA values and the Pt utilization (%) values were calculated and tabulated in Table 4.3. The results showed that the catalyst ink having C/N ratio of 12 (which had less Nafion solution) and the ink with no Nafion solution gave similar ESA values. Decrease in C/N ratio to 8 resulted in an increase in ESA which may be attributed providing of better contact but further decrease in C/N ratio to 4 (increase in Nafion amount) resulted in a decrease in ESA. As the Nafion loading increased the electrolytic conductivity increased in the electrodes. However as the Nafion loading further increased the performance decreased.

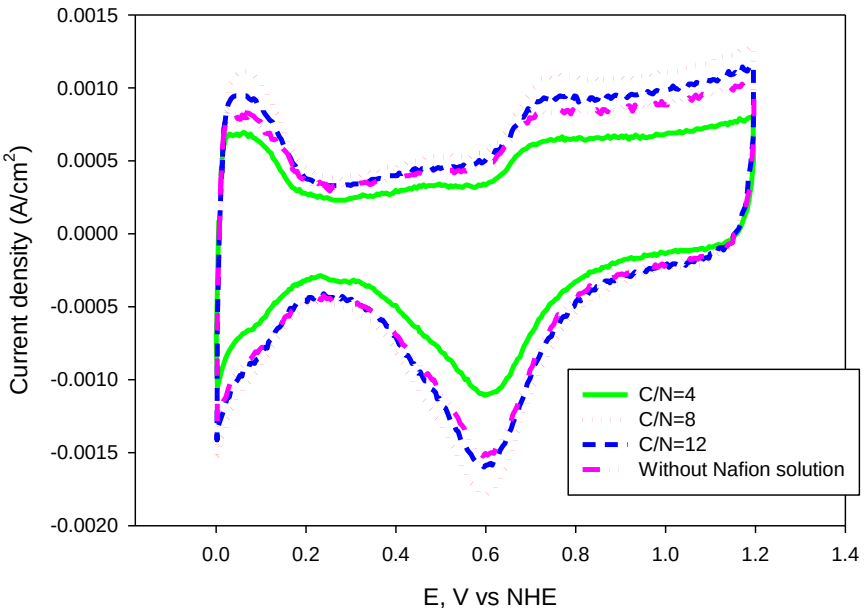

Figure 4.5 Cyclic voltammograms of Pt/V (20 %) (ETEK) having different C/N ratios in the catalyst ink taken before aging tests at a scan rate of 50mV/s in 0.1 M $HClO_4$ solution for 50 cycles

Antolini et al. (2002) studied the effect of Nafion loading in a catalyst layer on performance of a fuel cell. They have prepared inks having Nafion loadings of 0, 0.29, 0.67, 1.01 and 1.46 mg/cm^2. The performance of the fuel cell increased as the Nafion loading increased up to 0.67 mg/cm^2. Increase in the Nafion amount may block some active sites of the catalysts which cause ESA losses. Also, with an excess amount of Nafion, a thicker layer of polymer clogs the pores and builds a resistance to mass transfer. The fuel gases hardly transfers to the cathode side that may decrease the performance. In the same study, CV experiments were performed and similar to present case, ESA values increased up to 0.67 mg/cm^2 Nafion loading and then decreased as the loading increased.

In another study, Lobato et al. (2010) studied with a different polymer PBI for high temperature fuel cell applications. They have prepared catalyst inks having C/PBI ratios of 4, 8, 20 and 40. In CV tests, the highest ESA was gained from the catalyst ink having C/PBI ratio of 20. They have conluded that C/PBI ratio in the ink should be optimized and they also reported that the fuel cell performance tests were in accordance with the CV tests.

Table 4.3 Total metal surface areas (SA) and %Pt utilizations of the catalyst inks having different C/N ratios

C/N ratio	**SA (m^2/g)**	**Pt utilization (%)**
4	108	17
8	108	28
12	108	23
∞	108	21

The aging tests were performed for 1000 cycles at a scan rate of 20 mV/s between 0.6 V-1.2 V potential ranges where the platinum dissolution can be detected. In Figure 4.6, the cyclic voltammograms of the catalyst inks having different C/N ratios after Pt dissolution degradation tests were given. These voltammograms were taken

for 50 cycles at 50 mV/s scan rate between 0 V-1.2 V potential ranges. For all the catalyst inks the decrease in the ESA can be seen from Figure 4.6 as well as from Table 4.4.

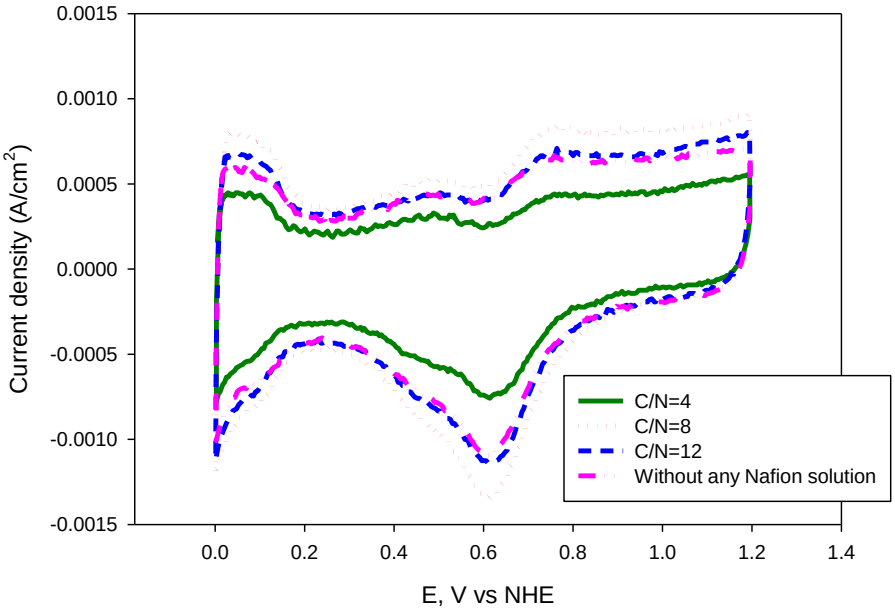

Figure 4.6 Cyclic voltammograms of Pt/V (20 %) (ETEK) having different C/N ratios in the catalyst ink taken after Pt dissolution test at a scan rate of 50mV/s in 0.1 M $HClO_4$ solution for 50 cycles

Ma Andersen et al. (2010) studied the effect of Nafion loading on the catalyst layer on Pt dissolution amount. They have tried commercial cathodes having ionomer loadings of 10, 20, 30, 40 and 50 %. The maximum ESA gained by CV experiments was the catalyst layer having 40 % of ionomer loading. They have detected the dissolved Pt by atomic absorption spectrophotometer and they have concluded that changing the amount of ionomer loading in the catalyst layer showed a significant effect on the electrochemical stability of the catalyst layer.

Table 4.4 showed that the highest ESA was obtained for C/N ratio of 8. The low and intermediate Nafion loadings (C/N ratios of 12 and 8) were resulted in similar ESA

losses but further increase in Nafion loading (C/N ratio of 4) resulted in an increase in %ESA loss.

Table 4.4 ESA values of catalyst layers having different C/N ratios in the inks

C/N ratios	**Average of the peak areas (A.V/cm^2)**	**ESA (m^2/g Pt)**	**Average of the peak areas (A.V/cm^2)**	**ESA (m^2/g Pt)**	**% ESA loss**
	BEFORE Pt dissolution test		**AFTER Pt dissolution test**		
4	5.4×10^{-5}	18	3×10^{-5}	10	44
8	9.1×10^{-5}	30	5.8×10^{-5}	20	33
12	7.2×10^{-5}	24	4.9×10^{-5}	17	29
∞	6.7×10^{-5}	23	4.4×10^{-5}	15	35

For carbon corrosion degradation tests, all the samples were kept at 1.2 V potentiostatic hold for 24 h. Carbon corrosion peaks appeared for all the catalysts between 0.2-0.6 V potential ranges. To calculate the charge in this region, first of all, the area under the curve of the resultant peak was found. The unit of the resultant area is in A.V/cm^2. So the result gives the charge per unit area (Eqn 4.4). The highest the charge per unit area means the highest amount of the surface functional groups. Sample calculation for area of the carbon corrosion peak is given in Appendix A.1.4.

$$Q = \text{Area of the peak (A.V/cm}^2\text{)} / \text{scan rate (V/s)} \times 1000 = \text{mC/cm}^2 \quad (4.4)$$

The corresponding carbon corrosion cyclic voltammograms for the catalysts prepared with different C/N ratios were given in Figure 4.7. The peaks corresponding to carbon corrosion located between 0.2-0.6 V potential ranges were getting more significant as the Nafion loading decreases (C/N ratio increases).

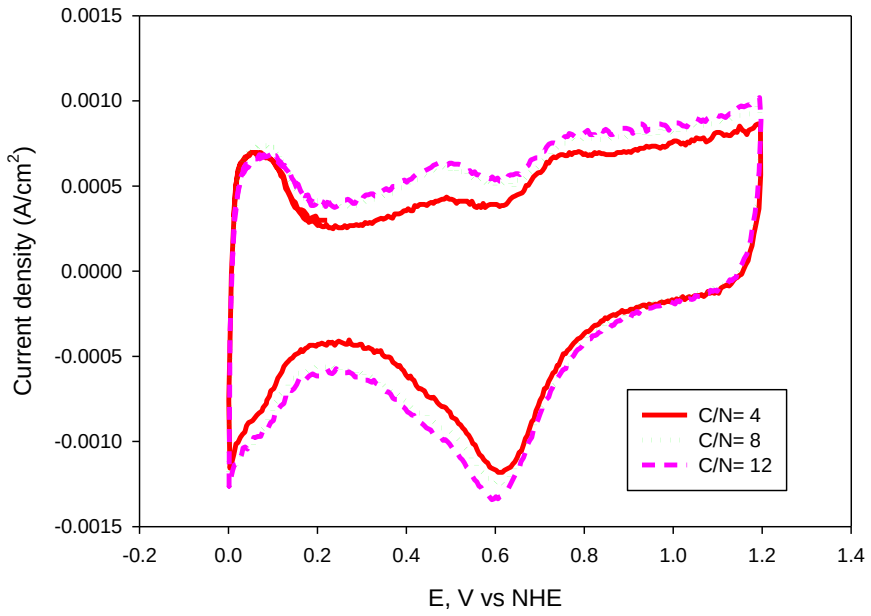

Figure 4.7 Cyclic voltammograms of the catalyst inks having different C/N ratios recorded after holding the electrodes at 1.2V for 24 h.

Cherstiouk et al. (2010) performed a study basing on searching the effect of Nafion loading on carbon corrosion. They have impregnated Nafion on Vulcan XC-72 with the loadings of 0, 0.16, 0.79 and 3.13 mg_{Nafion}/m^2. After potentiostatic hold at 1.1 V, they have detected the carbon corrosion peaks around 0.6 V which they have explained the reason basing on the formation of oxide groups on the surface of the carbon support. They have concluded from CV data that as the Nafion loading increases (C/N ratio decreases) up to 0.79 mg_{Nafion}/m^2, carbon corrosion decreases. Further increase to 3.13 mg_{Nafion}/m^2 carbon corrosion sudenly increases. They have reached two important points related with the impregnation of Nafion with carbon. The adsoprtion of ionomer on the surface of the carbon leading to micropore clooging of carbon and the structural degradations resulted with increase in corrosion currents. Due to impregnating excess amounts of Nafion, increase in corrosion currents causes swelling and deformation of carbon. These effects will produce microstrains in the carbon especially in the critical areas which the carbon is

connected with other particles. These structural imperfections will act as the source of active sites for carbon corrosion attack.

Table 4.5 Carbon corrosion peak areas of the catalyst layers having different C/N ratios in the catalyst ink

C/N ratio	**Carbon corrosion peak areas ($A.V/cm^2$)**	**Charge (Q)(mC/cm^2)**
4	3.9×10^{-5}	0.078
8	1.07×10^{-4}	0.214
12	1.46×10^{-4}	0.292

For all the catalyst inks, the ORR behaviours were investigated up to 2500 rpm. To compare the ORR performances of the catalyst inks, the current density versus potential relations were plotted at 1600 rpm angular velocity, as shown in Figure 4.8. Due to having the highest ESA value and %Pt utilization, catalyst ink having C/N ratio of 8 gave the highest performance whereas the ink having C/N of 4 showed the lowest. ORR results were consistent with the ESA and Pt utilization (%) results.

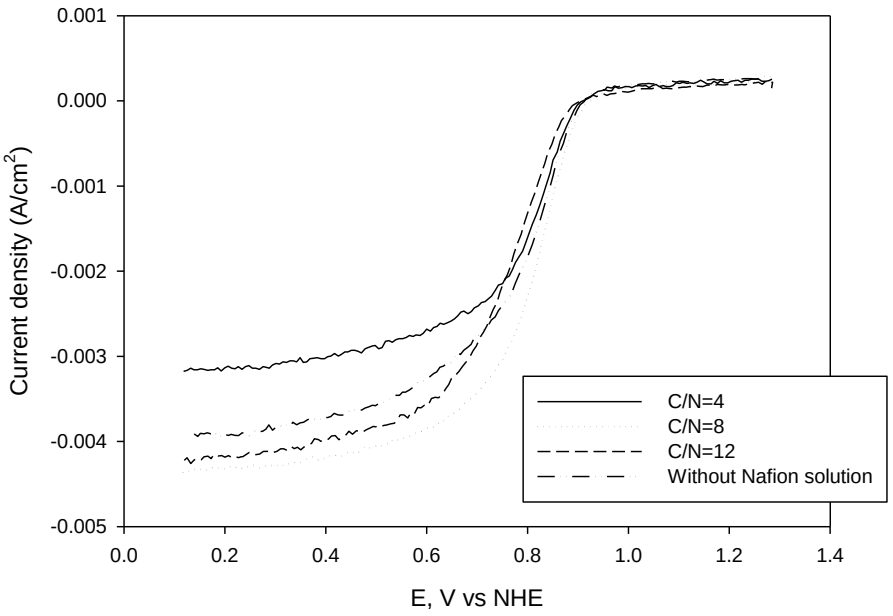

Figure 4.8 Hydrodynamic voltammogram of the catalysts taken before aging tests at a scan rate of 5mV/s in 0.1 M $HClO_4$ solution for 2 cycles at 1600 rpm

In Figure 4.9, the ORR behaviors of the catalyst inks were investigated after Pt dissolution tests. The highest performance was also belonging to the ink having C/N ratio of 8. That can be explained by the ink having C/N ratio of 8 had the highest ESA after Pt dissolution test (Table 4.4).

Lin and Shih (2007) investigated the ORR activity of the catalysts with different Nafion thicknesses. They have tried RDE (rotating disc electrode) experiments with different Nafion thicknesses in the range of 0.8 to 0.1nm. They have found that the ORR activity increased as the Nafion thickness decrased up to 0.3nm. Further decrease to 0.1 nm shows a sudden ORR activity loss. From this result, they have concluded that, the Nafion thickness should be optimized in order to get efficient performances.

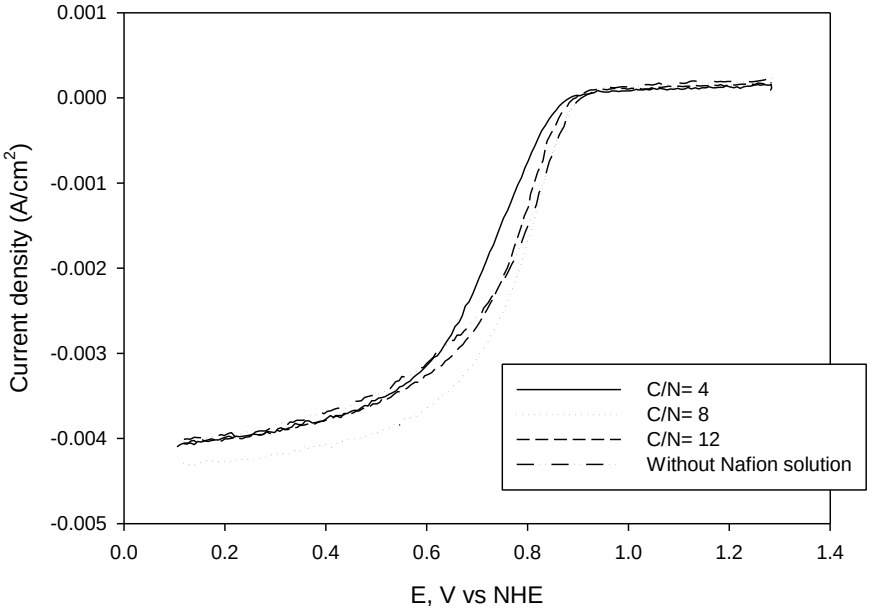

Figure 4.9 Hydrodynamic voltammogram of the catalysts taken after Pt dissolution tests at a scan rate of 50mV/s in 0.1 M $HClO_4$ solution for 50 cycles at 1600 rpm

In Figure 4.10, the hydrodynamic voltammogram of the catalyst inks at 1600 rpm angular velocity were shown after carbon corrosion tests. The performance comparison was more clear than Figure 4.9 (After Pt dissolution test). The ORR performances were consistent with the carbon corrosion amounts of the catalyst inks. Due to Figure 4.7 and Table 4.5, carbon corrosion increased as the C/N ratio increased (Nafion content decreased). However further increase in Nafion would cause sudden performance losses. In Figure 4.10, performance decrease can be seen with the same order of increasing carbon corrosion. This is a proof that carbon corrosion is a critical factor which affects the performances of the catalysts.

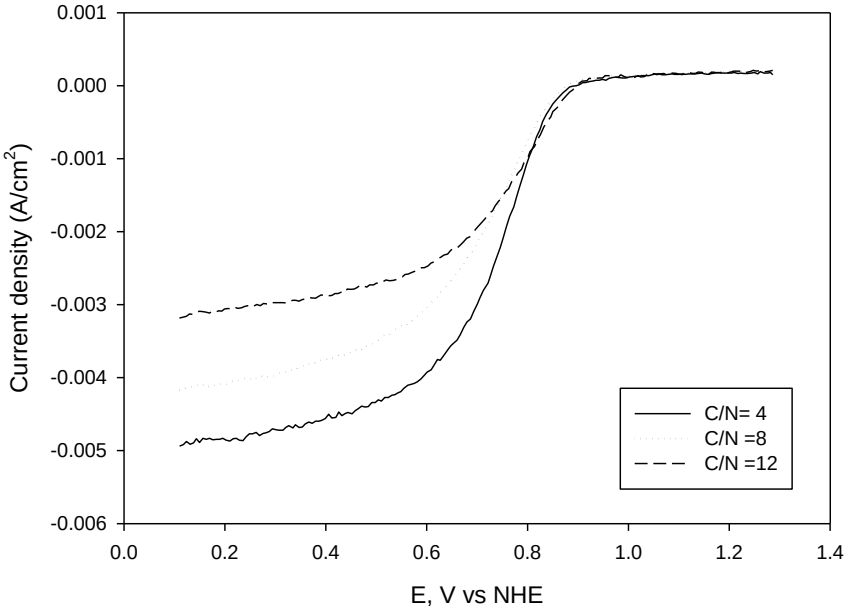

Figure 4.10 Hydrodynamic voltammogram of the catalysts taken after carbon corrosion tests at a scan rate of 5mV/s in 0.1 M $HClO_4$ solution for 2 cycles at 1600 rpm

Tafel slope losses were also calculated by using the ORR data taken before and after degradation tests shown in Table 4.6. Determination of Tafel slope losses is given in Appendix A.2.1. For Pt dissolution tests, potential losses were consistent with the ESA results. Catalyst ink having C/N ratio of 8 performed the highest ESAs both before and after Pt dissolution test and the ink having C/N ratio of 4 had the lowest ESAs. Moreover, it has the highest ESA loss (%) after degradation test so the result of having the highest potential loss of the catalyst ink with C/N ratio of 4 makes sense.

From carbon corrosion point of view, the least potential loss was belonging to the catalyst ink having C/N proportion of 8. Antolini et al. (2002) searched the ORR activity of the catalysts having different Nafion amounts on the GC (glassy carbon) electrode. As mentioned before, they have found an optimum Nafion loading of 0.67 mg/cm^2. Also, they have gained the best ORR activity from the catalyst having this Nafion loading. They have explained this behavior by two opposite effects of Nafion.

Positive effect was that, ESA of the catalysts increased by covering of Pt particles with Nafion. Also, Nafion enhances the proton transfer through the catalyst pores. Negative effect was clogging of the pores with excess amount of Nafion which then leads to lack of gas diffusion.

Table 4.6 Potential losses of the catalysts layers having different C/N ratios in the catalyst inks

C/N ratio	**Tafel slope loss (Pt dissolution) (Potential loss) (mV)**	**Tafel slope loss (Carbon corrosion) (Potential loss) (mV)**
4	18	21
8	7	20
12	17	24
∞	15	Not performed

4.1.3 Effect of different Pt percentages on commercial catalyst activity

In this part of the study, the effect of Pt percentages of the catalysts to the performance of the catalysts was investigated. The catalysts were all commercial having %Pt of 20, 50 and 70. Before starting the aging tests, cyclic voltammograms were taken for all the catalyst and shown in Figure 4.11. The corresponding SA and %Pt utilization values were also tabulated in Table 4.7.

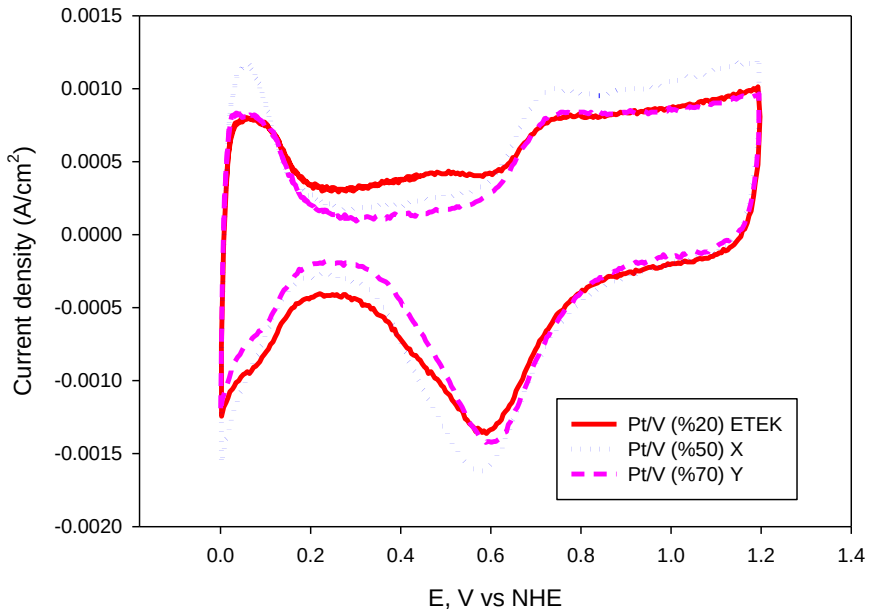

Figure 4.11 Cyclic voltammograms of catalysts having different Pt percentages taken before aging tests at a scan rate of 50mV/s in 0.1 M $HClO_4$ solution for 50 cycles

Table 4.7 Total metal surface areas (SA) and %Pt utilization of the catalysts having different %Pt

Catalyst	**SA (m^2/g)**	**Pt utilization (%)**
ETEK (20 %)	108	19
X (50 %)	117	26
Y (70 %)	88	30

The particle sizes of the catalysts were 2.6, 2.4, 3.2 nm, respectively. Smaller particle size is an important property for the catalyst in order to have higher total metal surface area (SA) and stability because smaller particles can disperse well and lack of agglomeration has been seen in those catalysts (Xing, 2004). In the present case, the best utilization was obtained from the catalyst having the highest %Pt. It can be seen that as the%Pt in the catalyst increased up to 70 %, the particle size did not increase significantly but this increase may have resulted in better utilization of the Pt metal

over the carbon support and lowers the amount of the Pt metal deposited on the micropores of the carbon support.

Figure 4.12 shows the cyclic voltammograms of the catalysts taken right after Pt dissolution tests. Table 4.8 shows the ESA values before and after the Pt dissolution tests. As can be seen from Table 4.8 that Pt/V (50 %) showed the highest ESA and Pt/V (20 %) had the lowest ESA.

Cho et al. (2007) and Xing (2004) performed durability tests on the catalysts having different %Pt. They have reported that as the %Pt increased, performance of the catalysts decreased. In those studies, particle sizes increased with increasing Pt percentages in the catalysts which leads to lower dispersion and higher agglomeration resulted in performance loss. In the present case, Pt/V 50 % had smaller particle size than Pt/V 20 % in spite of having higher Pt loading. That explains the result of the catalyst Pt/V %50 showed higher ESA than the other catalysts.

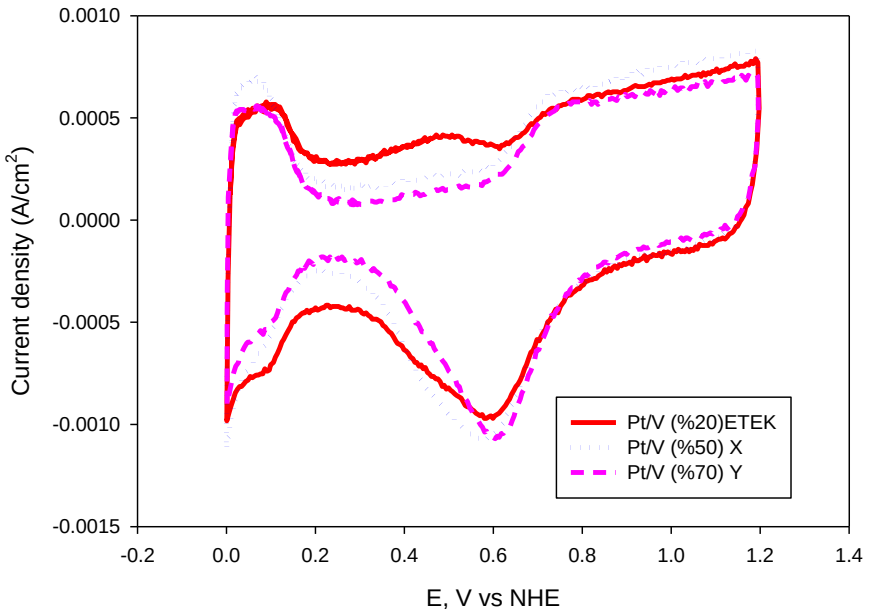

Figure 4.12 Cyclic voltammograms of catalysts having different Pt percentages taken after Pt dissolution tests at a scan rate of 50mV/s in 0.1 M $HClO_4$ solution for 50 cycles

Table 4.8 ESA values of catalysts having different %Pt (Pt dissolution test)

Catalysts (Pt/V)	**Average of the peak areas (A.V/cm^2)**	**ESA (m^2/g Pt)**	**Average of the peak areas (A.V/cm^2)**	**ESA (m^2/g Pt)**	**% ESA loss**
	BEFORE Pt dissolution test		**AFTER Pt dissolution test**		
%20 ETEK	6.55×10^{-5}	20	4×10^{-5}	12	40
%50 X	9.75×10^{-5}	30	6.1×10^{-5}	19	37
%70 Y	8.5×10^{-5}	26	5.8×10^{-5}	18	31

Another study, Merzougui and Swathirajan (2006) performed cyclic voltammetric experiments to the catalysts having Pt percentages of 46.5, 47.4 and 30 %. They have found that the highest ESA belonged to the catalysts having Pt percent of 30. On the other hand, the highest % ESA loss belonged to Pt/V 30 %, too. They have concluded that, the high ESA values at lower Pt loadings may be attributed to smaller particle sizes and good dispersions and the highest %ESA loss of the low %Pt catalysts may be due to high rates of Pt particle agglomerations due to carbon corrosion.

Figure 4.13 shows the cyclic voltammogram of the catalysts taken after carbon corrosion degradation tests. The characteristic carbon corrosion peaks can be seen for all the catalysts and the corresponding ESA values before and after the carbon corrosion tests were given in Table 4.9.

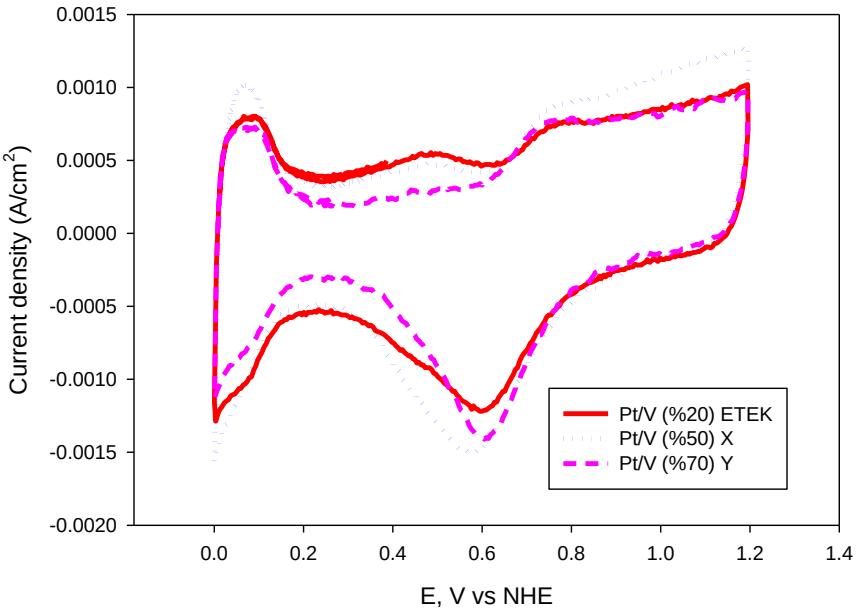

Figure 4.13 Cyclic voltammograms of catalysts having different Pt percentages recorded after holding the electrodes at 1.2V for 24 h

Table 4.9 ESA values of catalysts having different %Pt (carbon corrosion)

Catalysts (Pt/V)	**Average of the peak areas (A.V/cm^2)**	**ESA (m^2/g Pt)**	**Average of the peak areas (A.V/cm^2)**	**ESA (m^2/g Pt)**	**% ESA loss**
	BEFORE carbon corrosion test		**AFTER carbon corrosion test**		
%20 ETEK	6.55×10^{-5}	20	5.44×10^{-5}	17	**15**
%50 X	9.75×10^{-5}	30	7×10^{-5}	22	**27**
%70 Y	8.5×10^{-5}	26	6.35×10^{-5}	20	**23**

In Table 4.10, carbon corrosion peaks were shown in mC/cm^2 .The results indicated that as the %Pt in the catalyst increased, carbon corrosion decreased. It is obvious that as the %Pt over the carbon support increases the surface area of carbon decreases which results in a decrease in the carbon corrosion.

Table 4.10 Carbon corrosion peak areas of the catalyst having different %Pt

Catalysts (Pt/V)	**Carbon corrosion peak areas (A.V/cm^2)**	**Charge (Q)(mC/cm^2)**
%20 ETEK	8×10^{-6}	0.16
%50 X	6.53×10^{-6}	0.13
%70 Y	3.4×10^{-6}	0.07

In the study mentioned before by Merzougui and Swathirajan (2006), the higher % ESA loss in low % Pt loaded catalysts were explained by highest carbon corrosion. Indeed, the Pt agglomeration in those catalysts were attributed to highest carbon corrosion. This means that as the % Pt is decreased in the catalyst, the higher the carbon corrosion would be. In Table 4.10 and Figure 4.13, it was clearly seen that the carbon corrosion increased with decreasing %Pt of the catalysts.

Also, it can be seen from Figure 4.11 that the double layer capacitance was the highest in Pt/V %20 which enhances the carbon corrosion.

In Figure 4.14, the ORR behaviours of the catalysts taken at 1600 rpm, before aging tests can be seen. The highest ORR performance was gained from Pt/V %70 catalyst and the lowest performance was gained from Pt/V 50 %.

Antoine and Durand (2000) performed a study for searching the effect of Pt particle size on the ORR activity of the catalysts. They have tested Pt/V catalysts having %Pt of 20, 30 and 40 with particle sizes of 2.5, 3.4 and 4.1 nm. respectively. They have concluded that as particle size increased, the H_2O_2 production decreases which is the proof of higher ORR activity.

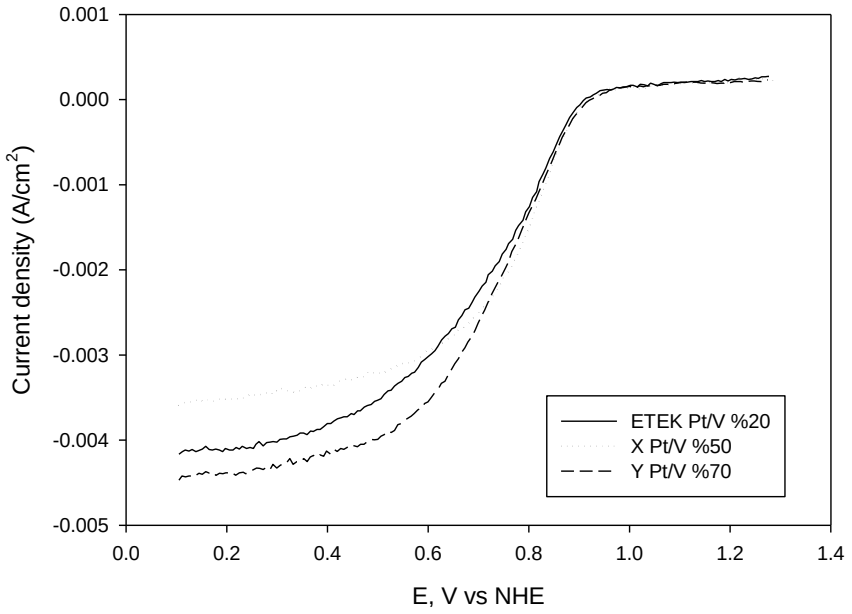

Figure 4.14 Hydrodynamic voltammogram of the catalysts taken before aging tests at a scan rate of 5mV/s in 0.1 M $HClO_4$ solution for 2 cycles at 1600 rpm

In Figure 4.15, the hydrodynamic voltammograms of the catalysts can be seen which were taken after Pt dissolution tests at 1600 rpm. The highest performance was taken from Pt/V 50 % catalyst and the lowest performance was gained from Pt/V 20 % catalyst. It makes sense that the Pt/V 20 % had the lowest performance which was also consistent with the literature. As mentioned before in the study of Antolini and Durand (2000), the ORR activity decreased as the Pt particle size decreased and the carbon content increased within the catalyst. Besides, 50 % Pt/V had a higher performance than Pt/V 70 %. This may be due to highest % ESA loss of the Pt/V 50 % catalyst (Table 4.8), which means increase in particle size growth leading to ORR activity increase.

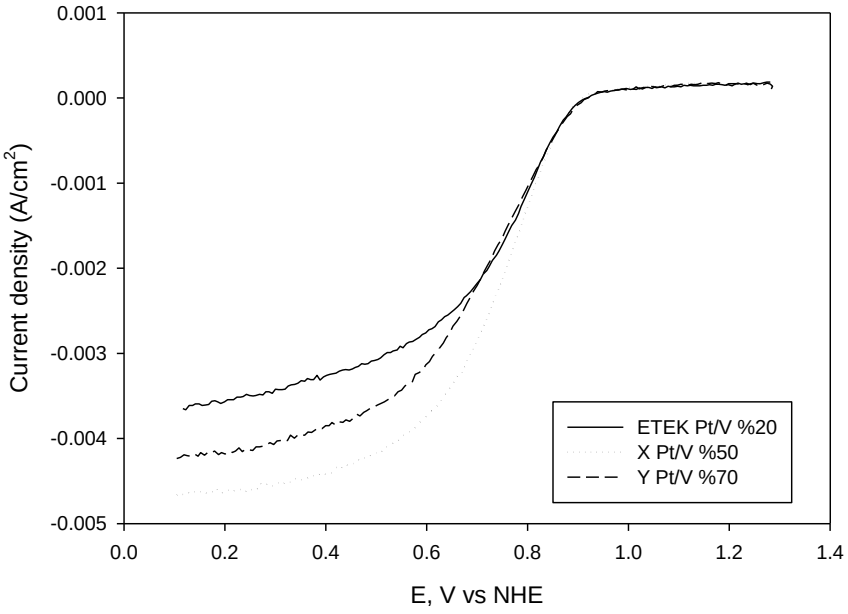

Figure 4.15 Hydrodynamic voltammogram of the catalysts taken after Pt dissolution tests at a scan rate of 5mV/s in 0.1 M $HClO_4$ solution for 2 cycles at 1600 rpm

In Figure 4.16, the hydrodynamic voltammograms of the catalysts can be seen which were taken after carbon corrosion tests at 1600 rpm. The highest performance was taken from the catalyst Pt/V 70 % and the lowest performance was gained from the catalyst Pt/V 20 %. The performances increased in the order of decreasing carbon corrosion.

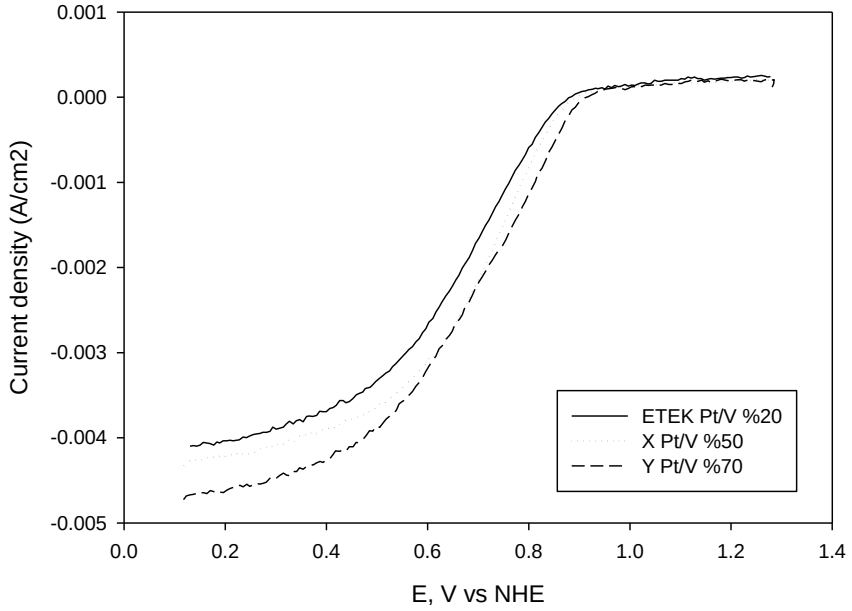

Figure 4.16 Hydrodynamic voltammogram of the catalysts taken after carbon corrosion tests at a scan rate of 5mV/s in 0.1 M $HClO_4$ solution for 2 cycles at 1600 rpm

In Table 4.11, the potential losses due to Tafel slopes were shown. For carbon corrosion tests, the potential losses were decreasing in the order of decreasing carbon corrosion. On the other hand for Pt dissolution test, the lowest potential loss was belong to Pt/V 70 % which makes sense according to literature mentioned before. The highest potential loss was belonging to Pt/V 50 % which has the smallest particle size. According to litearute, the ORR activity increases (H_2O_2 production decreases) as the Pt particle size increases. From this aspect, the highest potential loss of Pt/V 50 % makes sense.

Table 4.11 Potential losses of the catalysts having different %Pt

Catalysts (Pt/V)	**Tafel loss (Pt dissolution) (Potential loss) (mV)**	**Tafel loss (Carboncorrosion) (Potential loss) (mV)**
%20 ETEK	5	27
%50 X	13	17
%70 Y	3	9

4.1.4 Effect of different pH values on synthesized catalysts

The catalysts prepared in our laboratory were synthesized under different conditions including the pH of the environment. For determining the pH effect on the synthesized catalysts, cyclic voltammogram (HOR) and rotating disc voltammogram (ORR) experiments were carried on the catalysts synthesized by microwave irradiation technique. Three of the catalysts were used for the experiments having same Pt percentage (20 %) and synthesized in same microwave durations (50 s). Due to having different base concentrations pH values of them were measured as 1.4, 6.25 and 10. From XRD data, the particle sizes of the catalsysts were found as 3.98, 3.85, 3.32 nm, respectively (Bayrakçeken, 2008).

In Table 4.12 total metal surface areas of the catalysts were found according to their particle sizes. The catalyst synthesized under pH of 10 had the highest SA because of having the smallest particle size. Li et al. (2005) performed a study on Pt/CNTs synthesized under different pH values and investigated the particle size variation with pH. They have found that as the pH increased from 3.4 to 9.2, particle size of the catalysts decreased. Also, from TEM results, they have detected that at lower pH values. Pt particles were obviously agglomerated and did not show a good dispersion. On the other hand, at higher pH values (7.4 and 9.2) the dispersion of Pt particles was more homogeneous and no agglomeration can be seen.

Table 4.12 SA and %Pt utilizations of catalysts having % Pt of 20 and synthesized under microwave duration of 50s

Catalysts	**SA (cm^2/g)**	**Pt utilization (%)**
pH 1.4	70	15
pH 6.25	73	18
pH 10	84	17

Figure 4.17 shows the cyclic voltammograms of the catalysts synthesized under different pH values taken before aging tests. From Figure 4.17 and Table 4.13, it can be seen that the ESA values increased in the order of increasing pH. With increasing pH, the particle size of the catalysts decreases which is leading to a good dispersion and high surface area.

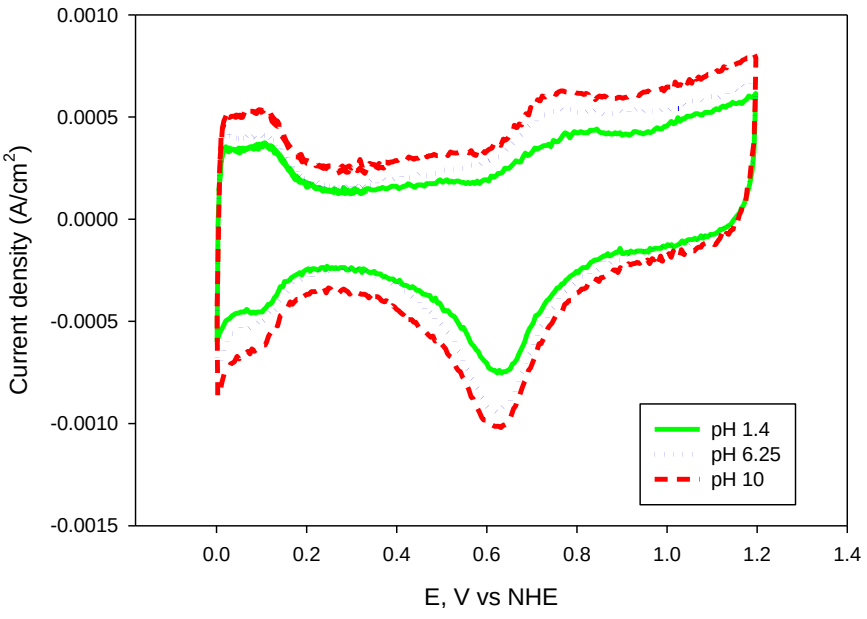

Figure 4.17 Cyclic voltammograms of catalysts synthesized under different pH values taken before aging tests at a scan rate of 50mV/s in 0.1 M $HClO_4$ solution for 50 cycles

Figure 4.18 shows the cyclic voltammograms of the catalysts taken just after the Pt dissolution tests. The ESA values in m^2/gr Pt were shown in Table 4.13, below. The highest ESA and the lowest ESA loss (%) after Pt dissolution test were belong to the catalyst synthesized under pH of 10.

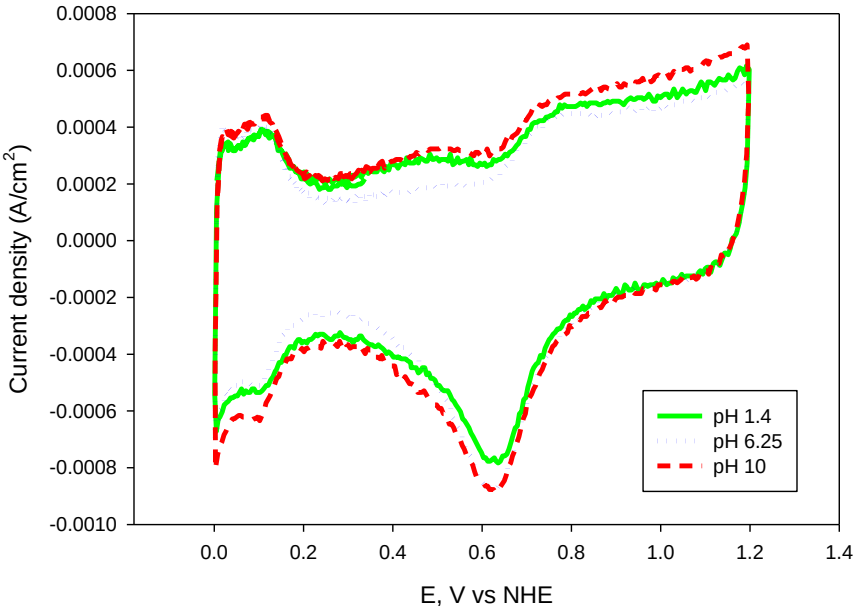

Figure 4.18 Cyclic voltammograms of catalysts synthesized under different pH values taken after Pt dissolution tests at a scan rate of 50mV/s in 0.1 M $HClO_4$ solution for 50 cycles

Table 4.13 ESA values of catalysts having % Pt of 20 and synthesized under microwave duration of 50s (Pt dissolution test)

Catalysts	**Average of the peak areas (A.V/cm^2)**	**ESA (m^2/g Pt)**	**Average of the peak areas (A.V/cm^2)**	**ESA (m^2/g Pt)**	**% ESA loss**
	BEFORE Pt dissolution test		**AFTER Pt dissolution test**		
pH 1.4	3.4×10^{-5}	11	3×10^{-5}	9	18
pH 6.25	4.2×10^{-5}	13	3.5×10^{-5}	12	8
pH 10	4.5×10^{-5}	14	3.7×10^{-5}	13	7

In Figure 4.19, cyclic voltammograms of the catalysts can be seen which were taken right after carbon corrosion degradation tests. Carbon corrosion can be observed for all the catalysts due to the peak arising from double layer between 0.2-0.6 V potential ranges. In Table 4.14, the ESA values before and after carbon corrosion tests can be seen. Also, in Table 4.15, the carbon corrosion peak areas were calculated in mC/cm^2. The highest carbon corrosion was seen in the catalyst synthesized at the pH of 1.4 and the lowest carbon corrosion was observed in the catalyst prepared under pH of 6.25.

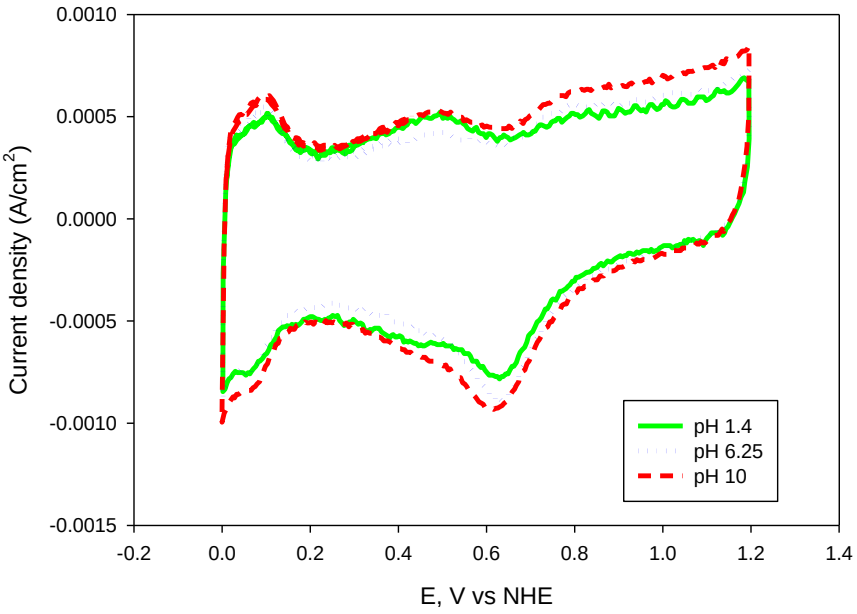

Figure 4.19 Cyclic voltammograms of catalysts having different synthesized under different pH values recorded after holding the electrodes at 1.2V for 24 h

Li and his co-workers (2005) studied the importance of the pH value of the environment which the catalyst is synthesized and they have got the best performance from the catalyst having the pH value of 7.4. In the present case, from carbon corrosion point of view, pH 6.25 gave the least carbon corrosion.

Table 4.14 ESA values of catalysts having % Pt of 20 and synthesized under microwave duration of 50s (carbon corrosion test)

Catalysts (Pt/V)	**Average of the peak areas (A.V/cm^2)**	**ESA (m^2/g Pt)**	**Average of the peak areas (A.V/cm^2)**	**ESA (m^2/g Pt)**	**% ESA loss**
	BEFORE carbon corrosion test		**AFTER carbon corrosion test**		
pH 1.4	3.4×10^{-5}	11	2.7×10^{-5}	8	27
pH 6.25	4.2×10^{-5}	13	3.4×10^{-5}	11	15
pH 10	$4.4 \times 10^{-}$	14	3.3×10^{-5}	10	29

Table 4.15 Carbon corrosion peak areas of the catalyst having % Pt of 20 and synthesized under microwave duration of 50s

Catalysts	**Carbon corrosion peak areas (A.V/cm^2)**	**Charge (Q) (mC/cm^2)**
pH 1.4	1.35×10^{-5}	0.27
pH 6.25	2×10^{-6}	0.04
pH 10	7×10^{-6}	0.14

In Figure 4.20, the hydrodynamic voltammograms of the catalysts were taken before degradation tests at 1600 rpm angular velocity. Performances were increasing in the order of increasing pH values.

In microwave irradiation technique, the synthesis undergoes in ethylene glycol solution. During synthesis, ethylene glycol is oxidized to acetate which would act as a stabilizer for metal particles. But under low pH values a low interaction between the acetate and Pt colloids occur. It seems that the pH of the synthesis solution is a

critical factor. At higher pH values, Pt particles would become more smaller and well dispersed which affect the performances of the catalysts in a positive manner (Bezerra et al., 2007).

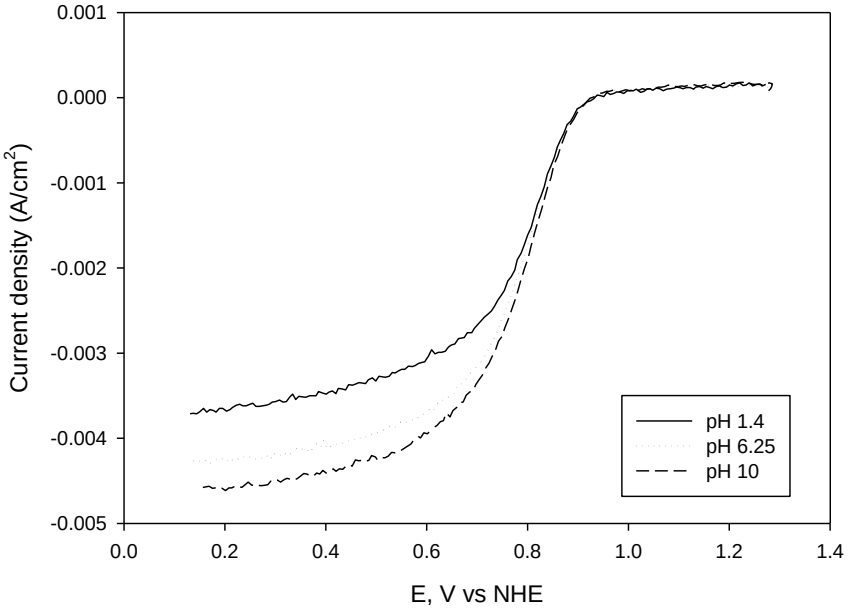

Figure 4.20 Hydrodynamic voltammogram of the catalysts taken before aging tests at a scan rate of 5mV/s in 0.1 M $HClO_4$ solution for 2 cycles at 1600 rpm

In Figure 4.21, the performances after RDE experiments taken at 1600 rpm were compared. The highest performance was taken from the catalyst synthesized under the pH of 6.25. This may be attributed to the higher corrosion resistance of the catalyst prepared at pH value of 6.25 because according to the Tables 4.14 and 4.15 the lowest ESA loss (%) and carbon corrosion was obtained from that catalyst.

In Figure 4.22, after carbon corrosion tests, the same performance trend was observed and the highest performance was obtained from the catalyst synthesized in the pH of 6.25. The catalyst synthesized in the pH of 6.25 showed better stability than the other catalysts.

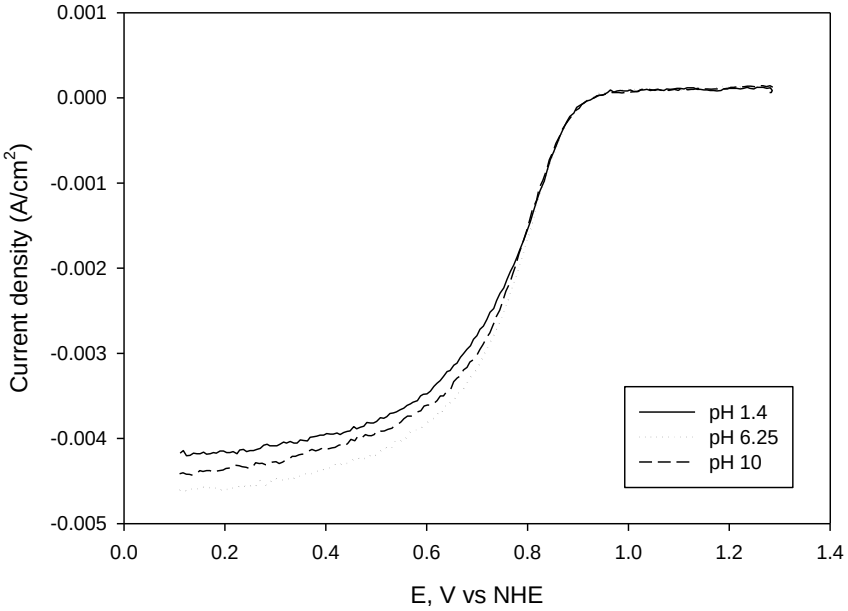

Figure 4.21 Hydrodynamic voltammogram of the catalysts taken after Pt dissolution tests at a scan rate of 5mV/s in 0.1 M $HClO_4$ solution for 2 cycles at 1600 rpm

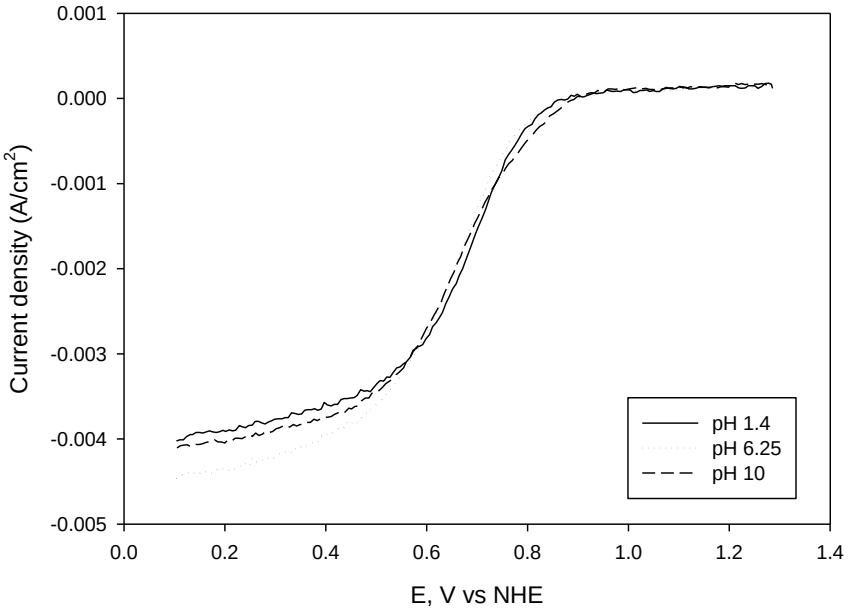

Figure 4.22 Hydrodynamic voltammogram of the catalysts taken after carbon corrosion tests at a scan rate of 5mV/s in 0.1 M $HClO_4$ solution for 2 cycles at 1600 rpm

In Table 4.16, the potential losses were summarized for the aging tests including Pt dissolution and carbon corrosion. There was not a significant potential loss detected due to Pt dissolution tests. On the other hand, considerable potential losses were observed due to carbon corrosion tests. The least potential loss was detected from the catalyst synthesized in the pH of 6.25. From ORR point of view, the moderate pH values were agreed to be more stable (Li et al., 2005).

Table 4.16 Potential losses of the catalysts having % Pt of 20 and synthesized under microwave duration of 50s

Catalysts	**Tafel loss (Pt dissolution) (Potential loss) (mV)**	**Tafel loss (Carbon corrosion) (Potential loss) (mV)**
pH 1.4	6	50
pH 6.25	3	36
pH 10	5	45

4.1.5 Effect of microwave duration on the performance of the catalysts

Cyclic and rotating disc voltammetry techniques were used in order to determine the effect of microwave duration on the performance of the catalysts. All the catalysts tested were having the same Pt loading (20 %) and synthesized under the pH of 1.4. This time the microwave durations were altered (Bayrakçeken, 2008).

Figure 4.23 showed the cyclic voltammograms of the catalysts synthesized at 50, 60 and 120 s microwave durations. The particle sizes were 3.68, 4.6 and 5.69 nm, respectively (Bayrakçeken, 2008). Total metal surface areas (SAs) and %Pt utilizations of the catalysts were shown in Table 4.17. Exposing the reaction medium to the microwave energy for long periods resulted in the increase in the temperature which caused to the agglomeration of the particles. Due to the increasing particle sizes, SA values are decreasing as the microwave duration of synthesis increases. In Table 4.18, the ESA values before and after the degradation tests were summarized. The highest ESA was obtained for the catalyst synthesized in microwave duration of 60 s.

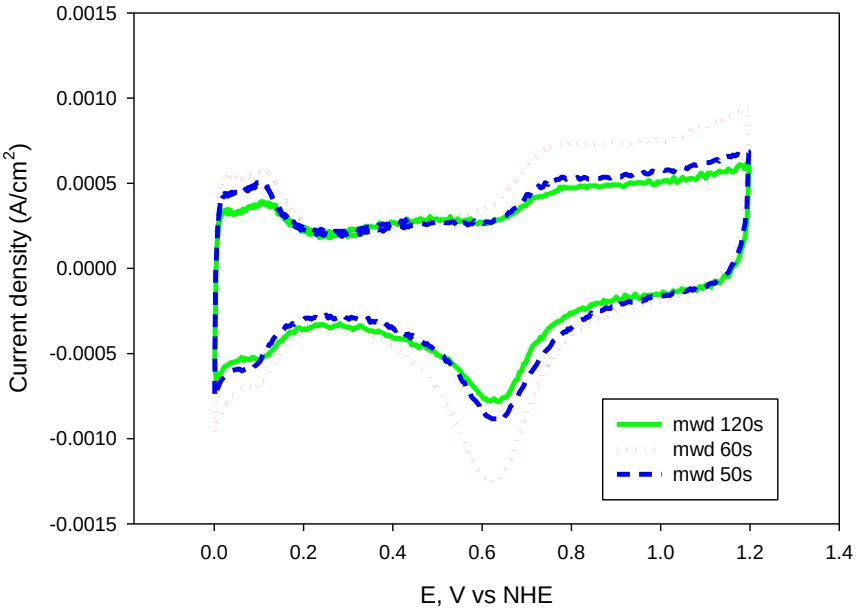

Figure 4.23 Cyclic voltammograms of catalysts synthesized at different microwave durations taken before aging tests at a scan rate of 50mV/s in 0.1 M $HClO_4$ solution for 50 cycles

In the study of Wang et al. (2007), Pt/C catalysts were synthesized under the microwave durations of 30, 60, 90 and 120 s, respectively. From cyclic voltammetry results, the highest catalytic activity was observed for the catalyst synthesized in 90 s microwave duration. This is an agreement that, suitable microwave duration should

be used in order to have catalysts having efficient catalytic activity. Smaller microwave durations (faster heating) would not be long enough for the formation of Pt nanoparticles. On the other hand, long duration causes rapid growth and agglomeration of Pt particles resulted to inefficient Pt/C catalysts.

In Figure 4.24 the cyclic voltammograms of the catalysts taken after Pt dissolution tests can be seen. In Table 4.18 the ESA values were given before and after Pt dissolution tests. In the study of Bayrakçeken et al (2008), these catalysts were tried in PEM fuel cell tests and the best performance was obtained from the MEA (membrane electrode assembly) having the catalyst synthesized in 60 s microwave duration. In CV tests, the catalysts synthesized at 50 and 120 s microwave durations showed similar ESA losses but the catalysts synthesized at 60 s duration showed the highest ESA loss.

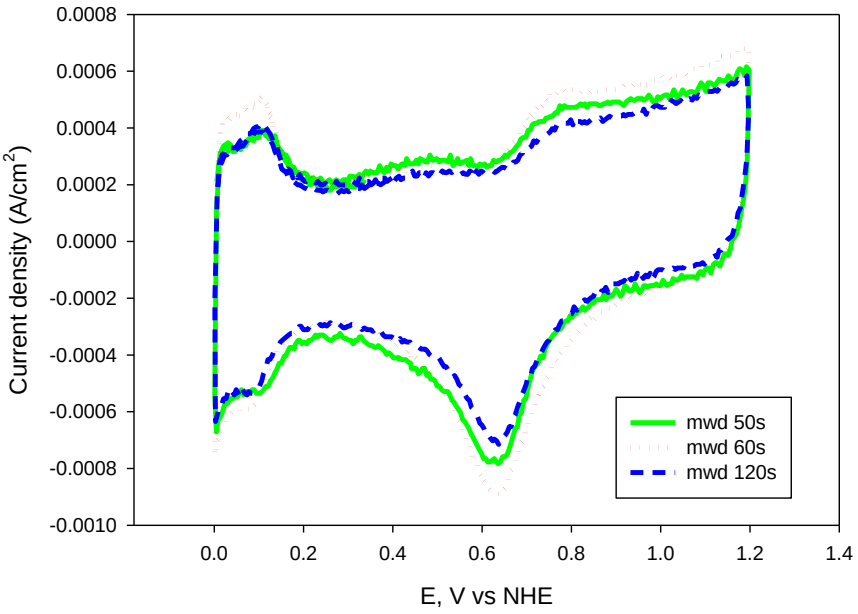

Figure 4.24 Cyclic voltammograms of catalysts synthesized at different microwave durations taken after Pt dissolution tests at a scan rate of 50mV/s in 0.1 M $HClO_4$ solution for 50 cycles

Table 4.17 SA and %Pt utilizations of catalysts having % Pt of 20 and synthesized under pH of 1.4 in different microwave durations

Catalysts	**SA (m^2/g)**	**%Pt utilization**
50 s	70	15
60 s	61	26
120 s	49	23

Table 4.18 ESA values of catalysts having % Pt of 20 and synthesized under pH of 1.4 in different microwave durations

Catalysts	**Average of the peak areas ($A.V/cm^2$)**	**ESA (m^2/g Pt)**	**Average of the peak areas ($A.V/cm^2$)**	**ESA (m^2/g Pt)**	**% ESA loss**
	BEFORE Pt dissolution test		**AFTER Pt dissolution test**		
50s	3.6×10^{-5}	11	3×10^{-5}	9	18
60s	5×10^{-5}	16	3.8×10^{-5}	12	25
120s	3.4×10^{-5}	11	3.2×10^{-5}	10	9

Cyclic voltammograms of the catalysts which were taken after carbon corrosion degradation tests are given in Figure 4.25. Also, in Table 4.19, the carbon corrosion peak areas were calculated in mC/cm^2. In Figure 4.25, the characteristic carbon corrosion peaks can be observed for all the catalysts at around 0.2 to 0.6 V. The highest carbon corrosion was belonging to the catalysts synthesized in 120 s and the lowest carbon corrosion belongs to the catalyst synthesized in 60 s.

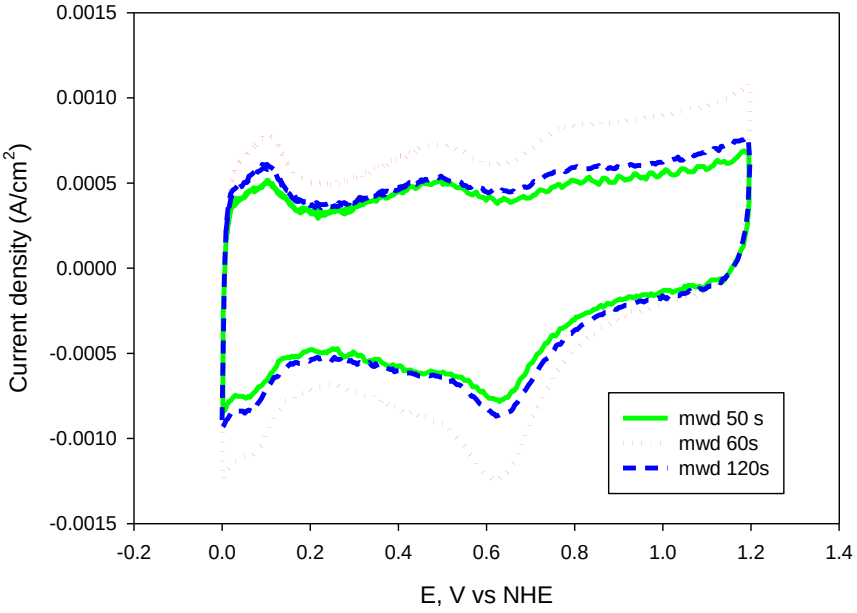

Figure 4.25 Cyclic voltammograms of catalysts having different synthesized under different different microwave durations recorded after holding the electrodes at 1.2V for 24 h

Table 4.19 Carbon corrosion peak areas of the catalyst having % Pt of 20 and synthesized under the pH of 1.4 in different microwave durations

Catalysts	**Carbon corrosion peak areas ($A.V/cm^2$)**	**Charge (Q) (mC/cm^2)**
50 s	1.4×10^{-5}	0.28
60 s	1.34×10^{-5}	0.27
120 s	1.6×10^{-5}	0.32

In Figure 4.26, the ORR activities of the catalysts were shown before degradation tests at 1600 rpm. The ORR activity of the catalysts increased as the microwave duration increased.

Bezerra et al. (2007) searched the heat treatment effect on the Pt/V catalysts. Long exposures of the catalysts to heat would increase the particle size growth which is a

negative effect on the perfromance of the catalyst. On the other hand, heat treatment enhances alloying degree and reorients the surface of the catalysts from amorphous to more ordered state. These factors would surely effect the ORR activitiy of the catalysts. The ORR performance of the catalyst increased as the microwave duration increased.

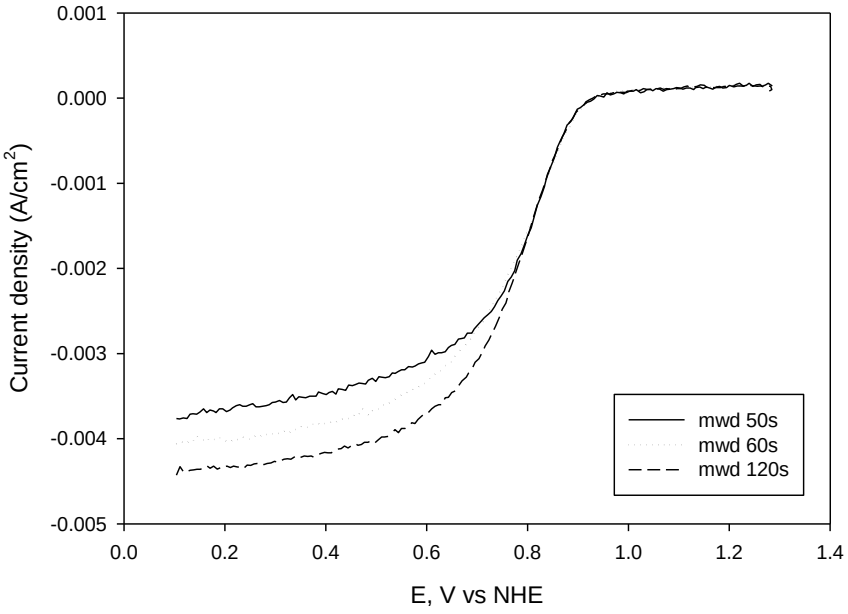

Figure 4.26 Hydrodynamic voltammogram of the catalysts taken before aging tests at a scan rate of 5mV/s in 0.1 M $HClO_4$ solution for 2 cycles at 1600 rpm

In Figure 4.27, ORR performances of the catalysts synthesized at different microwave durations taken after Pt dissolution tests were given. The best performance was obtained from the catalyst synthesized at microwave duration of 60 s and the lowest performance was obtained from the catalyst synthesized in the microwave duration of 50 s.

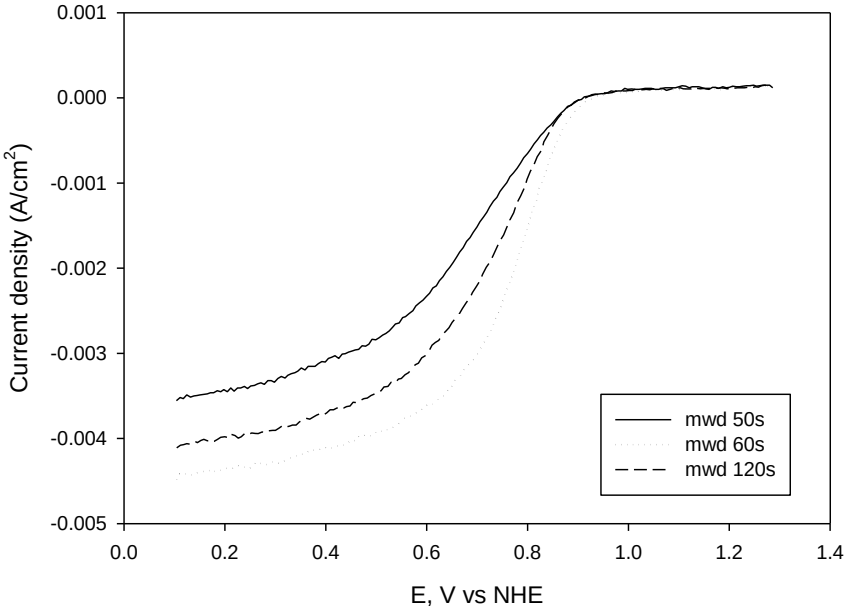

Figure 4.27 Hydrodynamic voltammogram of the catalysts taken after Pt dissolution tests at a scan rate of 5mV/s in 0.1 M $HClO_4$ solution for 2 cycles at 1600 rpm

In Figure 4.28, the performances of the catalysts can be seen prepared under different microwave durations after carbon corrosion tests. The highest performance was taken from the catalysts synthesized in 50s. and the lowest performace was taken from the catalyst synthesized under 120s. From Figure 4.25 and Table 4.19, the lowest carbon corrosion resistance was belong to the catalyst synthesized in 120 s and the other two catalysts synthesized under 50 and 60 s microwave durations showed similar carbon corrosion resistances. The lowest ORR performance of the catalyst synthesized under 120 s can be explained its lowest carbon corrosion resistance among other catalysts.

In the study of Wang et al.(2007), Vulcan XC72, Pt/V (20 %) and Pt/V prepared at 90 s were analyzed in BET for finding their surface areas. They have found out that, microwave irradiation decreased the surface area of carbon. Also, they have detected that, after long exposures (up to 120 s) surface area of carbon continued to decrease. For Figure 4.27, performance decrease of the catalysts in the order of increasing

microwave durations can also be explained by the decrease of carbon surface area of the catalysts due to extension of synthesis time.

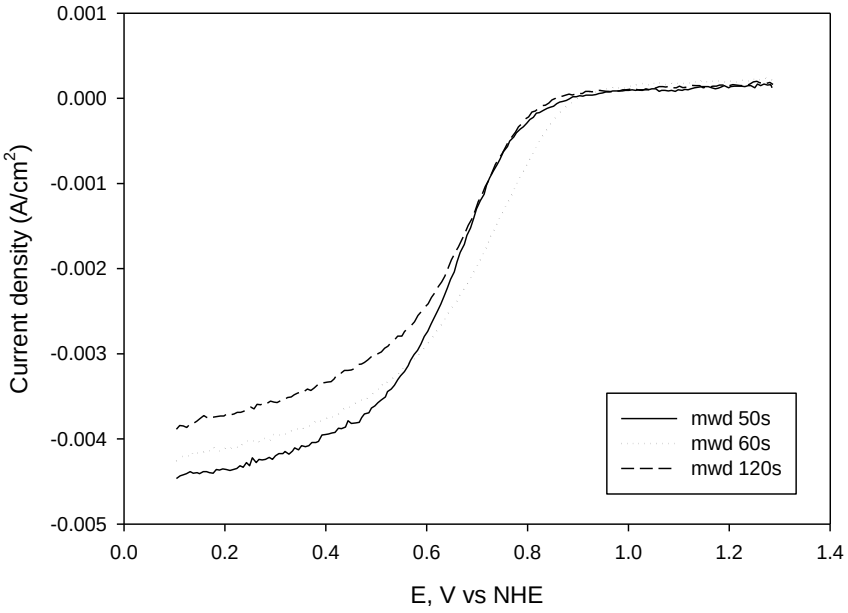

Figure 4.28 Hydrodynamic voltammogram of the catalysts taken after carbon corrosion tests at a scan rate of 5mV/s in 0.1 M $HClO_4$ solution for 2 cycles at 1600 rpm

The performance losses from Tafel slopes were shown in Table 4.20. Like the results of the catalysts having different pH values, potential losses due to Pt dissolution tests were not considerable but from carbon corrosion point of view, the potential losses were significant. Potential losses were decreasing as the microwave duration increases.

Table 4.20 Potential losses of the catalysts having % Pt of 20 and synthesized under the pH of 1.4 in different microwave durations

Catalysts	**Tafel loss (Pt dissolution) (Potential loss) (mV)**	**Tafel loss (Carbon corrosion) (Potential loss) (mV)**
50 s	6	49
60 s	10	35
120 s	7	30

4.2 Comparison of all the catalysts (Commercial and home made)

The comparison of the commercial and home made catalysts in terms of their durability for HOR and ORR were given in the tables below. It was observed that the home made catalysts gave similar Pt utilization results with the commercial ones (Table 4.2.1). By changing the catalyst preparation conditions the Pt utilization of the home made catalysts can be increased further. The best Pt utilization was observed for the catalyst prepared with the pH of 1.4 and microwave duration of 60 s. Bayrakçeken (2008) also showed that this catalyst gave the best PEMFC performance in the fuel cell environment and observed similar trend such as when the microwave duration increased further from 60 s, the performance started to decrease.

Electrochemical surface areas of the catalysts were found for before and after Pt dissolution degradation tests and also the corresponding ESA losses were given in Table 4.2.2 When the C/N ratio was set to the same value it was seen that home made catalysts showed a less ESA loss during Pt dissolution than commercial ones.

Table 4.2.3 shows the carbon oxidation peak areas of the commercial and home made catalysts after carbon corrosion degradation test. It was observed that for the same C/N ratio, when the loading of the Pt increased in the commercial catalysts which means that the amount of carbon decreasing, the carbon oxidation peak areas was also decreasing. From carbon corrosion point of view, catalysts 9 and 10 showed enhanced carbon corrosion properties when compared with the commercial catalysts. From C/N ratio point of view, catalyst ink having C/N ratio of 4 showed less carbon corrosion than the catalyst ink having the C/N ratio of 2.

ORR activities of the commercial and home made catalysts were also investigated before and after Pt dissolution and carbon corrosion degradation tests (Table 4.2.4). From Tafel slope potential losses of the catalysts were found after aging tests. Due to

Pt dissolution, catalysts 8, 9 and 10 showed lower potential losses which are comparable with the commercial catalysts. From carbon corrosion point of view, catalyst 12 showed nearly the same potential loss with the catalyst 1. All the prepared catalysts showed higher potential losses after carbon corrosion degradation tests.

Table 4.21 Total metal surface area (SA) and % Pt utilization

no	Catalysts	C/N ratio (Carbon/Nafion)	SA (m^2/g)	%Pt utilization
1	**Pt/V %20 ETEK**	2	108	19
2	**Pt/V %50 X(commercial)**	2	117	26
3	**Pt/V %70 Y(commercial)**	2	88	30
4	**Pt/V %20 ETEK**	4	108	17
5	**Pt/V %20 ETEK**	8	108	28
6	**Pt/V %20 ETEK**	12	108	23
7	**Pt/V %20 ETEK**	∞ (no Nafion solution)	108	21
8	**Pt/V % 20 pH 1.4, mwd 50s**	2	70	15
9	**Pt/V %20 pH 6.25, mwd 50 s**	2	73	18
10	**Pt/V %20 pH 10, mwd 50 s**	2	84	17
11	**Pt/V %20 pH 1.4 mwd 60 s**	2	61	26
12	**Pt/V %20 pH 1.4 mwd 120s**	2	49	23

Table 4.22 Electrochemical Surface Areas (ESA) before and after Pt dissolution

no	Catalysts	C/N ratio (Carbon/Nafion)	ESA Before (m^2/g Pt)	ESA After (m^2/g Pt)	ESA loss (%)
1	**Pt/V %20 ETEK**	2	20	13	35
2	**Pt/V %50 X(commercial)**	2	30	19	37
3	**Pt/V %70 Y(commercial)**	2	26	18	31
4	**Pt/V %20 ETEK**	4	18	10	44
5	**Pt/V %20 ETEK**	8	30	20	33
6	**Pt/V %20 ETEK**	12	24	17	29
7	**Pt/V %20 ETEK**	∞ (no Nafion solution)	23	15	35
8	**Pt/V % 20 pH 1.4, mwd 50s**	2	11	9	18
9	**Pt/V %20 pH 6.25, mwd 50 s**	2	13	12	8
10	**Pt/V %20 pH 10, mwd 50 s**	2	14	13	7
11	**Pt/V %20 pH 1.4 mwd 60 s**	2	16	12	25
12	**Pt/V %20 pH 1.4 mwd 120s**	2	11	10	9

Table 4.23 Carbon corrosion peak areas

no	Catalysts	C/N ratio (Carbon/Nafion)	Carbon corrosion peak areas (mC/cm^2)
1	**Pt/V %20 ETEK**	2	0.16
2	**Pt/V %50 X(commercial)**	2	0.13
3	**Pt/V %70 Y(commercial)**	2	0.07
4	**Pt/V %20 ETEK**	4	0.078
5	**Pt/V %20 ETEK**	8	0.214
6	**Pt/V %20 ETEK**	12	0.292
7	**Pt/V %20 ETEK**	∞ (no Nafion solution)	Not performed
8	**Pt/V % 20 pH 1.4, mwd 50s**	2	0.28
9	**Pt/V %20 pH 6.25, mwd 50 s**	2	0.04
10	**Pt/V %20 pH 10, mwd 50 s**	2	0.14
11	**Pt/V %20 pH 1.4 mwd 60 s**	2	0.27
12	**Pt/V %20 pH 1.4 mwd 120s**	2	0.32

Table 4.24 Tafel slope potential losses

no	Catalysts	C/N ratio (Carbon/Nafion)	After Pt dissolution test (mV)	After carbon corrosion test (mV)
1	**Pt/V 20% ETEK**	2	5	27
2	**Pt/V 50% X(commercial)**	2	13	17
3	**Pt/V 70% Y(commercial)**	2	3	9
4	**Pt/V %20 ETEK**	4	18	21
5	**Pt/V %20 ETEK**	8	7	20
6	**Pt/V %20 ETEK**	12	17	24
7	**Pt/V %20 ETEK**	∞ (no Nafion solution)	15	Not performed
8	**Pt/V % 20 pH 1.4, mwd 50s**	1.86	6	50
9	**Pt/V %20 pH 6.25, mwd 50 s**	2	3	36
10	**Pt/V %20 pH 10, mwd 50 s**	2	5	45
11	**Pt/V %20 pH 1.4 mwd 60 s**	2	10	35
12	**Pt/V %20 pH 1.4 mwd 120s**	2	7	30

CHAPTER 5

CONCLUSIONS

Durability is an important factor and very crucial for PEM fuel cells to become commercial and long lasting products. First of all, durability should be fully understood from components point of view. From this aspect, for getting quick results, accelerated degradation tests (ADTs) were agreed by most of the scientists to be performed to the components of the PEM fuel cell.

The main idea behind the durability tests performed on PEMFC components is to build a foresight about how the components would behave or what failure mechanisms they would show when they are really worked in PEMFC operations. Cyclic voltammetry and rotating disc voltammetry techniques were the ones accepted for testing the electrocatalysts. Many properties of the catalysts would be examined before and after aging tests with CV and RDE methods.

The aim of this study was to investigate the durability issues of the PEM fuel cell electrocatalysts by testing them via cyclic voltammetry and rotating disc voltammetry techniques. For this purpose, an accelerated degradation testing protocol was established and applied for determining the Pt dissolution and carbon corrosion behaviors of the catalysts.

Commercially available and already prepared catalysts having different properties (Pt percentages, prepared at different pH values and microwave durations) were tried. Besides, different catalyst ink compositions having different carbon to Nafion ratios with the same catalyst were also tested. Pt dissolution degradation tests were

performed between the potential range of 0.6–1.2V and carbon corrosion degradation tests were performed by keeping the catalyst film layer under potentiostatic hold of 1.2 V.

The results showed that physical properties and the catalyst preparation conditions strongly affect the performance and durability of the catalysts. Pt loading (%) which affect the particle size of the catalysts is an important parameter that influences the active surface area. On the other hand, Nafion loading is another important factor and should be optimized. pH of the catalyst preparation environment is another crucial property because at lower pH values, platinum cannot be impregnated into carbon and agglomerations occur in short times. Synthesis at lower microwave durations is not beneficial because time would not be enough for the Pt to be attached effectively to carbon. On the other hand, keeping the catalyst solution at high durations increases the particle size and corrosion properties of the catalysts.

All the home made catalysts were having 20% Pt loading except the catalysts having Pt loadings of 32 and 44%. The results of the Pt/V 20% catalysts (synthesized in different microwave durations and pH values) were compared with the commercial catalyst ETEK Pt/V 20%.

The testing protocol was succeeded for the characterization of the catalysts. Extention in testing durations would be applied in order to have more realistic results about the catalysts.

It was observed that the catalyst preparation conditions affect the Pt utilization of the home made catalysts. The best Pt utilization was observed for the catalyst prepared with the pH of 1.4 and microwave duration of 60 s. Home made catalysts showed a less ESA loss during Pt dissolution than commercial ones when the C/N ratio was set to the same value.

During the carbon corrosion test, it was observed that for the same C/N ratio when the loading of the Pt increased in the commercial catalysts which means that the amount of carbon decreasing the carbon oxidation peak areas was also decreasing. Home made catalyst prepared at pH of 6.25 showed the lowest carbon oxidation peak area than the commercial ones. Catalyst ink having C/N ratio of 4 showed less carbon corrosion than the catalyst ink having the C/N ratio of 2 with commercial catalysts.

ORR activities of the commercial and home made catalysts were also investigated before and after Pt dissolution and carbon corrosion degradation tests. All of the home made catalysts gave higher potential losses after carbon corrosion test. But they gave similar potential losses after Pt dissolution degradation tests.

These results showed that microwave irradiation method seems to be a promising catalyst preparation technique and if the preparation conditions improved further the catalyst properties can also improved. It is essential to determine the durability of the electrocatalysts for long term durable fuel cells.

REFERENCES

Antolini E., Giorgi L., Pozio A., Passalacqua E., *Influence of Nafion loading in the catalyst layer of gas-diffusion electrodes for PEFC,* Journal of Power Sources 77 (2002) 136-142

Antoine O., Durand R., *RRDE study of oxygen reduction on Pt nanoparticles inseide Nafion: H_2O_2 production in PEMFC cathode conditions*, Journal of Applied Electrochemistry 30: 839-844, 2000

Ball S.C., Hudson S.L., Thompsett D., Theobald B., *An investigation into factors affecting the stability of carbons and carbon supported platinum and platinum/cobalt alloy catalysts during 1.2 V potentiostatic regimes at a range of temperatures*, Journal of Power Sources 171 (2007) 18-25

Barbir F., *Fuel Cell Technology*, Springerelink, 2006

Barbir F., *PEM Fuel Cells*, *Elsevier*, 2005

Bayrakçeken A., Smirnova A., Kitkamthorn U., Aindow M., Türker L., Eroğlu İ., Erkey C., *Pt-based electrocatalysts for polymer electrolyte membrane fuel cells prepared by supercritical deposition technique*, Journal of Power Sources, 179 (2008) 532-540

Bayrakçeken A., *Platinum and platinum-ruthenium based catalysts on various carbon supports prepared by different methods for PEM fuel cell applications*, PhD thesis, METU, Ankara, 2008

Bayrakçeken A., Cangül B., Zhang L.C., Aindow M., Erkey C., *PtPd/BP2000 electrocatalysts prepared by sequencial supercritical carbon dioxide deposition*, International Journal of Hydrogen Energy 35(2010 11669-11680

Bernay C., Marchand M., *Cassir M., Prospects of different fuel cell Technologies for vehicle applications*, Journal of Power Sources 108 (2002) 139-152

Bezerra C., Zhang L., Liu H., Lee K., Marques A., Marques E., Wang H., Zhang J., *A review of heat-treatment effects on activity and stability of PEM fuel cell catalysts for oxygen reduction reaction*, Journal of Power Sources 173 (2007) 891-908

Biocharfarming,www.biocharfarming.files.wordpress.com/2008/10/fuel_cell_diagram_scientificcomputing.jpg, last accessed at 25.12.2010.

Borup R.L., Davey J.R., Garzon F.H., Wood D.L., Inbody M.A., *PEM fuel cell electrocatalyst durability measurements*, Journal of Power Sources, 163 (2006) 76-81

Büchi F.N., Inaba M., Schmidt T.J., *Polymer Electrolyte Fuel Cell Durability*, Springer, 2009

Chen C., Levitin G., Hess D.W., Fuller T.F., *XPS investigation of Nafion® membrane degradation*, Journal of Power Sources 169 (2007) 288-295

Chen G., Zhang H., Ma H., Zhong H., Electrochemical durability of gas diffusion layer under simulated proton exchange membrane fuel cell conditions, International Journal of Hydrogen Energy, 34 (2009) 8185-8192

Cherstiouk O.V., Simonov P.A., Fenelonov V.B., Savinova E.R., Influence of Nafion® ionomer on carbon corrosion, J.Appl. Electrochem (2010) 40: 1933-1939

Cho Y., Park H., Cho Y., Jung D., Park Y., Sung Y., *Effect of platinum amount in carbon supported platinum catalyst on performance of polymer electrolyte membrane fuel cell*, Journal of Power Sources, 172 (2007) 89-93

Cleghorn S.J.C., Mayfield D.K., Moore D.A., Rusch G., Sherman T.W., Sisofo N.T., Beuscher U., *A polymer electrolyte fuel cell life test: 3 years of continuous operation*, Journal of Power Sources, 158 (2006) 446-454

Dam V.A.T., Bruijn F.A., *The stability of PEMFC electrodes: Platinum dissolution vs potential and temperature investigated by quartz crystal microbalance*, Journal of Electrochemical Society, 2007(154) 494-499

David K., Gosser Jr., Cyclic *Voltammetry, Simulation and Analysis of Reaction Mechanisms*, VCH Publishers Inc., 1993)

De Brujin F.A., Dam V.A.T., Janssen G.J.M., *Review: Durability and Degradation Issues of PEM Fuel Cell Components*, Wiley Interscience, DOI: 10, 1002 / fuce. 200700053

De Bruijn F.A., Dam V.A.T., Janssen G.J.M., *Review: Durability and degradation issues of PEM fuel cell components*, FUEL CELLS, 08, 2008, No. 1-3-22

Güvenatam B., *Development of different carbon supports for proton exchange membrane fuel cell electrocatalysts*, MsC Thesis, METU, Ankara, 2010

Hung Y., El-Khatib K.M., Tawfik H., *Testing and evaluation of aluminium coated bipolar plates of PEM fuel cells operating at 70 C*., Journal of Power Sources 163 (2006) 509-513

Kangasniemi K.H., Condit D.A., Jarvi T.D., *Characterization of Vulcan electrochemically oxidized under simulated PEM fuel cell conditions*, Journal of the Electrochemical Society, 151 (4) E125-E132 (2004)

Le Canut J. M., Latham R., Merida W., Harrington D.A., *Impedance study of membrane dehydration and compression in proton excahnge memberane fuel cells*, Journal of Power Sources, 192 (2009) 457-466

Lee C., Merida W., *Gas diffusion layer durability under stady-state and freezing conditions*, Journal of Power Sources, (2007) 164

Li X. Chen W., Zhao J., Xing W., Xu Z., *Microwave polyol synthesis of Pt(CNTs catalsysts: Effects of pH on particle size and electrocatalytic activity for methanol electrooxidation*, Carbon 43 (2005) 2168-2174

Lin R-B., Shih S-M., Kinetics of hydrogen oxidation reaction on Nafion-coated Pt/C electrodes under high overpotentials, Journal of the Chinese Institute of Chemical Engineers 38 (2007) 365-370

Litster S., McLean G., *PEM fuel cell electrodes*, Journal of Power Sources, 30 (2004) 61-76

Liu D., Case S., *Durability study of proton exchange membrane fuel cells under dynamic testing conditions with cyclic current profile*, Journal of Power Sources, 162 (2006) 521-531

Lobato J., Canizares P., Rodrigo M.A., Linares J.L., Pinar F.J., *Study of the influence of the amount of PBI-H_3PO_4 in the catalytic layer of a high temperature PEMFC*, International Journal of Hydrogen Energy 35 (2010) 1347-1355

Ma Andersen S., Madsen L., Skou E.M., *Studied on PEM fuel cell noble metal catalyst dissolution*, Solid States Ionics, 2010, (Article in Press)

Merzougui B., Swathirajan S., *Rotating disk electrode investigations of fuel cell catalyst degradation due to potential cycling in acid electrolyte*, Journal of The Electrochemical Society, 152 (12) A2220-A2226 (2006)

Middelman E., Kout W., Vogelaar B., Lenssen J., De Waal E., *Bipolar plates for PEM fuel cells*, Journal of Power Sources, 118(2003) 44-46

O'Hayre R. , Lee S.J. ,Cha S.W, Prinz F.B., *A sharp peak in the performance of sputtered platinum fuel cells at ultra-low platinum loading*, J. Power Sources 109 (2002) 483–49

Shao Y., Yin G., Gao Y., *Understanding and approaches for the durability issues of Pt-based catalysts for PEM fuel cell*, Journal of Power Sources, 171 (2007) 558-566

Shao Y., Yin G., Gao Y., *Understanding and approaches fort he durability issues of Pt-based catalysts for PEM fuel cell*, Journal of Power Sources, 171 (2007) 558-566

Schmittinger W., Vahidi A. A *review of main parameters influencing long-term performance and durability of PEM fuel cells*, Journal of Power Sources, 180 (2008) 1-14

Tang H., Peikang S., Jiang S.P., Wang F., Pan M., *A degradation study of Nafion proton exchange membrane of PEM fuel cells*, Journal of Power Sources 170 (2007)85-92

Wang J., Yin G., Shao Y., Zhang S., Wang Z., Gao Y., *Effect of carbon black support corrosion on the durability of Pt/C catalyst*, Journal of Power Sources 171 (2007) 331-339

Williams M.V., Begg E., Bonville L.J., Kunz H.R., Fenton J.M., Characterization of gas diffusion layers for PEMFCs, Journal of electrochemical society, 151 (8) A1173-A1180 (2004)

Wind J., Spah R., Kaiser W., Böhm G., *Metallic bipolar plates for PEM fuel cells*, Journal of Power Sources, 105 (2002) 256-260

Wu J., Zi Yuan X., Martin J.J., Wang H., Zhang J, Shen J., Wu S., Merida W., *A review of PEM fuel cell durability: Degradation mechanisms and mitigation strategies*, Journal of Power Sources, 184 (2008) 104-119

Xing Y., *Synthesis and Electrochemical Characterization of Uniformly-Dispersed High Loading Pt Nanoparticles on Sonochemically-Treated Carbon Nanotubes*, J. Phys. Chem. B 2004, 108, 19255-19259

Yu J., Matsuura T., Yoshikawa Y., Islam N., Hori M., *Lifetime behaviour of a PEM fuel cell with low humidification of feed stream*, Phys.Chem., 2005, 7, 373-378

Zhang S., Yuan X., Wang H., Merida W., Zhu H., Shen J., Wu S., Zhang J., *A review of accelerated stress tests of MEA durability in PEM fuel cells*, International Journal of Hydrogen Energy 34 (2009) 388-40

APPENDIX A

SAMPLE CALCULATIONS

A.1 Cyclic Voltammetry results

A.1.1 Electrochemical Surface Area (ESA)

Figure A.1 shows a typical cyclic voltammogram taken from a cyclic voltammetry experiment.

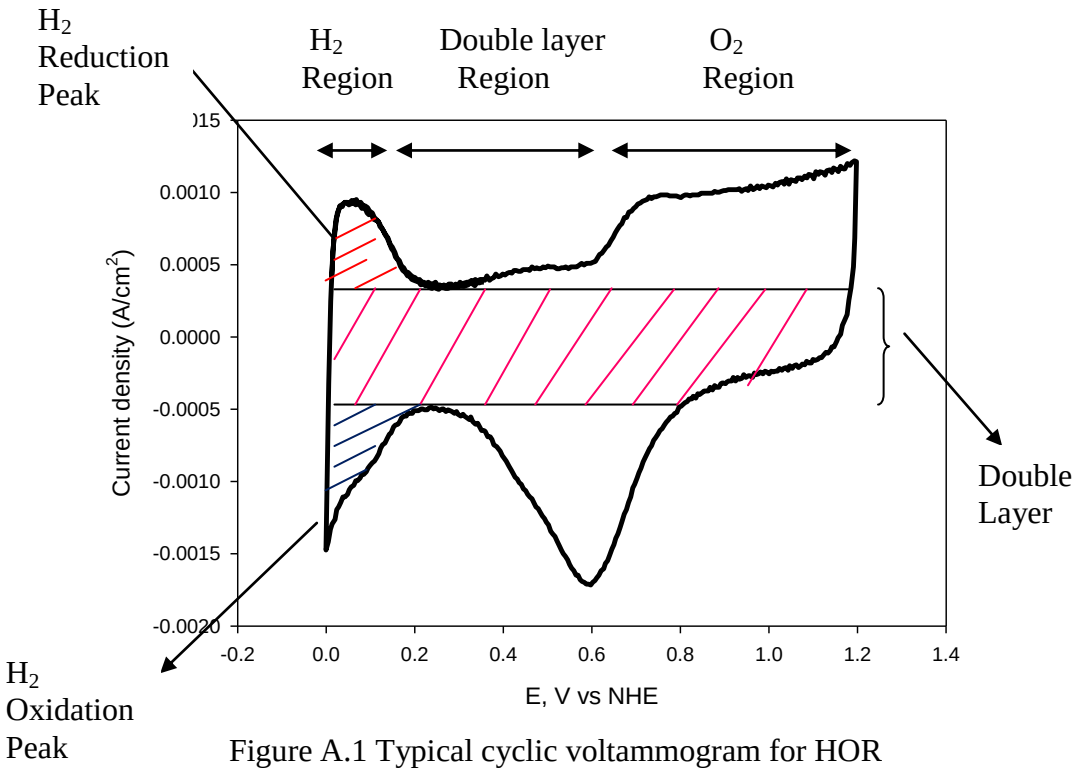

Figure A.1 Typical cyclic voltammogram for HOR

The ESA of Pt/V (20 %), pH 6.25 was calculated before aging tests was 4.2 $\times 10^{-5}$ A.V/cm^2. The calculation of ESA in m^2/g Pt was shown below.

$$ESA = \frac{0.000042}{0.21 \times 50 \times 28} \times 10^8 = 13 \text{ m}^2/\text{g Pt}$$

A.1.2 Metal Total Surface Area (SA)

The particle diameter of Pt/V (20 %), pH 6.25 was found from XRD as 3.85 nm. The calculation of its SA was shown below.

$$SA = \frac{6}{\rho \times d} \times 1000 = \frac{6}{21.4 \times 3.85} \times 1000 = 73 \text{m}^2/\text{g Pt}$$

A.1.3 Pt utilization (%)

Pt utilization (%) of Pt/V (20 %), pH 6.25 catalyst is shown below.

$$Pt_{ut} (\%) = \frac{13}{73} \times 100 = \%18$$

A.1.4 Carbon corrosion

Carbon corrosion mainly occurs at around 0.6 V. In Figure A.2, the cyclic voltammogram shows a typical result of carbon corrosion test taken before and after aging tests (potentiostatic hold of the catalyst at 1.2 V for 24 h). The blue dashed curve shows a certain peak between 0.4-0.6 V which corresponds to the carbon corrosion peak.

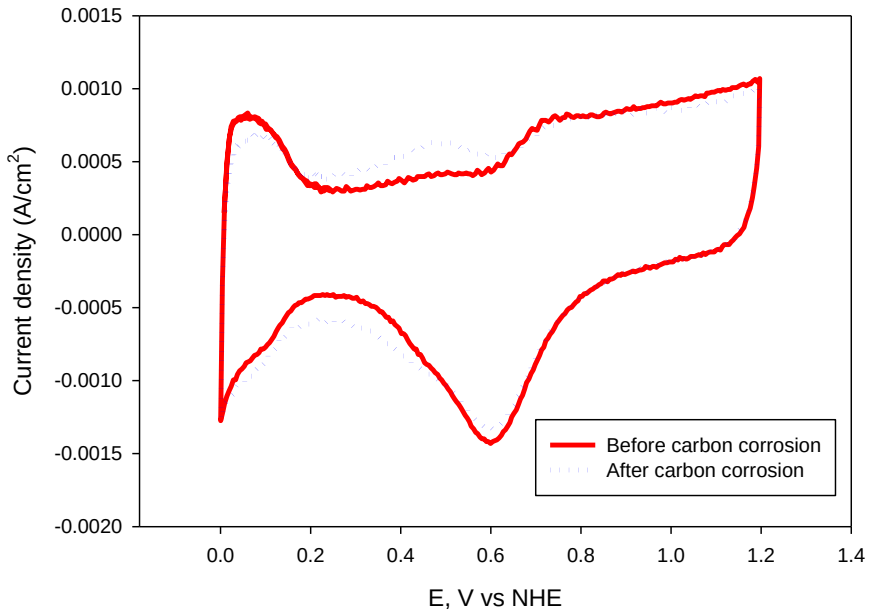

Figure A.2 Typical result of a catalyst after carbon corrosion aging test

The area of the carbon corrosion peak was found by using the software OriginLab 7.5. The area of the carbon corrosion peak was found as 2 $\times 10^{-6}$ A.V/cm^2 for Pt/V (20 %), pH of 6.25 catalysts. The charge found was shown below.

$Q = 2 \times 10^{-6} / 0.05 \times 1000 = 0.04$ mC/cm^2

A.2 Rotating Disc Voltammetry Results

A.2.1 Potential losses (Tafel plots)

Figure A.3 is a typical hydrodynamic voltammogram (forward scan) taken from an experiment carried out at 5 mV/s scan rate. Hydrodynamic voltammograms were taken at 100, 400, 900, 1600 and 2500 rpm angular velocities. For each angular velocity 1 cycle was taken. This behavior should be seen for all the experimental results. This means that as the angular velocity increases the stagnant layer on the GC electrode gets thinner (mass transfer limitation effect decreases) which the

transfer of ions to the surface of the electrode becomes easier. As much as the ions transfer to the surface of the electrode, current will increase.

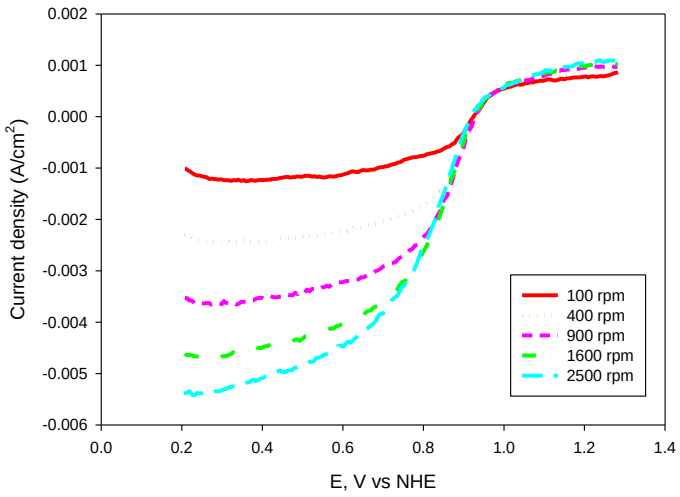

Figure A.3 Typical hydrodynamic voltammogram taken from RDE experiments

Tafel plots are obtained from plotting E (voltage) versus log (- i_k) (current occurring due to kinetic rates of the reactions). With the data obtained from RDE experiments for each of the angular velocity and for before and after test results Tafel plots were drawn. Figure A.4 is a typical result taken form an experiment for before and after test at 400 rpm angular velocity.

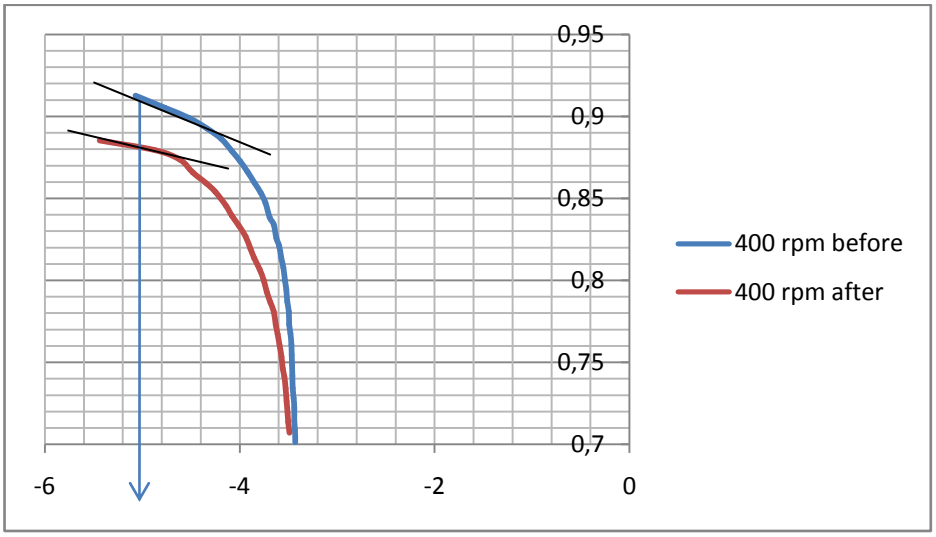

Figure A.4 Typical voltammogram taken from E vs log (-ik) for before and after test for 400 rpm

For all angular velocity values, the potential loss is found from the upper part of the curves where the potential loss is at its highest value. From the slopes taken, for the same current density the potentials were read from the data and the difference gives the potential loss of the catalyst for the specified angular velocity after aging test. Taken the average of potential losses gained from each angular velocity values gave the resultant potential loss. Potential losses were found for both Pt dissolution and carbon corrosion aging tests.

APPENDIX B

REPRODUCIBILITY

To determine the reproducibility of the tested catalysts in cyclic and rotating disc voltammetry, same tests were carried on for different batches. The cyclic voltammograms of the same catalyst can be seen which were taken for two different runs beore and after ageing tests (Figure B.1, Figure B.2).

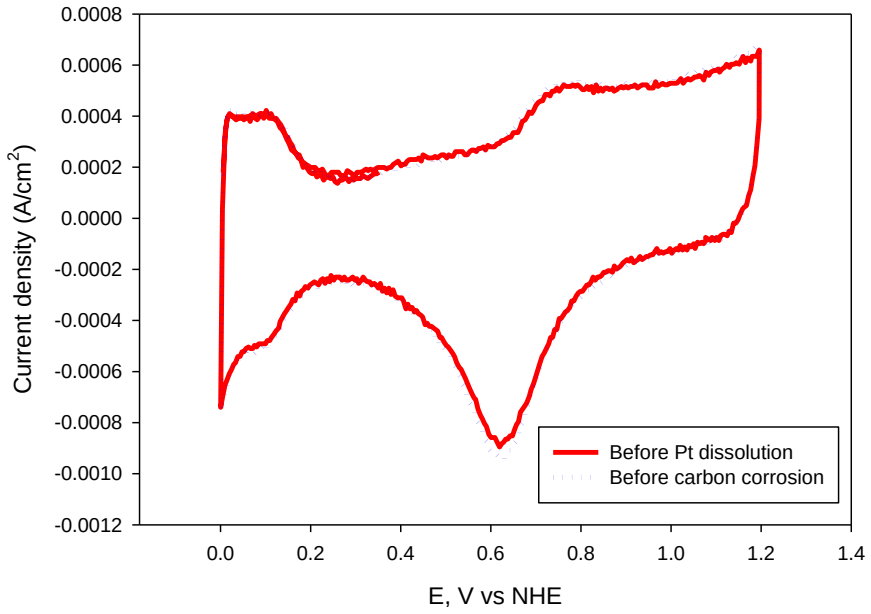

Figure B.1 Cyclic voltammograms taken from the calayst Pt/V (20 %), pH 6.25, mwd 50 s

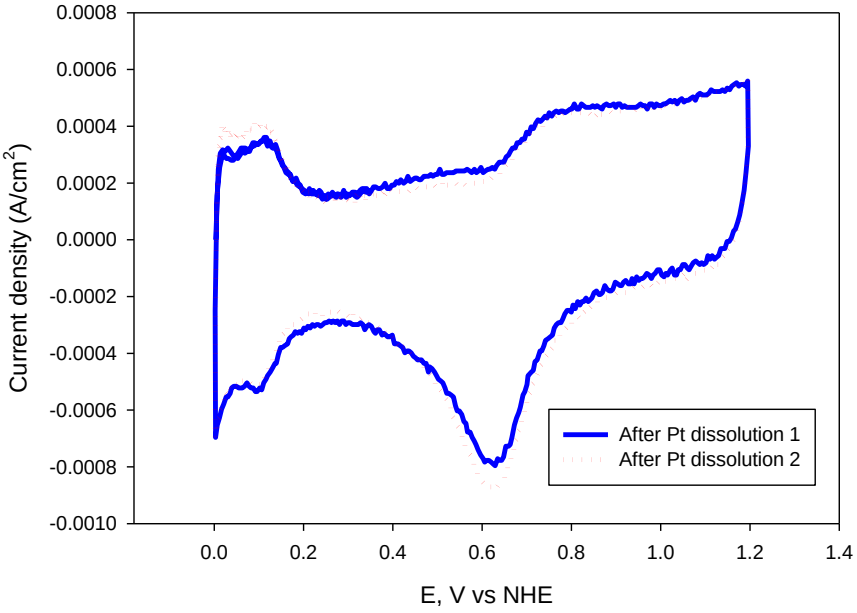

Figure B.2 Cyclic voltammograms taken from the calayst Pt/V (20 %), pH 6.25, mwd 50 s (After Pt dissolution test from two different runs)